GAMMA IRRADIATION OF NONLINEAR GR-S

Blachford

THE EFFECTS OF GAMMA RADIATION ON NONLINEAR POLY(BUTADIENE-CO-STYRENE)

by

John Blachford, B.Eng.(McGill)

A thesis submitted to the Faculty of Graduate Studies and Research in partial fulfilment of the requirements for the degree of Doctor of Philosophy

Department of Chemistry,
McGill University,
Montreal, Quebec.

April, 1963

ACKNOWLEDGEMENTS

Grateful acknowledgement is made to Dr. R. F. Robertson for valuable advice and encouragement.

The author would also like to thank the Pulp and Paper Research Institute of Canada for osmotic pressure data and Mr. H. G. Sanderson of the Chemistry Department for the ultracentrifuge data.

Gratitude must also be expressed to the National Research Council of Canada for the award of a Studentship and for additional financial support from grant A.605.

TABLE OF CONTENTS

LIST OF FIGURES

LIST OF TABLES

NOMENCLATURE

Symbol	Meaning	Units
A'	The number of monomer units in a sample	-
A,a,	Absorbancy and absorbancy index, respectively	-
a,a'	Exponent in the empirical relationship between intrinsic viscosity and molecular weight for M_v and M_w, respectively	-
a_1,a_2,a_3	Coefficients in the expansion of $_{sp}/c$ as a power series in concentration	-
B	Weight or abbreviation of N-phenyl-β-napthylamine	g.
b	Thickness of sample used in ultraviolet spectrophotometry	cm.
C_c	Correction factor to account for small volume of system connected to the McLeod gauge	-
c	Concentration of solids in solution	$g.dl.^{-1}$
D	Molecules of B destroyed per weight average primary molecular of polymer	-
E_p,E_b	Electron densities of polymer and B, respectively	electrons $g.^{-1}$
F	Right side of equation 38	-
F,	Force opposing the motion of a mole of molecules through solution with velocity f_f	g.
f,f_o	Frictional coefficients for a polymer molecule at a finite and at infinite dilution, respectively	$g.sec.^{-1}$
f_n	Functionality of nonlinearity	-
G	Fraction of polymer that is insoluble	-
G_g	Molecules of gas produced per 100 e.v. of obsorbed radiation	molecules/100 e.v.

G_{gp}, G_{gb}	Values of G_g for pure polymer and pure B, respectively	molecules/100 e.v.
G_s, G_x	Scissions and crosslinks produced per 100 e.v. of absorbed radiation	-
g	Ratio of mean-square size of a non-linear to a linear molecule of the same molecular weight	-
h^3	Ratio of intrinsic viscosity of a non-linear to a linear molecule of the same molecular weight according to Stockmayer-Fixman theory (72)	-
h_2, h_1	Difference in mercury levels of the McLeod gauge after and before gas expansion	cm.
I_o, I	The initial and transmitted intensity of light in ultraviolet spectrophotometry	ergs.sec.^{-1}
i	The inhibitor effect in a radiation induced chain reaction producing crosslinks	-
j	Used in defining a Schulz-Zimm distribution (87)	-
K, K_1	Constants in the relationship between intrinsic viscosity and molecular weight for M_v and M_w respectively	dl.g.^{-1}
K_s	Constant in the relation $s_o = K_s \bar{M}_{\eta s}^{\gamma}$	-
k'	Huggin's constant equal to $a_2/[\eta]^2$ if $a_3=0$	dl.g.^{-1}
k_s	Coefficient relating sedimentation coefficient to concentration	dl.g.^{-1}
$\bar{M}_n, \bar{M}_w, \bar{M}_{\eta s}, \bar{M}_v$	Number, weight, sedimentation-viscosity, and viscosity average molecular weights, respectively	-
$\bar{M}_{nog}$	Number average molecular weights before crosslinking for the gel fraction	-
$\bar{M}_{no}, \bar{M}_{wo}$	Number average and weight average weights, respectively before irradiation	-

$\bar{M}_{noo}$,$\bar{M}_{woo}$	Number average and weight average molecular weights, respectively of the primary linear molecules	-
M_v^c,M_v^h	From the Mark Houwink equation for low and high temperature of polymerization	-
$\bar{M}_{cg}$	Molecular weight per crosslink unit	-
m,m_w	Number and weight average number of crosslink units per molecule	
N	Avogadro's number	-
n	Exponent to which $[\eta]$ must be raised to keep k' constant, $\frac{\eta_{sp}}{c} = [\eta] + k'[\eta]^{n}c$	
P	Parameter relating f_o to the root-mean-square end-to-end distance	-
P	Polymer or polymer weight	g.
P,	Pressure at the point in the cell at which s_p is measured	dynes.cm.$^{-1}$
p,p_o	Ratio of main chain fractures to chain units for a given dose and for unit dose, respectively	-
Q_o,Q_R	Weight fraction of soluble B before and after irradiation	-
q,q_o	Portion of units crosslinked for a given dose and for unit dose	-
q_g,q_{oa}	Same as q except only gel fraction considered and irradiation in air, respectively	
R	Radiation dose	rads
R_g	Radiation dose required to initiate gelation	rads
R_{gc},R_{ga}	Values of R_g for crosslinking, and for both crosslinking and degradation, respectively	rads
R'	The gas constant, 82.057 cm.^{3}atm.deg.$^{-1}$mole^{-1}	
R_o	Dose required to cause the nonlinearity found in the unirradiated polymer	rads

$r, \sqrt{\overline{r^2}}, \sqrt{\overline{r_0^2}}$	Distance between the ends of a polymer chain, root-mean-square end-to-end distance averaged over all configurations, and the same for unperturbed molecules, respectively	cm.
S	Fraction of soluble polymer	-
s, s_0	Sedimentation coefficients for molecule at a finite and infinite dilution, respectively	sec.
s_p	Sedimentation coefficient uncorrected for pressure	sec.
u	Degree of polymerization	-
$\bar{u}_n, \bar{u}_w$	Number and weight average degree of polymerization	-
V_1	Molar volume of solvent	cc.
V_2, V_3	Dilution volumes in ultraviolet spectrophotometry	ml.
v_s, v_p	Specific volume of polymer solution and polymer, respectively	-
v, v_0	Partial specific volume at finite and infinite dilution, respectively	-
v_1	Volume fraction of polymer in swollen gel	-
v_f	Translational velocity of a polymer molecule in sedimentation	$cm.sec.^{-1}$
W	Energy absorbed per ion pair produced	e.v.
W	Sample weight for extraction or gas evolution	g.
W_c	Cumulative weight used in obtaining molecular weight distribution curves	-
W_g, W_b	Weight of gel and of benzene associated with gel, respectively	g.
w	Weight of monomer units	g.
X_m, X_1	Distance from maximum ordinate to centre of rotor, and the same magnified by a factor P_m	cm.

Y	Moles of gas evolved per gram of sample	moles/g.
z	Used in defining a Schulz-Zimm molecular weight distribution	-
γ	Exponent in the relationship between s_o and M	-
γ_p	Correction factor for the dependence of s on P,	cm.dynes^{-1}
δ	Crosslinking coefficient, number of crosslink units per weight average primary molecule	-
δ_o	Crosslinking coefficient for the unirradiated polymer	-
η_o, η	Viscosity of solvent and solution, respectively	poises
η_r, η_{sp}	Relative and specific viscosities, respectively	-
$[\eta]$	Intrinsic viscosity	dl.g.$^{-1}$
$[\eta]_b, [\eta]_l$	Intrinsic viscosities of nonlinear and linear molecules, respectively	dl.g.$^{-1}$
$[\eta]_R, [\eta]_o$	Intrinsic viscosities after and before irradiation, respectively	dl.g.$^{-1}$
μ	Correction factor for the effect of pressure, $s_p = s(1-\mu P,)$	cm.dynes^{-1}
ρ_s, ρ_o, ρ_p	Densities of solution, solvent, and polymer	g.cc.$^{-1}$
σ, γ_1	Correction factors for chain entanglements in swelling $\gamma_1 = 1 + \sigma M_{cg}$	-
W_u	Weight fraction of polymer of degree of polymerization u	-
Φ	Parameter relating the intrinsic viscosity to the root-mean-square end-to-end distance	cm.^{2}dynes^{-1}
Ω	Constant used in correcting η_o for pressure	cm.^{2}dynes^{-1}
χ	Interaction coefficient for solvent with polymer	-

χ_1, χ_2, χ_3	Coefficients in the expansion of χ as a power series in v_2	-
φ	Factor to correct v_0 for the effects of pressure	cm.^{2}dynes^{-1}
ω	Angular velocity	radians sec.$^{-1}$
ω_s	Factor used to correct swelling results for steric hindrance	-

INTRODUCTION

GENERAL

Although the effects of radiation on inorganic and small organic molecules had been studied for many years, it was only in 1952 that work began on the examination of the changes produced by radiation in organic polymers. Early in this work it was found that on exposure to radiation the chains of some polymers were joined while the chains of others were broken. The reactions producing these changes are still not completely understood.

Surprisingly little study has been devoted to the effect of radiation on the copolymer of butadiene and styrene which is the basic constituent of the synthetic rubber GR-S. Almost all previous work has been of a practical nature. It is the purpose of this thesis to examine the basic changes which occur when this polymer is irradiated in air and in vacuum, in the pure state and containing an antioxidant. The changes in solution properties are the only physical changes investigated in this work. The chemical effects studied are the amount and composition of the gas evolved, and the changes in the infrared and ultraviolet spectra.

The dominant reaction of γ radiation on GR-S is chain-joining (1). Chain-joining might have occurred during polymerization of the sample studied in the present work. The extent to which the chains of the unirradiated material are joined must be known to interpret correctly the radiation induced changes in solution properties. To determine the extent of linkage between the chains the polymer was fractionated and each fraction was characterized by weight, intrinsic viscosity, and sedimentation coefficient. These data were also used to find the molecular weight distribution of the molecules in the polymer as a further index of the extent of chain joining.

RADIATION-CHEMICAL PROCESSES

Primary Reactions:

The common property of high energy radiation whether in the form of gamma rays, beta particles, or alpha particles is the ability to produce ions in any substance exposed to this radiation. Although the energy associated with high energy radiation is greater than that binding an orbital electron to its nucleus or an atom to its neighbour, it is usually less than that required to affect the binding force within the atomic nucleus. The high energy radiation used in the work to be reported was gamma radiation from Co^{60}.

When a Co^{60} source is used to irradiate a substance almost all of the gamma radiation is dissipated by Compton scattering. This involves the inelastic collision between an incident photon and an electron of the substance. The electron is ejected while the photon continues in a different direction but with lower energy. The ejected electron is called a Compton recoil electron. Such electrons have a broad spectrum of energies and are responsible for almost all observable ionizations and all chemical changes (2). A Compton recoil electron can react with electrons of other atoms to produce ionization or excitation. An atom is said to be excited when one of its electrons is raised to a higher energy level. An electron ejected by a Compton recoil electron is known as a secondary electron. It may return immediately to the atom from which it came, or it may join a neutral molecule to produce a negatively charged molecule, or it may gradually lose its energy until it becomes a subexcitation electron which can no longer excite the type of atom from which it came. Burton et al. (3) believe that a secondary electron can rarely escape the field of the positive ion, whereas Platzman (4) claims that it almost always escapes.

The mechanism by which an irradiated molecule decomposes will determine the speed of the decomposition. According to the Franck-Condon principle (5) the time taken for an electron transition to occur is very much shorter than is needed for an appreciable change in the distance between nuclei of the irradiated molecule. Therefore, there is insufficient time for the nucleus to move into position even though the excited state may itself have a stable level and dissociation occurs in 10^{-13} second, the time of an atomic vibration. The excited level might give a stable molecule, but it might also intersect another level which allows dissociation. Under these conditions dissociation is called predissociation (6) and takes much longer than 10^{-13} second to occur. In this longer time other processes such as emission of radiation or collision may remove most of the excess energy and prevent dissociation. Internal conversion is said to occur if the excess energy is used to increase the vibrational energy of the molecule. A process similar to pyrolysis may occur if the vibrational energy is sufficiently high. If the electron shift of the molecule has been from an inner level, a molecule which has energy in excess of that required for ionization will result. If this excess energy is transferred internally to another electron energy level to give ionization, the process is called preionization (6). But preionization will be absent if the excess energy is lost by other processes.

Because all electrons in a molecule are equally likely to be affected by radiation, the probability of dissipating energy in a particular part of a molecule is proportional to the electron density in that region. Therefore, primary events in a given molecule will occur at random. This consideration led Burton (3) to state the "principle of non-specificity" as follows:

"Where special chemical factors can be neglected, the nature and quantity of the products resulting from irradiation are determined by the nature and number of parent groups which are present in the molecule of the irradiated substance."

When the principle is applied to the production of, say, methane molecules from a compound, the number of methane molecules is determined by the number of methyl groups in the compound. Thus, in the homologous series of aliphatic hydrocarbons the ratio of methane to hydrogen produced is almost a linear function of the ratio of the methyl and hydrogen groups in the parent molecule. Generally, however, "special chemical factors" prevail and the principle is not followed. One cause of specificity is energy transfer from one part of a molecule to another. Another cause is related to the nature of aromatic groups; in a molecule such as benzene electronic resonance stabilization will cause any activated state to lose its energy through internal conversion. In the solid phase the Franck-Rabinovitch cage will encourage two radicals formed following a carbon-carbon bond break to unite, and then specificity might appear to occur in the solid phase to a much greater extent than it in fact does.

Ions and excited molecules produced by radiation are located close to the path, or "track", of the ionizing particle or photon. The average energy loss by the photon or particle per unit path is known as the linear energy transfer, LET, and is expressed in kilovolts per micron. Its value depends on the energy and type of radiation. The low value of 0.20 found (7) for the Compton recoil electrons of gamma rays implies that the ions and excited states are spaced quite far apart along the track. Chemical yields which depend on the initial interaction of active species should increase with increasing LET, whereas products caused by free radicals which have escaped initial recombination will be most abundent for low LET radiation.

According to Chapiro (8) secondary electrons produced in the track of a Compton recoil electron can ionize three or four molecules and excite an equal number before becoming subexcitation electrons, and about ten active species will be enclosed in a small volume of less than ten molecules in diameter. Such sites of dense ionization and excitation are called spurs or clusters. Diffusion and reaction will rapidly decrease the concentration of active molecules in spurs.

Even though the individual reactions produced in a system may not be known, the sensitivity of the substance may be expressed in terms of the number of changes produced by a given radiation dose. The G value is the number of chemical changes of a given nature produced per 100 e.v. absorbed.

Ionization or excitation of a polymer molecule may render it unstable and thus cause decomposition. The resulting fragments might then react with each other or with neutral molecules producing new molecules which might be unstable. Excited molecules often decompose into radicals. An ion frequently breaks into two fragments, an ion and a radical. For polymers, no dependence of products on LET has been found.

The energy absorbed in a polymer can be calculated from the time of exposure, the intensity of the radiation, the electron density of the sample, and the sample thickness. The unit of radiation flux most often used is the roentgen. It is defined as the quantity of X or gamma radiation such that the associated corpuscular emission for 0.001293 grams of air produces, in air, ions carrying one e.s.u. of electricity of either sign. If the energy absorbed per ion pair formed in air is 34 e.v., then the energy absorbed per roentgen is 88 ergs per gram of air (9). For gamma radiation from Cobalt-60 the energy absorbed per gram of any substance is directly proportional to the number of electrons per gram. Therefore, if the intensity in roentgens per hour is known the number of ergs absorbed per gram of substance per hour can be calculated provided the electron density is also known. The amount of energy absorbed is expressed in rads, one rad being equal to an energy absorption of 100 ergs per gram. The thickness of of the samples used in this work was small enough to have a negligible effect on intensity.

In many of the theoretical calculations predicting changes in the solution properties of polymers by radiation it is assumed that such changes occur at random throughout the polymer. Because of the space between tracks and between groups of active molecules in the tracks this will be true only above a dose of 500 rads for gamma radiation. Doses much greater than this were used in this work.

Reactions of Irradiated Molecules

The various reaction mechanisms proposed for irradiated polymers are in many instances developed from and supported by reactions in simple organic compounds. For example, radiation induced chain-joining and chain degradation in polymers are closely related to condensation and scission in low molecular weight organic substances; similarly, double bond formation and gas evolution occur during radiation of either kind of molecule.

The degree of chain joining and degradation caused by irradiation of a pure polymer in a vacuum has been found to be directly proportional to the radiation dose, and is independent of the radiation intensity (10,11). Any mechanism proposed to explain chain-joining or chain-degradation must account for these two characteristics. Temperature dependence, and the great protective effects of small amounts of certain additives must also be considered in any such mechanism. Proposed mechanisms fall into four groups: (a) those based on an ionic reaction, (b) those assuming a combination of two mobile radicals produced independently, (c) those in which two adjacent radicals are formed directly or indirectly as a result of a single ionization or excitation, and (d) those involving the reaction of a radical with a double bond which was in the molecule initially or was produced by the radiation.

To differentiate between these mechanisms the yield and composition of the gases evolved on irradiating a polymer, the changes in infrared and ultraviolet spectra, and the effect of additives on these properties must be investigated. Studies of the changes in solution properties induced by radiation will not differentiate between these mechanisms, but such studies may reveal the effect of radiation on the hydrodynamic shape of the molecule. A classification of radiation reaction mechanisms based on changes in molecular shape, but incorporating the other classification given above, will now be presented. Each mechanism will be considered separately.

Degradation:

Miller and Lawton (12) suggested that vinyl polymers degrade when two side chains are attached to a single carbon, but crosslink when a carbon atom has only a single or no side chain. There are exceptions to this generalization, and for polymers other than the vinyl type no general rule can be applied. To explain this generalization Miller proposed that fracture followed by disproportionation would occur when a hydrogen is removed by an irradiation process from a tertiary carbon atom, because resonance stabilization is impossible for this type of atom. Wall (13) considers the cause of degradation to be steric hindrance rather than lack of resonance stabilization.

Cyclization:

If two units of the same molecule join together, a loop will be formed. Dole et al. (14) have obtained experimental evidence for cyclization, and have given several possible explanations for cyclization.

Endlinking:

If the end of a molecule joins to a point other than the end of another molecule a trifunctional link, or endlink, is formed. Davison (15) claims that some of the products he obtained on irradiating low molecular weight organic compounds can only be explained by such a reaction. He suggests that both thermal and highly excited radicals, R^{*}, known as "hot" radicals, may be formed. The latter arise from the decomposition of an ion, followed by recapture of an electron by an ionized fragment.

$$R_1R_2 \rightsquigarrow R_1R_2^{+} + e \longrightarrow R_1\cdot + R_2^{+} + e \longrightarrow R_1\cdot + R_2^{*}$$

$$R_2^{*} + R_3H \longrightarrow R_2H + \cdot R_3$$

$$\cdot R_3 + \cdot R_1 \longrightarrow R_1R_2$$

The sign $\rightsquigarrow$ designates a primary radiation chemical process. The reaction of an end radical of one molecule with another molecule will give an endlink. Dole (14) proposes that if a molecule ends with a vinyl, the following reaction may occur.

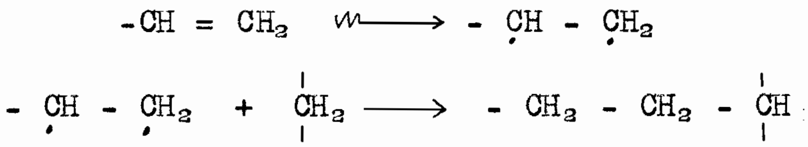

$$-CH = CH_2 \rightsquigarrow -\underset{\bullet}{CH} - \underset{\bullet}{CH_2}$$

$$-\underset{\bullet}{CH} - \underset{\bullet}{CH_2} + \overset{|}{\underset{|}{CH_2}} \longrightarrow -CH_2 - CH_2 - \overset{|}{\underset{|}{CH}}$$

Crosslinking:

A crosslink is formed when a point other than an end-point of one molecule joins to a similar point of another molecule. The most frequently employed mechanism involving thermal radicals is (16):

$$R_1H \rightsquigarrow R_1\cdot + H\cdot$$

$$R_2H \rightsquigarrow R_2\cdot + H\cdot$$

$$R_1\cdot + R_2\cdot \longrightarrow R_1R_2$$

$$H\cdot + H\cdot \longrightarrow H_2$$

A mechanism based on "hot" radicals is (16):

$$R_1H \rightsquigarrow R_1^{*}\cdot + H\cdot$$

$$R_1^{*} + R_2H \longrightarrow R_1R_2 + H\cdot$$

$$H\cdot + H\cdot \longrightarrow H_2$$

In the first mechanism the radicals must be mobile so that they can come together and react, or the hydrogen radical must be "hot" so that it can abstract a hydrogen very close to $R_1\cdot$ and permit the two R radicals to immediately join (17).

The mechanism advocated by Dole for endlinking can be used for crosslinking if the vinyl group is not at the end of the chain (14).

Another mechanism (18) involving unsaturation is that a positive charge formed during irradiation will migrate along the chain to a double bond, and enter a more stable energy state by association with the double bond. Neutralization of such an olefin ion would release sufficient energy to break at least two carbon hydrogen bonds. If hydrogen abstraction reactions followed at least four radicals close to the unsaturated group would be produced. Probably two of the radical sites would be on the olefin molecule. Intermolecular combination would then give a crosslink.

Unsaturation occurs if a hydrogen radical, liberated by radiation, abstracts a second hydrogen from an adjacent carbon. Some of this unsaturation may be removed by hydrogenation (19). For olefins a critical figure for unsaturation has been found to be about one double bond per twenty carbon atoms (20). Below this degree of unsaturation, exposure to radiation increases the degree of unsaturation, while above it, the unsaturation is decreased.

A simple ionic mechanism has been proposed by Weiss (21).

$$\begin{aligned} R_1H &\rightsquigarrow R_1H^+ + e \\ R_1H^+ + R_2H &\longrightarrow R_1R_2 + H_2^+ \\ H_2^+ + e &\longrightarrow H_2 \end{aligned}$$

or

$$\begin{aligned} R_1H &\rightsquigarrow R_1H^+ + e \\ R_1H^+ + R_2H &\longrightarrow R_1R_2^+ + H_2 \\ R_1R_2^+ + e &\longrightarrow R_1R_2 \end{aligned}$$

Double bond formation may also occur.

$$- CH_2 - \overset{+}{CH_2} - CH_2 - \longrightarrow - CH_2 - CH = CH - + H_2^+$$

Libby adversely critized Weiss's theory on thermochemical grounds, and suggested several ionic mechanisms of his own (22). The primary reaction suggested by Libby is:

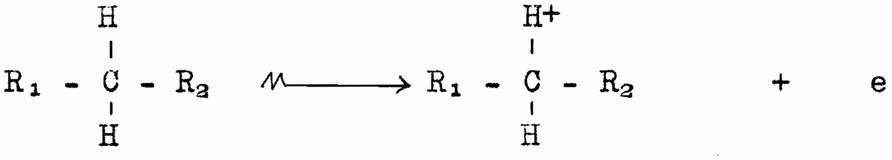

$$R_1 - \underset{H}{\overset{H}{C}} - R_2 \rightsquigarrow R_1 - \underset{H}{\overset{H+}{C}} - R_2 + e$$

Three different reactions may now occur. According to the first suggested reaction the ion radical can abstract a hydrogen atom.

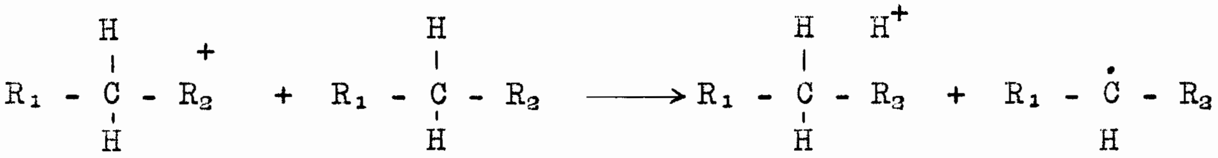

$$R_1 - \underset{H}{\overset{H}{C}} - \overset{+}{R_2} + R_1 - \underset{H}{\overset{H}{C}} - R_2 \longrightarrow R_1 - \underset{H}{\overset{H}{C}} - \overset{H^+}{R_2} + R_1 - \underset{H}{\dot{C}} - R_2$$

An electron can then interact with the positive ion:

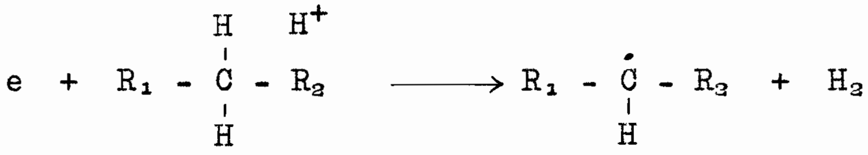

$$e + R_1 - \underset{H}{\overset{H}{C}} - \overset{H^+}{R_2} \longrightarrow R_1 - \underset{H}{\dot{C}} - R_2 + H_2$$

and the two radicals may then join to give a crosslink. The second possibility suggested by Libby is ion radical decomposition to give a hydrogen radical and a carbonium ion. The latter then reacts as follows:

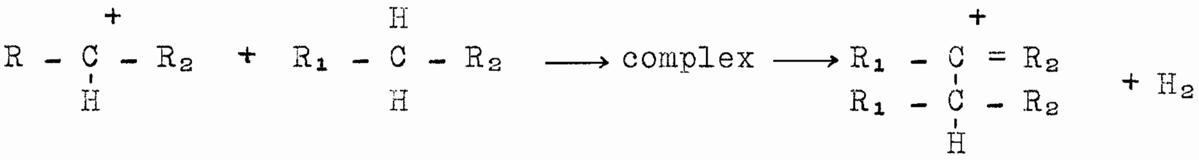

$$R-\overset{+}{\underset{H}{C}}-R_2 + R_1-\overset{H}{\underset{H}{C}}-R_2 \longrightarrow \text{complex} \longrightarrow \begin{matrix} R_1-\overset{+}{C}=R_2 \\ R_1-\underset{H}{C}-R_2 \end{matrix} + H_2$$

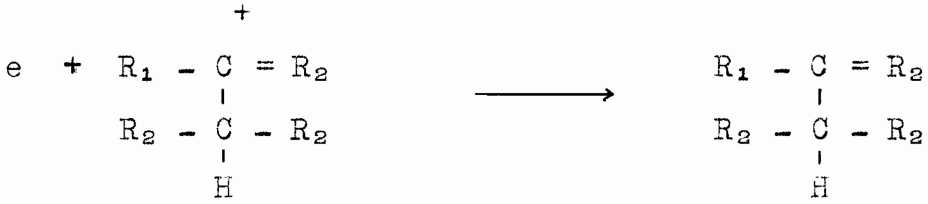

$$e + \begin{matrix} R_1-\overset{+}{C}=R_2 \\ | \\ R_2-\underset{H}{C}-R_2 \end{matrix} \longrightarrow \begin{matrix} R_1-C=R_2 \\ | \\ R_2-\underset{H}{C}-R_2 \end{matrix}$$

The final reaction possibility of Libby's is that the hydrogen radical resulting from ion radical decomposition abstracts a hydrogen from a neighbouring neutral molecule to give a radical which can join with the radical produced when the carbonium ion is neutralized. Libby calculates that the chance of the hydrogen atom abstraction occurring close to the radical formed on neutralization is very small, because the hydrogen radical will diffuse away quickly. If the hydrogen radical is "hot" this difficulty is overcome. The carbonium ion is extremely electrophilic, and should therefore react rapidly with olefins. In such a case, no hydrogen will be evolved because of the presence of the double bond.

Crosslinking by a Chain Reaction:

In the case of crosslinking by a chain reaction a single ionization or excitation will give rise to more than one link. Pearson suggests the following reaction (23):

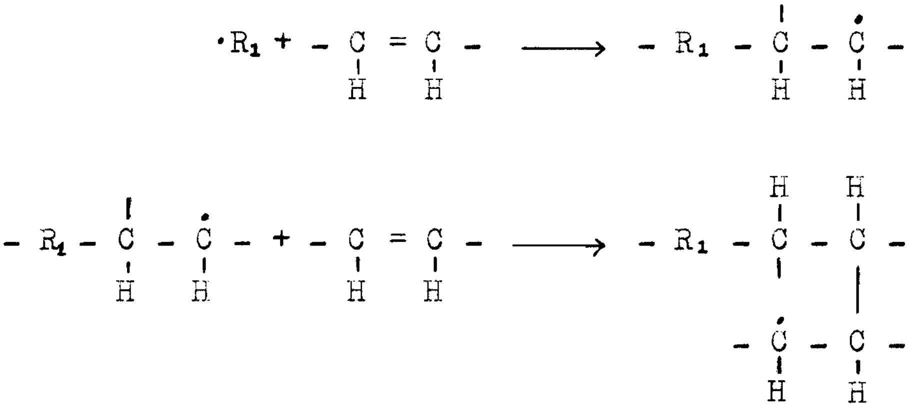

$$\cdot R_1 + -\underset{H}{C}=\underset{H}{C}- \longrightarrow -R_1-\underset{H}{\overset{|}{C}}-\underset{H}{\dot{C}}-$$

$$-R_1-\underset{H}{\overset{|}{C}}-\underset{H}{\dot{C}}- + -\underset{H}{C}=\underset{H}{C}- \longrightarrow \begin{array}{cccccc} & & H & & H & \\ & & | & & | & \\ -R_1 & - & C & - & C & - \\ & & | & & | & \\ & - & \dot{C} & - & C & - \\ & & H & & H & \end{array}$$

The resulting radical can then attack another double bond, and so form the basis for a chain reaction. Either a vinylene double bond or a vinyl double bond might be involved in such a reaction.

With low molecular weight olefins it has been found that the energy required per crosslink decreases with increasing unsaturation, but not by as much as would be expected if a chain reaction occurred (24). The gas yield was less in this case than for a saturated compound. These results suggest that after one radical joins to a double bond the resulting radical is destroyed by a hydrogen radical, and no chain reaction occurs.

Isomerization:

Golub (25) found that on irradiating pure polybutadiene an equilibrium cis-trans ratio of about one to four was attained after a certain critical dose dependent on the initial cis-trans ratio.

Protection

Internal protection will occur if a component of a molecule protects the rest of the molecule from radiation. On the other hand, external protection will occur if one or more molecules is protected by another molecular species.

Aromatic groups within a molecule are particularly effective as internal protectors; their range of protection extends to four or five surrounding atoms (26,27). Because the protector is removing energy from surrounding atoms one would expect that it would be more sensitive to radiation than when irradiated in its pure form. This appears to occur in the case of vinyl groups in polethylene where they act as protectors (17). A group within a molecule can protect surrounding atoms by energy transfer only if it has excited states lying energetically lower than those of the atoms it is to protect. A similar criterion applies in the case of charge transfer except ionized rather than excited states are involved (28).

Several different mechanisms may operate in external protection. One definite possibility is energy transfer from the polymer to the protective agent. For this to occur the difference in excited state levels must be the same as in the case of internal protection (28). Here no chemical change occurs in the polymer, but the protector might be destroyed, or it might rid itself of the excess energy by heat or radiation emission. The time required for the energy transfer to occur depends on the transfer mechanism, and determines which reactions will be prevented. A slow process such as predissociation might be inhibited, but the fast process of direct dissociation will not.

Rather than trap electronic excitation energy, an additive may promote distribution of the initially localized energy among vibrational and rotational degrees of freedom of the polymer molecules. This is a quenching mechanism. A quencher may also enhance another mode of decomposition. Usually but not always the quencher is chemically unchanged (28).

Crosslinking, endlinking or, one of the other mechanisms mentioned above, can be prevented if the protector rapidly repairs the damage in the polymer following a radiation induced chemical change, by replacing an electron or hydrogen removed from the polymer by one of its own. The additive must have ionized states lying lower than those of the polymer if charge transfer is to occur. This type of protection might cause the decomposition of the additive.

The additive might trap, rather than donate, electrons. If neutralization then occurs between the negatively charged additive and the positively charged polymer molecule, the resulting excited polymer molecule might have less energy and hence might be more stable than if neutralization was by a free electron (28).

Finally the entire additive might join a polymer radical or ion and thereby prevent crosslinking or the other reactions. If B represents a solute or additive molecule, the following reaction could occur:

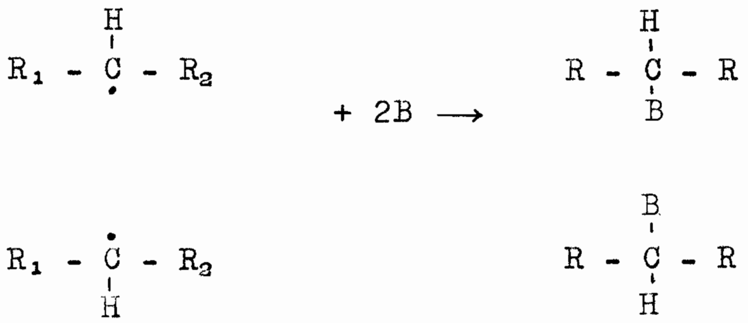

$$\begin{matrix} R_1 - \overset{H}{\underset{\bullet}{C}} - R_2 \\ \\ R_1 - \overset{\bullet}{\underset{H}{C}} - R_2 \end{matrix} + 2B \longrightarrow \begin{matrix} R - \overset{H}{\underset{B}{C}} - R \\ \\ R - \overset{B}{\underset{H}{C}} - R \end{matrix}$$

Effects of Oxygen

The presence of oxygen may cause an increase or a decrease in either degradation or crosslinking depending on the polymer. Very few polymers are insensitive to oxygen during irradiation. Apart from protecting the polymer from radiation by being an efficient electron acceptor, oxygen can oxidize the polymer as in the absence of radiation (29). Alexander and Toms (30) proposed that an oxygen molecule combines with an electron to give an ion which can attack the polymer. Oxidation might also occur by an excited molecule combining with oxygen.

If immediately following irradiation in vacuo, the polymer is exposed to air and if radicals formed during irradiation are trapped within the polymer, these radicals will react with oxygen of the air. This type of oxidation has been observed with several polymers (31).

SOLUTION PROPERTIES OF SOLUBLE POLYMERS

The radiation induced changes in the solution properties of the polymer will be markedly dependent on the molecular weight distribution and the degree of nonlinearity in the polymer before irradiation. The theoretical background necessary to evaluate the effect of these two variables will now be given.

Molecular Weight Averages

In general the molecules of a polymer sample cover a wide range of molecular weights. Ideally, the description of a polymer sample would include the specification of the entire distribution of molecular weights, but for practical reasons only certain averages molecular weights are used.

M, the molecular weight of a molecule and u the degree of polymerization are related by the equation

$$M = uw$$

where w is the weight of a monomer unit. If n(M) represents the number of polymer molecules of molecular weight M, the number average molecular weight can be defined by

$$\bar{M}_n = \frac{\Sigma n(M)M}{\Sigma n(M)}$$

and the weight average molecular weight by

$$\bar{M}_w = \frac{\Sigma n(M)M^2}{\Sigma n(M)M}$$

Generally the form of the distribution is not known, and any finite number of average molecular weights can correspond to an infinite number of distributions.

Fractionation

All fractionation techniques are based on the premise that the solubility of a homogeneous polymer fraction decreases with molecular weight. In fractional precipitation the addition of a nonsolvent to a solution of a polydisperse polymer progressively precipitates fractions of decreasing molecular weight. Fractionation may also be produced by a reduction in solubility by cooling. The fraction of polymer molecules of a particular chain length remaining in the dilute phase has been related to the ratio of the volume of the precipitate to that of the supernatant phase (32). This relation shows that the fractionation is most efficient if the starting solution is very dilute and small fractions are collected. Schulz's (33) theoretical fractionation using eight fractions and a very dilute starting solution shows considerable overlap of the molecular weight distributions of the fractions. Refractionation will sharpen the fractions somewhat; but as shown theoretically there will always be a "head" and a "tail" to each fraction (33).

Configuration and Dimensions of a Linear Polymer Molecule

A polymer molecule consists of a large number of bonds all of which are connected together by atoms to form a single unit. These bonds are generally known as statistical elements or segments. One valuable way of describing the configuration of such a molecule is in terms of a segment density distribution about the center of gravity of the polymer coil. Flory showed that the segment density will be Gaussian in form if the effect of the volume excluded by each segment to other segments in a polymer chain is not taken into account, and effects of polymer-solvent interaction are ignored (34).

Under special conditions the excluded volume effect will be exactly compensated by polymer-solvent interaction. In what is known as a good solvent, the energy of interaction between a polymer element and an adjacent solvent molecule will exceed the mean of the energies of interaction between the polymer-polymer and solvent-solvent pairs. In such a solvent a molecule will tend by expansion to reduce the frequency of contacts between pairs of polymer elements. In a poor solvent, polymer-polymer contacts will be favoured, and the molecule will contract. Because solvent power is temperature dependent the excluded volume effect will be exactly compensated by this tendency to contract at a unique temperature, the theta temperature, for a given polymer in a given solvent. A polymer molecule at the theta temperature is said to be unperturbed.

Although no experimental method will give detailed information about the molecular configuration, certain average dimensions can be obtained. One such average dimension is the root-mean-square end-to-end distance denoted by $\sqrt{\overline{r^2}}$ for a perturbed and by $\sqrt{\overline{r_0^2}}$ for an unperturbed molecule. These two dimensions have been related by Flory (35) in the equation

$$\sqrt{\overline{r^2}} = \alpha \sqrt{\overline{r_0^2}}$$

where α is the excluded volume factor. This α factor is related to temperature and theta temperature, the molecular weight and density of polymer, and the molar volume of the solvent. A modified relation between $\sqrt{\overline{r^2}}$ and $\sqrt{\overline{r_0^2}}$ has been proposed by Kurata et al.(36) which is in better agreement with experiment close to the theta temperature than Flory's relation. At temperatures well above the theta temperature Flory's theory gives better agreement then Kurata's.

Relation of Molecular Dimensions to Hydrodynamic Properties

Before examining several of the many theories relating hydrodynamic properties to molecular dimensions, the definitions of some hydrodynamic solution properties will be given.

The intrinsic viscosity, $[\eta]$, represents the contribution of the dissolved polymer to the viscosity of the solution, η . If η_o is the viscosity of the solvent the relative viscosity, η_r, is η/η_o, and the specific viscosity, η_{sp}, is (η_r-1). On dividing the specific viscosity by the concentration, c, in grams per 100 ml. of solution, the reduced viscosity η_{sp}/c is obtained. The reduced viscosity is related to the intrinsic viscosity by

$$\lim_{c \longrightarrow 0} (\eta_{sp}/c) = [\eta]$$

The sedimentation coefficient may be defined by

$$s = \frac{dX/dt}{\omega^2 X} \qquad \text{...........} \quad (1)$$

where dX/dt is the velocity at which the molecule sediments, and ω^2X is the centrifugal field. Because s is concentration dependent the value of the sedimentation coefficient at zero concentration s_o is usually employed.

The frictional properties of dilute solutions can be studied in terms of the "molecular frictional coefficient", f. This coefficient is defined by the equation

$$F' = Nfv_f$$

where F' is the force opposing the motion of a mole of molecules moving through the solution with a velocity v_f and N is Avogadro's number. At zero concentration f becomes f_o.

The coefficients f_o and s_o can be related by the Svedberg equation (37)

$$s_o = \frac{M(1-v_o \rho_o)}{Nf_o} \quad \text{........ (2)}$$

where v_o is the polymer partial specific volume at zero concentration and ρ_o is the density of the solvent.

The hydrodynamic properties have been related to the polymer chain dimensions by considering model systems. One of the first models to be proposed was a free-draining coil. In this model the chemical groups are considered to be beads which offer individual hydrodynamic resistance to the flow of the solvent. It is assumed that the beads are small and widely separated and the solvent can stream through the molecule. Only a few real molecules even approximate this model.

A more realistic model provides for the trapping of solvent within the molecule. As the number of segments in the chain increases the disturbance of flow by peripheral beads becomes so large that the beads in the interior do not interact with the exterior solvent. Brinkman, Debye and Bueche (38,39) and Kirkwood and Riseman (40) developed hydrodynamic theories in which the trapping of solvent was considered. Even though somewhat different models were used in the two theories, both theories led to identical equations relating intrinsic viscosity and molecular weight.

$$[\eta] = KM^{a} \qquad \text{...........} \; (3)$$

where K is a constant for a given polymer in a given solvent, and a varies from 0.5 to 1.0 as M increases from zero to infinity. Peterlin (41) found that in the range of M generally studied the changes in coil permeability are very small and therefore a is constant.

Mandelkern and Flory (42) introduced the equivalent hydrodynamic sphere model. This consists of an impermeable sphere of such a radius that it is identical to the actual molecule in frictional and viscosity properties. Assuming the radius of this equivalent sphere, the effective hydrodynamic radius, to be proportional to the root-mean-square end-to-end distance of the polymer molecule, Flory (43) derived

$$f_o = \eta_o P(\overline{r_o^2})^{1/2} \qquad \text{..........} \ (4)$$

where P is a "universal" constant the value of which depends on the ratio of the effective hydrodynamic radius to $\sqrt{\overline{r_o^2}}$.
According to Flory the intrinsic viscosity is

$$[\eta] = \Phi \left[\frac{(\overline{r_o^2})}{M} \right]^{3/2} M^{1/2} \quad \alpha^3 \qquad \text{......}(5)$$

where Φ is another "universal" constant. This equation is equivalent to equation 3 because α is directly proportional to M raised to some power. On combining equations 2, 4, and 5 one obtains

$$\frac{s_o\,[\eta]^{1/3}}{M^{1/3}} = \frac{(\Phi)^{1/3}\,(P)^{-1}\,(1-v_o\,\rho_o)}{\eta_o\,N} \qquad \text{.......} \ (6)$$

Theoretically, $(\Phi)^{1/3}\,(P)^{-1}$ should be a constant equal to 2.11×10^6 if the same equivalent sphere can be used for both f_o and intrinsic viscosity (43). It has been found experimentally to be a constant, but with a value (44,45) of 2.5×10^6, applicable to flexible chain molecules. For hard spheres it has been calculated (46) to be 2.12 x 10^6, and for long rod-like molecules it may be greater than 2.5 x 10^6.

Although Flory's theory agrees more closely with experimental data than the other theories mentioned, there is still considerable experimental evidence that shows the Flory treatment to be not entirely correct. Krigbaum and Carpenter (47) found that ϕ decreased as the "goodness" of the solvent increased. Throughout the Flory theory it is assumed that the polymer segment density at any temperature is approximately Gaussian in form. Several theories hold that this assumption is incorrect, and is the main cause of the discrepancy between theory and experiment (17,47,48). Despite these objections, Flory's theory, uncorrected for non-Gaussian effects, will be used in the present work.

Concentration Dependence of Viscosity and Sedimentation

Since hydrodynamic properties reflect the behavior of individual molecules only at infinite dilution, experimental data on viscosity and sedimentation rate must be extrapolated to zero concentration before such data become unequivocal.

The most general expression for relating viscosity to concentration (49) is

$$\frac{\eta_{sp}}{c} = a_1 + a_2c + a_3c^2 \qquad \text{......} \; (7)$$

Equation 7 is most commonly employed in the form

$$\frac{\eta_{sp}}{c} = [\eta] + k'[\eta]^2 c \qquad \ldots\ldots\ldots(8)$$

provided c is low. The constant k' is known as the Huggins constant, and for a given solvent, temperature, and polymer, its value is generally constant (50).

The intrinsic viscosity can also be obtained from the extrapolation to zero concentration of the plot of $\ln \eta_{r/c}$ versus c. In this case the viscosity equation has the form

$$\frac{\ln \eta_r}{c} = [\eta] - \beta[\eta]^2 c \qquad \ldots\ldots\ldots(9)$$

MacFarlane and McLeod have shown that k' must be close to 0.3 if this equation is to be used (51).

According to Cragg and Bigelow, the value of the coefficient a_2 of equation 7 reflects the long-range hydrodynamic interaction of pairs of single molecules, the formation of doublets, and intermolecular attraction or repulsion (52). Simha (53) showed that long-range interaction of single molecules depends partly on the nature of the units of the polymer and their arrangement, and on the density of the coil which the molecule forms. This density factor in turn depends on intramolecular attraction, density of branching, solvent, and temperature. A doublet makes a contribution because it dissipates more energy than two isolated spheres (54). Probably triplets and larger aggregates contribute to the higher terms in equation 6.

Jones (55) has shown experimentally that the effect of molecular orientation on k', although often neglected, can be important in certain instances.

The concentration dependence of the sedimentation coefficient has not been examined either experimentally or theoretically as thoroughly as has the concentration dependence of viscosity. The empirical equation generally used to describe the variation of s with c for flexible chains is

$$s = \frac{s_o}{1 + k_s c} \qquad \ldots\ldots\ (10)$$

where the value of the coefficient k_s increases with molecular weight (56).

The theories of Burgers (57) and Flory (43) have been used (58) to derive a relationship between k_s and the intrinsic viscosity.

$$\frac{k_s}{[\eta]} = 1.66 \qquad \ldots\ldots\ (11)$$

The value 1.66 includes the quantity $(\Phi^{1/3} P^{-1})^{-3} = (2.5 \times 10^6)^{-3}$. The validity of this equation is in doubt since many experimental results (59) support this equation while others (60,61) do not.

The Effect of Polydispersity

The relation between intrinsic viscosity and molecular weight given in equation 3 was first suggested by Mark and Houwink (62,63). The experimental values of a and K can be obtained from viscosity studies on a series of monodisperse fractions of known molecular weight. When the equation is applied to a polydisperse sample a viscosity average molecular weight is obtained. This may be defined as (64)

$$\bar{M}_v = \left[\frac{\sum n(M)M^{1+a}}{\sum n(M)M}\right]^{1/a} \qquad \text{.........} \quad (12)$$

Obviously, $\bar{M}_v$ will have a value between $\bar{M}_n$ and $\bar{M}_w$, unless a = 1, in which case $\bar{M}_v = \bar{M}_w$. Because $0.5 < a < 1$, $\bar{M}_v$ will be closer to $\bar{M}_w$ than to $\bar{M}_n$.

The molecular weight obtained when equation 2 is applied to a polydisperse sample is denoted by $\bar{M}_{\eta s}$. The value of $\bar{M}_{\eta s}$ relative to $\bar{M}_v$ and $\bar{M}_w$ will depend on the analytical technique employed in determining the value of s_o.

Cragg's theory (52) predicts that the Huggins constant, k', is not affected by polydispersity provided k' involves only hydrodynamic interaction. A definite relationship between k' and polydispersity is predicted by Tompa (65). There is a considerable amount of experimental evidence both for (66,67), and against (68,69) such a dependence.

Wales and Van Holde (58) claim that k_s in equation 10 is characteristic of the low molecular weight components, and therefore, $k_s/[\eta]$ should decrease with increasing polydispersity because $[\eta]$ is close to being a weight average value.

Effect of Nonlinearity

Monodisperse Sample:

It is obvious that the root-mean-square end-to-end distance of a nonlinear molecule will be less than that of a linear molecule of the same molecular weight. This fact in conjunction with equations 2, 4, and 5 indicates that $[\eta]$ will be less and s_o will be greater for the nonlinear molecule. Using the subscripts b and l to denote nonlinearity and linearity, the ratio of the root-mean-square end-to-end distance of a linear molecule to that of a nonlinear molecule is given by

$$g = \frac{\sqrt{(\overline{r_o^2})_b}}{\sqrt{(\overline{r_o^2})_l}} \qquad \text{........(13)}$$

where g has been related to the number of trifunctional or tetrafunctional units per molecule (70). A trifunctional unit corresponds to a branch or an endlink, while a tetrafunctional unit corresponds to a crosslink unit. A crosslink involves two crosslink units.

Combining equation 13 with 5 yields at the theta temperature

$$\frac{[\eta]_b}{[\eta]_1} = g^{3/2} \quad \text{........} \quad (14)$$

where $[\eta]_b$ and $[\eta]_1$ are the intrinsic viscosities of a nonlinear and a linear molecule respectively of the same molecular weight. This equation does not agree very satisfactorily with experimental data (71) since it tends to exaggerate the effect of nonlinearity. Stockmayer and Fixman (72) attributed this exaggeration to the root-mean-square radius not being simply related to the hydrodynamic behavior of the molecule when the shape of the molecule is changed, since the form of the segment distribution is changed. The effective hydrodynamic radius will be less sensitive to nonlinearity than is the root-mean-square radius. The theory of Stockmayer and Fixman gives the ratio

$$\frac{[\eta]_b}{[\eta]_1} = h^3 \quad \text{.........} \quad (15)$$

where h is related to g. A recent theory by Zimm and Kilb (73) predicts that

$$\frac{[\eta]_b}{[\eta]_1} = g^{1/2} \quad \text{..........} \quad (16)$$

Both equations 15 and 16 are derived from modifications of the Kirkwood and Riseman theory. Two other theories, one by

Bueche (74) and the other by Kotliar and Podgar (75,76), agree fairly closely with equation 16. The relationship between $[\eta]_b/[\eta]_1$ and the number of tetrafunctional units per molecule, m, for several of these theories in shown in Fig. 1.

Although the individual values of ϕ and P vary with nonlinearity the product $(\phi)^{1/3}(P)^{-1}$ does not, since the powers to which these quantities are raised result in a cancellation of the nonlinearity effect. Experiments with branched dextran support this (77). Therefore the following equation can be written.

$$\frac{(s_o)_b\,[\eta]_b^{\;1/3}}{M_{\eta s}^{\;2/3}} = (\phi)^{1/3}\,(P)^{-1}\,\frac{(1 - v_o\,\rho_o)_b}{N\eta_o} \quad \ldots . \; (17)$$

In this equation it can be assumed that $(1 - v_o\,\rho_o)_b$ is equal to $(1 - v_o\rho_o)_1$. Therefore, if $M_{\eta s}$ is the same for the linear and nonlinear material then

$$(s_o)_1[\eta]_1^{\;1/3} = (s_o)_b\,[\eta]_b^{\;1/3} \quad \ldots\ldots \; (18)$$

On combining equations 1, 2, and 3, the equation

$$(s_o)_1 = K_s\,[\eta]^{\gamma} \quad \ldots\ldots \; (19)$$

is obtained, where K_s and γ are analogous to the corresponding terms in equation 3. Substituting equation 19 into 18 gives

$$K_s\ [\eta]_l^{(3\gamma + 1)/3} = (s_o)_b\ [\eta]_b^{1/3} \qquad \text{......} (20)$$

Therefore, if $(s_o)_b$ and $[\eta]_b$ are known for a monodisperse fraction of nonlinear polymer, then from known values of K_s and γ the value of $[\eta]_l$ for the nonlinear polymer can be obtained from equation 20. From the ratio $[\eta]_b/[\eta]_l$, m is obtained from Fig. 1. If a polymer is fractionated and m is found for each of the fractions, the weight average value of m for the unfractionated material, m_w, can be calculated.

Even though many investigations have been made on the relation between the Huggins constant, k', and the degree of nonlinearity, no definite conclusions have yet been reached. It would be expected that a greater density of the coil of a nonlinear molecule would cause k' to be higher than for a linear molecule of the same molecular weight and composition. Because the value of k' depends on the outer contacts of the polymer molecule with the solvent, a difference in the segment density distribution of a nonlinear and linear molecule should become particularly important if the difference is near the outer surface of the molecule. The Huggins constant, k', has

Fig. 1

Intrinsic viscosity as a function of degree of nonlinearity according to three theories.

■ Zimm-Kilb (73)
● Stockmayer-Fixman (72)
▲ based on equation 14

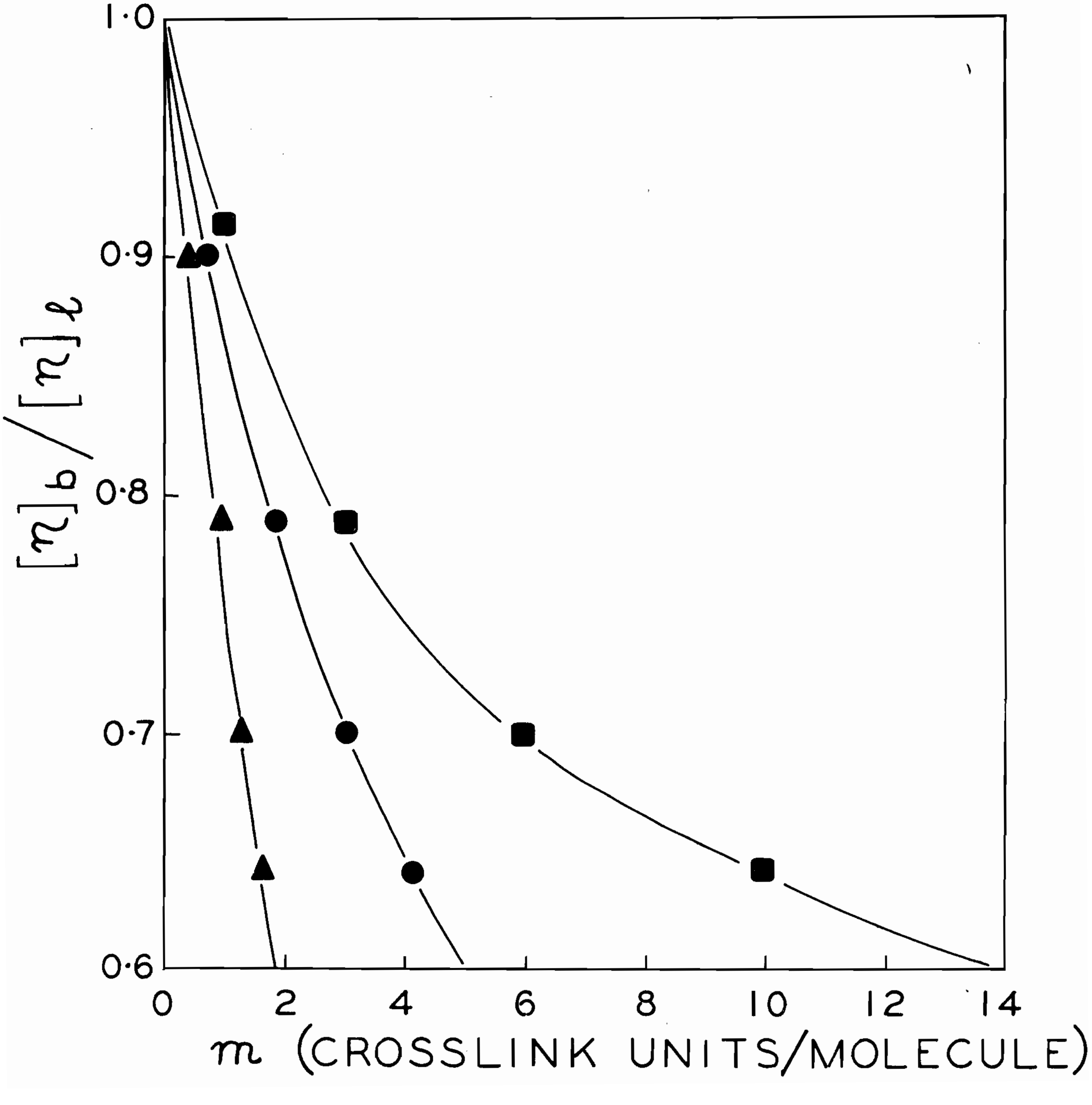
1·0
0·9
0·8
0·7
0·6
$[\eta]_b / [\eta]_\ell$
0
2
4
6
8
10
12
14
m (CROSSLINK UNITS/MOLECULE)

been found to increase with increasing nonlinearity so frequently (68,59,78-83) that it is tempting to conclude that a definite relation exists between the two. Experiments have been reported however, in which k' does not increase with nonlinearity (84,85).

The results of Moore, Greear, and Sharp (86) indicate that k_s is slightly less for a nonlinear molecule than for a linear molecule of the same molecular weight.

Polydisperse Sample:

A polymer sample may be heterogeneous in molecular weight, in distribution of branches on molecules, in length of branches, and in functionality of the branch units. The last two factors have been shown to have only a very small effect on solution properties (73).

The random, or "most probable", molecular weight distribution, M.W.D., is the distribution most frequently found for linear polymers. It is a special case of the Schultz-Zimm distribution (87). If W_u is the weight fraction of polymer of degree of polymerization u, then the Schultz-Zimm distribution may be expressed as

$$W_u du = \frac{z^{(j+1)} u^j e^{-zj}}{\Gamma(j+1)} du \qquad \ldots\ldots\ldots(21)$$

where $z = \frac{j}{\bar{u}_n} = \frac{j+1}{\bar{u}_w} = \frac{1}{\bar{u}_v} \frac{[\Gamma(j+1+a)]^{1/a}}{[\Gamma(j+1)]^{1/a}}$ and $\bar{u}_n$, $\bar{u}_w$, and $\bar{u}_v$ denote number, weight, and viscosity average degrees of polymerization respectively. When the parameter j is equal to one, equation 21 describes a random, or "most probable" distribution.

Random crosslinking will occur if the probability that any given structural unit become a crosslink unit is independent of the other units in the same molecule. Molecules may become randomly crosslinked either during or after polymerization. If random crosslinking is imposed on a polymer with a random molecular weight distribution, the distribution will be broadened according to the theories of Stockmayer (88), Saito (89), and Kotliar (75). Stockmayer's theory applies only to an initial random molecular weight distribution, but the other theories apply to the other types of distributions as well. The theories of Stockmayer and Kotliar give

$$\frac{\bar{M}_w}{\bar{M}_n} = \frac{2 - \delta/2}{1 - \delta} \qquad \ldots\ldots\ (22)$$

where δ is the crosslinking coefficient, the number of crosslinked units per weight average primary, or initial, molecule. When the molecules of a sample have become highly crosslinked, some will no longer be soluble. The point at which insolubility begins is the gelation point. The gelation point corresponds to a value of unity for δ. The weight average number of crosslinked units per molecule, m_w, is related to δ by the equation

$$m_w = \frac{\delta}{1 - \delta} \qquad \ldots\ldots\ldots (23)$$

To distinguish the values of δ, $\bar{M}_w$ and $\bar{M}_n$ of the irradiated polymer from those of the unirradiated polymer the symbols δ_o, $\bar{M}_{wo}$ and $\bar{M}_{no}$ will be used for the unirradiated polymer. Furthermore, the symbols $\bar{M}_{woo}$ and $\bar{M}_{noo}$ will be used to denote the respective weight and number averages of the primary linear molecules.

There are three methods which can be employed to determine the value of δ_o. In the first method the values of $\bar{M}_{wo}$ and $\bar{M}_{no}$ can be obtained from light scattering and osmometry, respectively, and δ_o found from equation 22. In the second method the value of the ratio $\bar{M}_{wo}/\bar{M}_{no}$ can be obtained from the experimentally determined molecular weight distribution and so found from equation 22. In the third method the polymer can be fractionated and the degree of crosslinking in each fraction obtained from equation 20 and

Fig. 1, and m_w is thus obtained and finally δ_o from equation 23. Two assumptions are made in applying these methods; that crosslinking is random, and that it is imposed on a random molecular weight distribution.

RADIATION INDUCED CHANGES IN SOLUTION PROPERTIES

As already mentioned, any one or any combination of the following reactions might occur on irradiating a polymer: degradation, endlinking, cyclization, crosslinking, and crosslinking by a chain reaction. The manner in which changes in solution properties occur with irradiation aids in distinguishing between these possibilities, and indicates to what extent they occur for a given dose of radiation. These changes also provide an experimental test of many theories of polymer properties.

Viscosity

Unless specifically stated otherwise the theories on polymer irradiation to be discussed assume that either degradation or crosslinking, or the two simultaneously, occur on irradiating a polymer, and that these changes are imposed on a random initial molecular weight distribution. In these theories the two processes are treated as independent; first degradation occurs and then crosslinking. One other assumption inherent in the theories is that δ_o is zero, implying that all the molecules of the unirradiated material are linear. Each of the theories relates the change in $[\eta]$ on irradiation to three distinct factors: the effect of the nonlinearity of the molecules, the effect of the change in molecular weight and the effect of the change in molecular weight distribution.

Before discussing each theory the nomenclature commonly employed must be given. The gelation dose, R_g, is the dose of radiation in megarads corresponding to the gelation point. R is the dose in megarads. $[\eta]_R$ and $[\eta]_o$ are the intrinsic viscosities after and before irradiation, respectively. The term a' is from the equation

$$[\eta]_o = K_1 \bar{M}_w^{\ a'} \qquad \text{........(24)}$$

The symbols, q_o and p_o represent the number of crosslinked units and breaks per chain unit per unit dose respectively. If no degradation occurs then p_o/q_o is zero, and R/R_g is δ (90).

Schultz, Roth, and Rothman (90) use the Stockmayer-Fixman theory (72) to relate the effect of nonlinearity to viscosity, and another theory by Stockmayer (88) to relate the effect of the change in the molecular weight and the M.W.D. to viscosity. Schultz's theoretical results are shown in Fig. 2 for a' = 0.7. The maximum which appears in some of the theoretical curves is perculiar to this theory.

Fig. 2

Effect of radiation on intrinsic viscosity according to Schultz' theory.

● $p_o/q_o = 0$

○ $p_o/q_o = 0.4$

□ $p_o/q_o = 1.0$

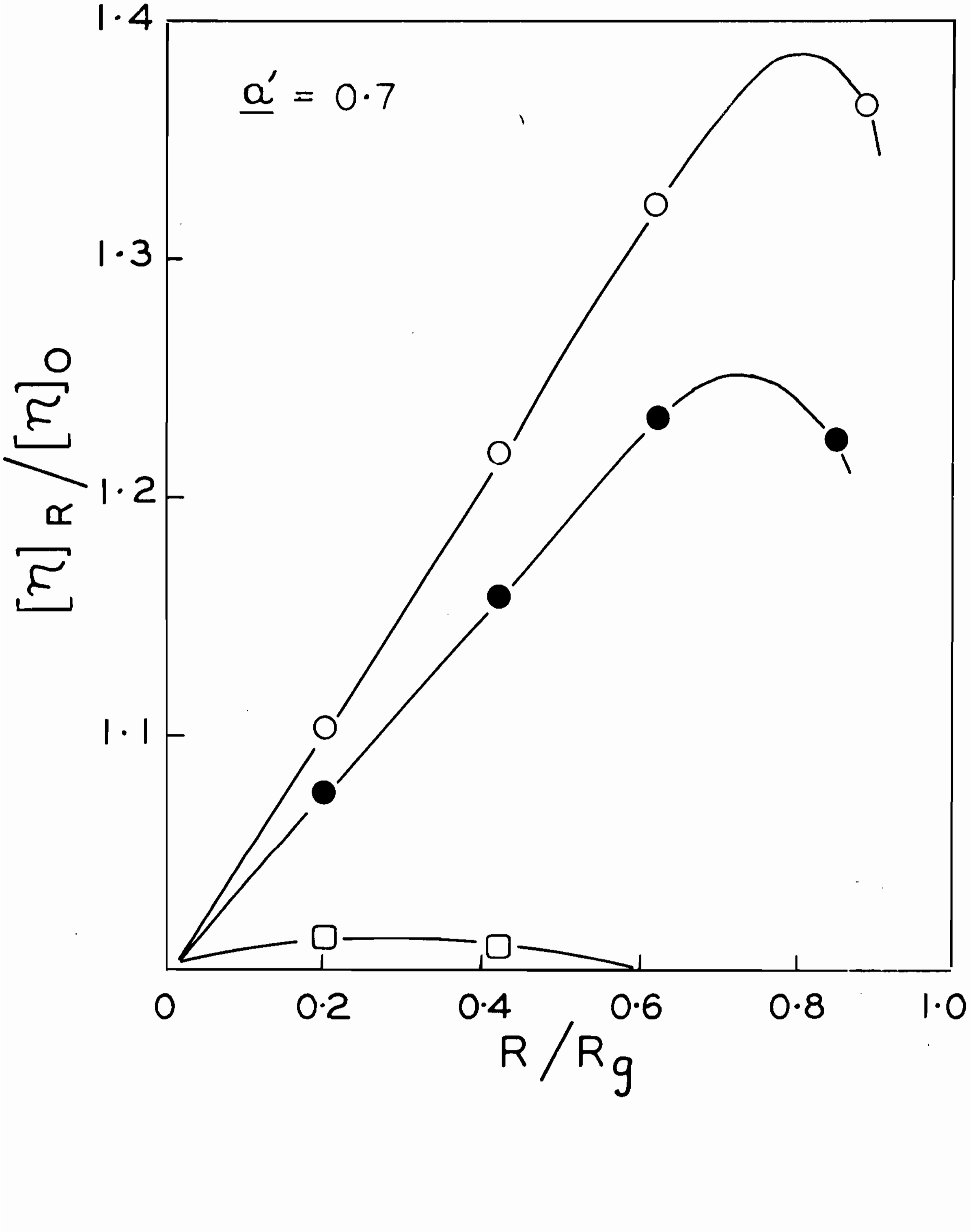

$\underline{\alpha}' = 0{\cdot}7$
1·4
1·3
1·2
1·1
$[\eta]_R / [\eta]_O$
0
0·2
0·4
0·6
0·8
1·0
R / R_g

Kilb (91) bases his theory on the ratio

$$\frac{[\eta]_b}{[\eta]_l} = g^{1/2} \qquad \text{.......} \ (16)$$

and on a modification of the Stockmayer molecular weight distribution theory. The theoretical curves given in Fig. 3 show the effect of both p_o/q_o and a on the relation of viscosity to dose.

Using equation 16 but their own distribution theory Kotliar and Podgor (75) obtained theoretical curves similar to Kilb's, except a smaller increase is predicted in $[\eta]_R/[\eta]_o$ at low values of R/R_g and a greater increase is predicted at high values, particularly if p_o/q_o is greater than zero. Unlike others, Kotliar and Podgor have calculated changes for several kinds of initial molecular weight distributions. According to these authors the increase in intrinsic viscosity with dose is reduced if the M.W.D. is narrowed.

The curves in Fig. 4 are from Katsuura's theory (92). He used a modified Debye-Bueche theory for viscosity, and theories by Karaoka (93) and Saito (89) for changes in molecular weight and molecular weight distribution. Dole (94) has severely critized Saito's theory (89), and therefore indirectly Katsuura's.

Fig. 3

Effect of radiation on intrinsic viscosity according to Kilb's theory.

– – – $\underline{a} = 0.75$

——— $\underline{a} = 0.68$

······ $\underline{a} = 0.50$

○ $p_o/q_o = 0$

△ $p_o/q_o = 0.5$

□ $p_o/q_o = 1.0$

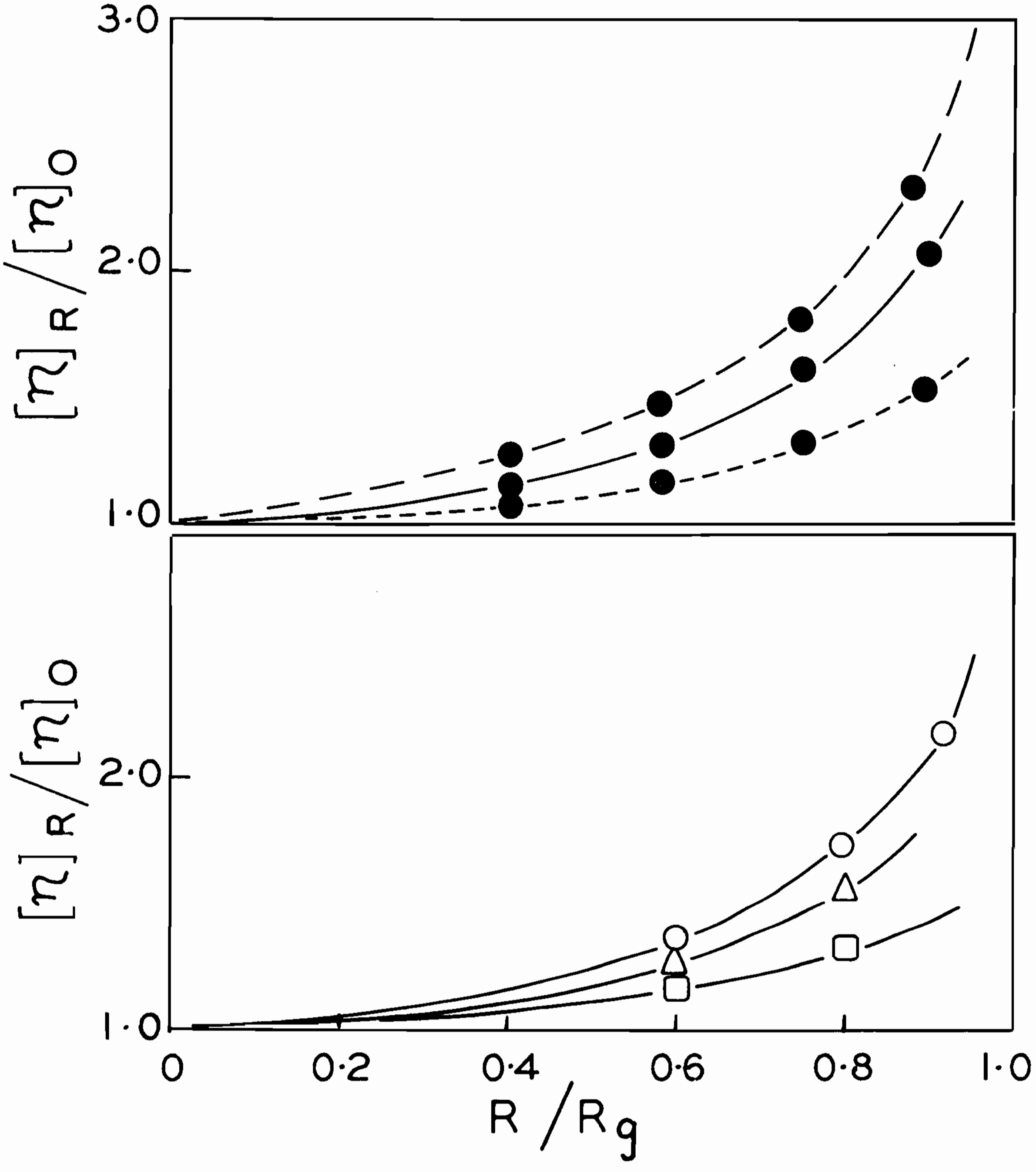
3·0
2·0
1·0
$[\eta]_R/[\eta]_0$
2·0
1·0
$[\eta]_R/[\eta]_0$
0
0·2
0·4
0·6
0·8
1·0
R/R_g

Fig. 4

Effect of radiation on intrinsic viscosity according to Katsuura's theory.

— — — $a = 0.8$

——— $a = 0.7$

.... $a = 0.6$

○ $p_o/q_o = 0$

□ $p_o/q_o = 1$

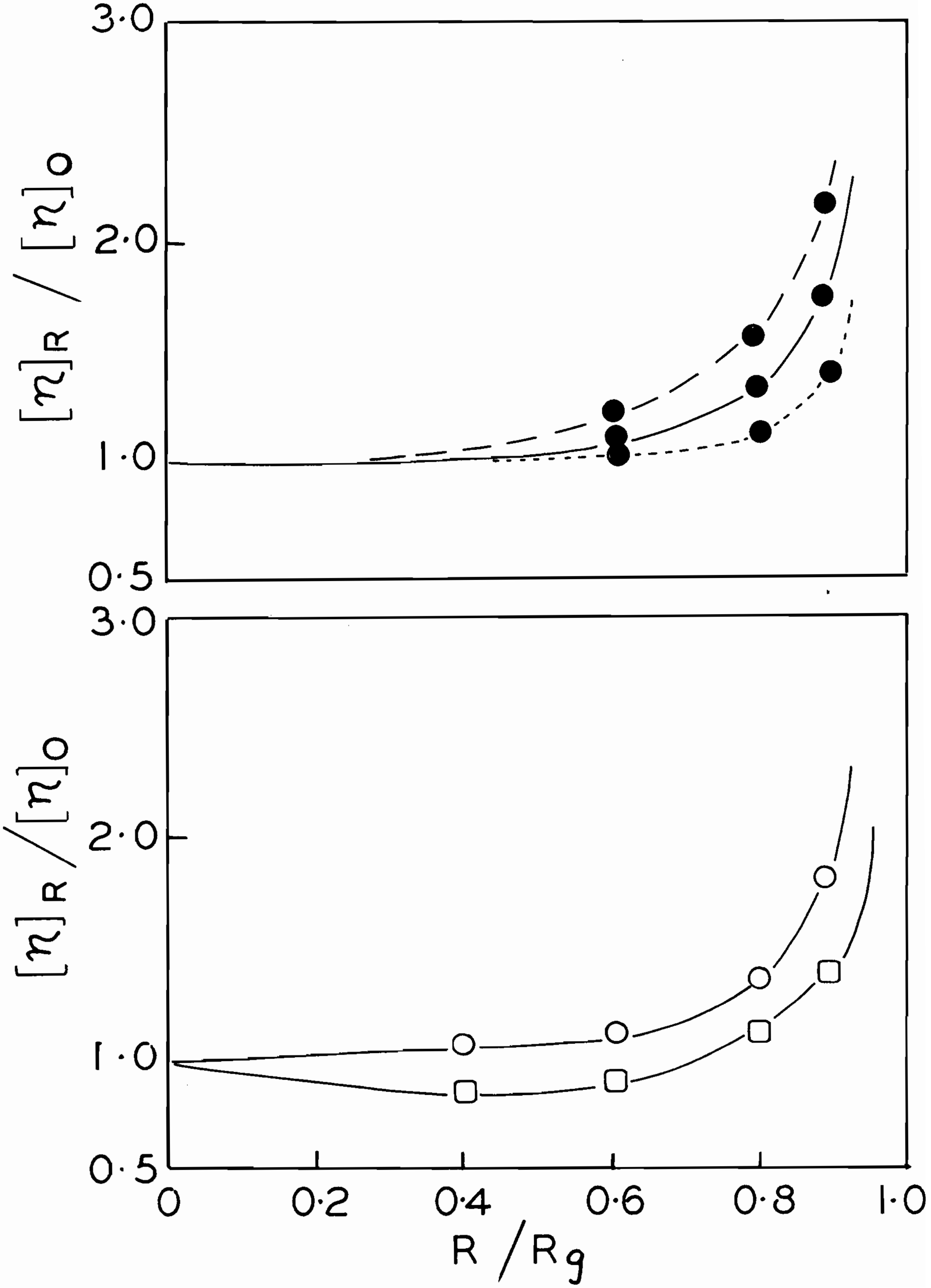
3·0
2·0
1·0
0·5
[η]R / [η]o
3·0
2·0
1·0
0·5
[η]R / [η]o
0
0·2
0·4
0·6
0·8
1·0
R / Rg

These theories provide a further method for the determination of δ_o. If crosslinking alone occurs, and the initial molecular weight distribution is a random one, then (95)

$$\bar{M}_{no} = \frac{\bar{M}_{noo}}{(1 - \delta_o/4)} \qquad \text{.......} \quad (25)$$

and

$$\bar{M}_{wo} = \frac{\bar{M}_{woo}}{1 - \delta_o} \qquad \text{.......} \quad (25a)$$

where $\bar{M}_{no}$ and $\bar{M}_{noo}$ are the number average molecular weights after and before crosslinking, respectively, and $\bar{M}_{wo}$ and $\bar{M}_{woo}$ are the corresponding weight averages. If $\bar{M}_{no}$ is obtained from osmometry then on assuming a value of δ_o, $\bar{M}_{noo}$ can be found from equation 25. For a sample of linear molecules with a random distribution the following equation can be used (87).

$$[\eta] = K\,\Gamma(2 + a)\,\bar{M}_{noo}^{a} \qquad \text{......} \quad (26)$$

where K and a are the same as in equation 2. On substituting $\bar{M}_{noo}$ in this equation an intrinsic viscosity is obtained which corresponds to the intrinsic viscosity before crosslinking. If the intrinsic viscosity of the crosslinked material is known, a ratio of the two viscosities is obtained which corresponds to the viscosity ratios of Figs. 2, 3, and 4 and therefore δ_o is found, which for no degradation is equal to

R/R_g. A successive approximation procedure is employed to obtain the correct value of δ_o.

Solubility

The treatment of changes in solubility is similar to that of changes in intrinsic viscosity, except for solubility no hydrodynamic theories are needed. Because of this the effect on the solubility of other processes than crosslinking and degradation, such as endlinking, cyclization and crosslinking by a chain reaction, have been examined. It is assumed in the treatment of solubility changes that all processes occur randomly, and crosslinking and degradation can be treated as separate events. All treatments of solubility assume δ_o to be zero, that is, the polymer before irradiation is assumed to be linear.

The analysis of solubility data is simplest if only crosslinking occurs. As the crosslinking coefficient increases above unity, the sample can be separated by solution techniques into two fractions, gel and sol. The sol is soluble in the usual solvents and contains both slightly crosslinked material and original molecules. The gel is those molecules which have been linked together to form a three dimensional network. As the dose increases the amount of crosslinking increases and so does the amount of gel. The manner in which the gel fraction, G, increases with δ can be written (95) for any initial distribution as

$$G = (1 - S) = \delta G - \frac{1}{2!}\frac{\bar{M}_z}{\bar{M}_w} \delta^2 G^2 + \frac{1}{3!}\frac{\bar{M}_4\bar{M}_z}{\bar{M}_w^{\,2}} \delta^3 G^3 \qquad \ldots(27)$$

where S is the sol fraction and

$$\bar{M}_z = \frac{\Sigma n(M)M^3}{\Sigma n(M)M^2} \qquad \text{and} \qquad \bar{M}_4 = \frac{\Sigma\, n(M)M^4}{\Sigma\, n(M)M^3}$$

For an initial random molecular weight distribution, M.W.D., equation 27 becomes

$$S + \sqrt{S} = 2/\delta \qquad \ldots\ldots\ldots (28)$$

Because the crosslinking coefficient is R/R_g if there is no degradation, the value of R_g can be obtained from extrapolating a plot of $S + \sqrt{S}$ versus $1/R$ to the point where $S + \sqrt{S} = 2$.

From the values of R_g and $\bar{M}_{wo}$ the value of the number of crosslinks formed per 100 e.v. absorbed, G_x, can be calculated. If the dose is expressed in Mrads, unit dose corresponds to the absorption of 0.624×10^{20} e.v. per gram or $1.04 \times 10^{-4}w$ e.v. per unit chain of molecular weight w. By definition, q_o crosslinked units are produced by this amount of energy. Therefore,

$$G_x = 0.48 \times 10^6 \frac{q_o}{w} \qquad \ldots\ldots\ldots (29)$$

If the crosslinking density, q, is the proportion of main chain units crosslinked by a radiation dose **R**, then

$$q = q_o R \qquad \ldots\ldots\ldots\ldots (30)$$

From equation 30 and the definition of the crosslinking coefficient, the following equation is obtained:

$$\delta = q_o \bar{u}_w R \qquad \text{......} \ (31)$$

On combining equation 31 with equation 29 for $R = R_g$ the desired equation is found to be:

$$G_x = \frac{0.48 \times 10^6}{R_g \bar{M}_w} \qquad \text{......} \ (32)$$

Only when the radiation induced process is crosslinking alone can the relation between percentage sol and R be corrected for the effect of nonlinear molecules in the unirradiated polymer. If the extent of crosslinking in the unirradiated polymer is equivalent to a dose R_o, then

$$\frac{R_o}{R_o + R_g} = \delta_o \qquad \text{........} \ (33)$$

From the deviation between the experimental results and the theoretical curves of Fig. 5 and 6, the value of δ_o can be found provided irradiation causes only crosslinking and provided the crosslinks in the unirradiated polymer have been caused by a random process. The value of % sol for a given ratio R/R_g will be greater than that corresponding to the appropriate theoretical curve of Fig. 5 because the true or effective ratio is $\dfrac{R + R_o}{R_g + R_o}$.

Fig. 5

Theoretical dependence of S on the degree of crosslinking.

— — — $\bar{M}_w/\bar{M}_n = 1$
——— $\bar{M}_w/\bar{M}_n = 2$
.... $\bar{M}_w/\bar{M}_n = \infty$
● $p_o/q_o = 0$
○ $p_o/q_o = 0.5$
□ $p_o/q_o = 1$

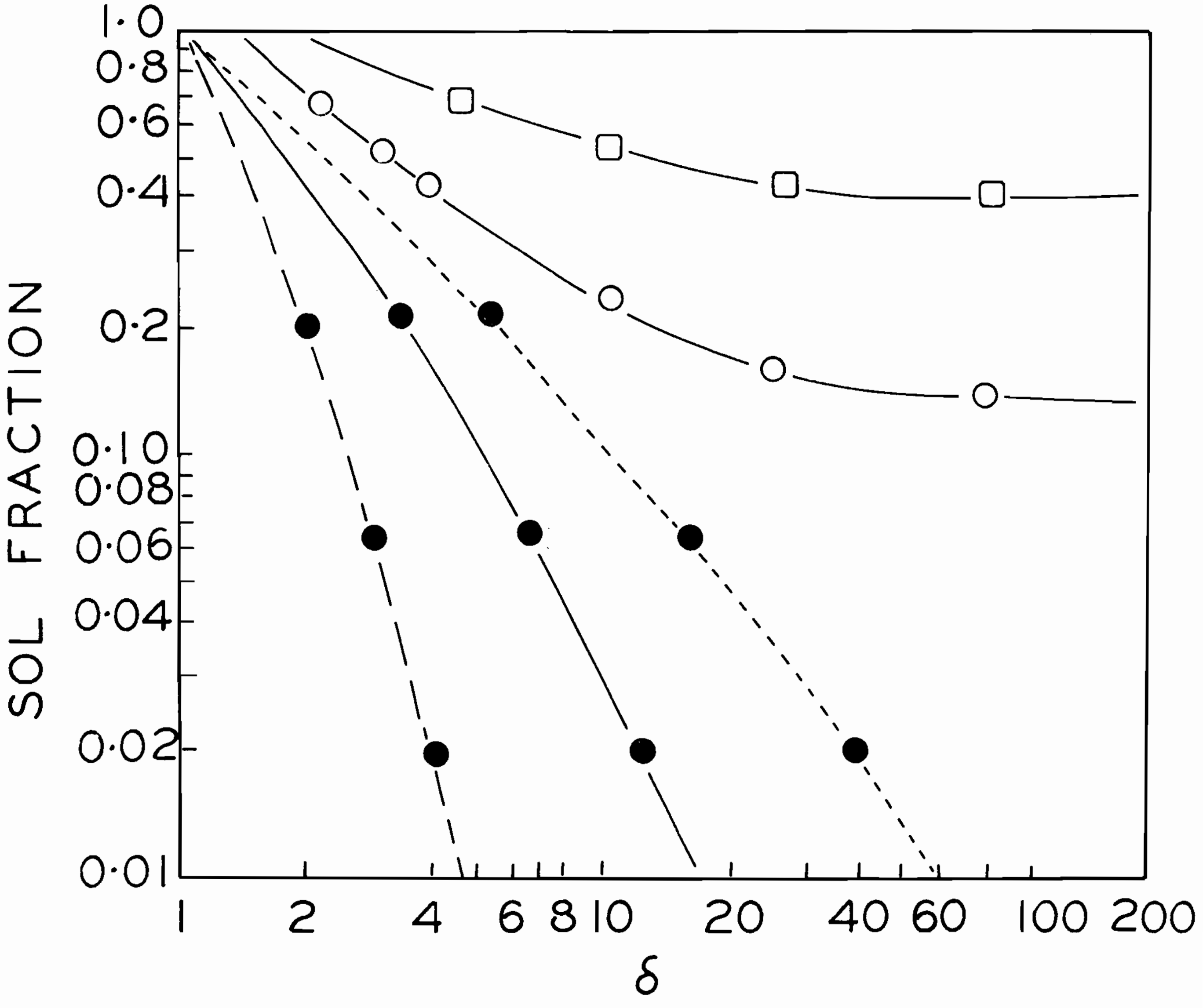
SOL FRACTION
1·0
0·8
0·6
0·4
0·2
0·10
0·08
0·06
0·04
0·02
0·01
1
2
4
6
8
10
20
40
60
100
200
δ

According to Charlesby (96), for concomitant crosslinking and degradation equation 28 can be written as

$$S + \sqrt{S} = \frac{p_o}{q_o} + \frac{1}{q_o \bar{u}_n R} \quad - \ldots\ldots (34)$$

Both p_o and q_o can therefore be obtained from a plot of $S + \sqrt{S}$ versus 1/R. G_s is the number of chain fractures or breaks per 100 e.v. and can be related to p_o and w.

$$G_s = \frac{0.96 \times 10^6 p_o}{w} \quad \ldots\ldots\ldots (35)$$

Figs. 5 and 6 illustrate two methods of plotting solubility data for different initial values of the M.W.D. and for different degrees of degradation. In the case of an arbitrary initial M.W.D. the distribution is first modified by fracture and then the effect of crosslinking is calculated using equation 27. When the number of fractures per average initial molecule is greater than about three, the plots of Fig. 6 will not be linear at low doses but will become so asymptotically as the dose increases. Therefore, at sufficiently high doses equation 34 can be applied.

Charlesby (97) has made a mathematical analysis of endlinking for the case of an initial random molecular weight

Fig. 6

Theoretical dependence of $S + \sqrt{S}$ on the degree of crosslinking.

— — — $\bar{M}_w/\bar{M}_n = 1$

——— $\bar{M}_w/\bar{M}_n = 2$

······ $\bar{M}_w/\bar{M}_n = \infty$

● $p_o/q_o = 0$

○ $p_o/q_o = 0.5$

□ $p_o/q_o = 1.0$

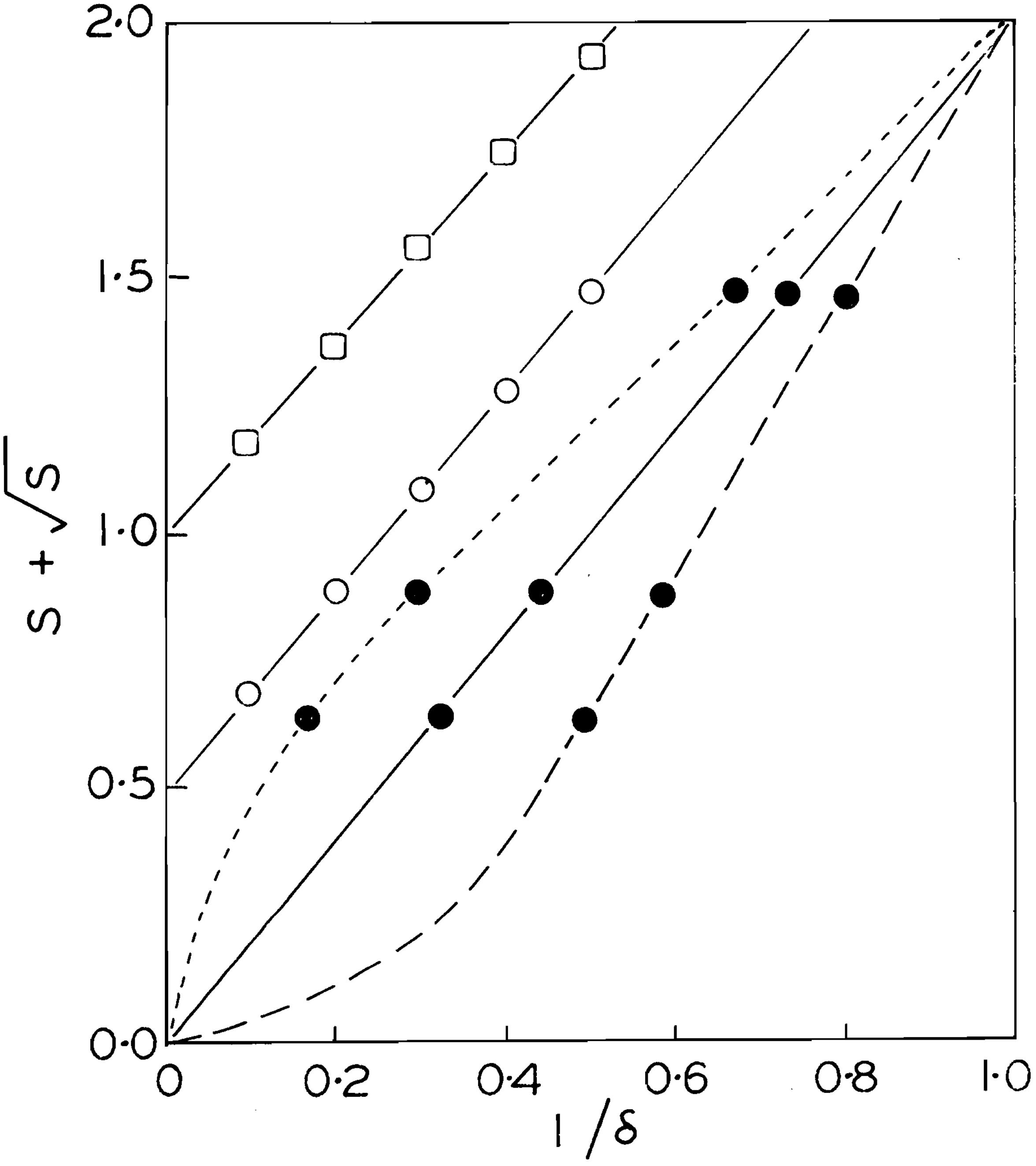
2·0
1·5
1·0
0·5
0·0
0
0·2
0·4
0·6
0·8
1·0
$S+\sqrt{S}$
$1/\delta$

distribution. He found that for such a distribution the quantitative difference in the sol versus dose curves between endlinking and crosslinking could be obscured through minor differences in M.W.D. Saito (89) has examined this problem for initial distributions of various types including a random one. For an initial random M.W.D. Saito's results agreed with those of Charlesby.

Charlesby (98) bases a mathematical analysis of crosslinking by a chain reaction on the assumption that the chain reaction is inhibited by some inherent process such as resonance stabilization, and not by termination through combination, disproportionation or chain transfer. Unlike the previous cases, log S versus R gives essentially a straight line (99). If i represents the inhibiting effect, then the average number of crosslinks formed by each chain reaction is (1 - i)/i. Charlesby's analysis (98) leads to the expressions

$$R_g = \frac{0.5 \times 10^6 \, i^2}{G_x \bar{M}_w} \quad \ldots\ldots\ldots\ldots (36)$$

$$\frac{d(\log S)}{dR} = 0.45 \times 10^{-6} \, \frac{G_x \bar{M}_n}{i} \quad \ldots\ldots\ldots\ldots (37)$$

These equations can be solved simultaneously to give i and G_x.

Saito (89) has considered the effect of simultaneous crosslinking and cyclization. The rate of increase with increasing dose of molecular weight, intrinsic viscosity and gel fraction as found for systems in which crosslinking alone occurs, will be significantly reduced in the presence of cyclization. The extent of this reduction is predicted quantitatively by his theory. There is no definite proof that cyclization ever occurs on irradiating a pure polymer in the solid state. Considering the large number of other variables the detection of cyclization by examining solution properties would be very difficult.

Swelling

The gel fraction of a crosslinked polymer will swell in a solvent to an extent determined by the density of crosslinks, the solvent, the functionality of the nonlinearity, and the temperature. There is a tendency for solvent to penetrate the gel. This mixing tendency, expressed as the entropy of dilution, may be augmented or diminished by the heat of dilution, a measure of the interaction energy between solvent and solute molecules. As the network is swollen the chains between crosslink units are elongated, and an elastic force is developed which opposes swelling. A state of equilibrium is ultimately reached. The smaller the average molecular weight between crosslinks, $\bar{M}_{cg}$, the less will be the swelling.

An expression relating $\bar{M}_{cg}$ to the extent of swelling is given by Flory (100) as

$$\bar{M}_{cg} = \frac{-\rho_p V_1 (v_2^{1/3} - 2 v_2/f_n)}{\chi v_2^2 + \ln(1 - v_2) + v_2} \qquad \text{........(38)}$$

where ρ_p is the density of the polymer, v_1 is the molar volume of the solvent, v_2 the volume fraction of polymer in the swollen gel, χ is the interaction coefficient between the polymer and the solvent, and f_n is the functionality of the units causing nonlinearity.

In a real network some chains will have free ends. On correcting for the effect of "free ends" equation 38 becomes

$$\frac{\bar{M}_{cg}}{(1 - 2\bar{M}_{cg}/\bar{M}_{nog})} = F \qquad \text{........(39)}$$

where F is the right side of equation 38, and $\bar{M}_{nog}$ is the number average molecular weight of the molecules in the gel before crosslinking. This correction by Flory (100) agrees well with experimental data (101), and is similar to the theoretical predictions of others (102, 103).

James and Guth (104) have adversely criticized Flory's theory and proposed another, and Wall and Flory (105), and Hermans (106) have criticized the theory of James and Guth. However, experimental data has been reported (107) which supports the Flory theory. Two other theories (108, 109) have been developed which agree with the Flory interpretation. None of the theories account for the excluded volume effect, an effect probably very important near a crosslink junction (106). All the theories so far proposed fail to account for the steric hindrance effect which must be present when the molecular chains connecting the crosslinks lie on top of each other.

Natural rubber chemically crosslinked to a known extent (110) has been used to test equation 39. This equation overestimated the number of crosslinks, the discrepancy being attributed to chain entanglements which result in physical crosslinks. In attempting to correct for this discrepancy, Blanchard and Wooton (111) arrived at the following equation.

$$\bar{M}_{cg} = w_s + \gamma_1 F \left(1 - 2\bar{M}_{cg}/\bar{M}_{nog}\right) \quad \ldots\ldots. \quad (40)$$

In this equation γ_1 is an entanglement factor, and ω_s a steric hindrance factor. γ_1 is related to $\bar{M}_{cg}$ by the equation

$$\gamma_1 = 1 + \sigma \bar{M}_{cg} \quad \ldots\ldots\ldots \quad (41)$$

where σ is a constant for a given system. Using Mullins (110) results for natural rubber, Blanchard and Wooton found no steric hindrance, and σ equal to 0.414×10^{-4}.

Once $\bar{M}_{cg}$ is obtained the value of the crosslinking density in the gel, q_g, can be calculated. For a gel specimen containing A' monomer units the number of crosslinked units will be q_g A'. For each primary chain there will be two free ends. Therefore, if the primary molecular weight is $\bar{M}_{nog}$, then the total number of chains is $q_gA' + A'w/\bar{M}_{nog}$ (112). Since the average length of terminal chains is the same as internal chains (112), the molecular weight of each chain, $\bar{M}_{cg}$, will be given by

$$\bar{M}_{cg} = \frac{A'w}{q_gA' + A'w/\bar{M}_{nog}} = \frac{w}{q_g + w/\bar{M}_{nog}} \quad \ldots .(42)$$

If $\bar{M}_{noo}$ is the molecular weight of the primary molecules then (113)

$$\bar{M}_{nog} = \bar{M}_{noo} \ (1 + \sqrt{S}\ ) \quad \ldots\ldots\ldots(43)$$

Substituting the equation derived by Flory (113)

$$q_g = q \ (1 + S) \quad \ldots\ldots\ldots(44)$$

in equation 42 gives q in terms of $\bar{M}_{cg}$.

$$q = \frac{(1 - \bar{M}_{cg}/\bar{M}_{nog})\ w}{(1 + S)\ \bar{M}_{cg}} \quad \ldots\ldots\ldots(45)$$

If both q and R are known, then q_o and G_x can be obtained from equations 29 and 30. If the unirradiated polymer contains nonlinear molecules then R_o must be added to R if the correct values of q_o and G_x are to be obtained. These values are compared to the corresponding values calculated using solubility results. Generally these equations are valid if only crosslinking occurs and degradation is absent.

Many experiments indicate that the interaction coefficient between solvent and polymer, χ, is not a constant (114-117), but increases with increasing v_2. This effect is particularly serious if a poor solvent is used (116). A general expression for the increase in χ is (118):

$$\chi = \chi_1 + \chi_2 v_2 + \chi_3 v_2^2 + \ldots \qquad \ldots\ldots\ldots (46)$$

where χ_1, χ_2 and χ_3, for a polymer of infinite molecular weight are 0.5, 0.33, and 0.25 respectively.

SOLUTION PROPERTIES OF THE UNIRRADIATED POLYMER

EXPERIMENTAL

Materials

The GR-S sample obtained from the Polymer Corporation, was prepared by emulsion polymerization and contained impurities of fatty acid soap, fatty acid and "Polygard" antioxidant. The Company estimated that about 20% of the polybutadiene portion was vinyl-1,2, 7% was cis-1,4, and 73% was trans-1,4. According to Binder (119) these values indicate that the polymerization was at about 5°C.

Reagent grade benzene and methanol made by Fisher Scientific Company were used as solvents in all experiments. The antioxidant obtained from Eastman Organic Chemicals was N-phenyl-β-napthylamine and will be denoted by B or $(Ar)_2NH$.

Fractionation

The following technique was used in the fractionation of the polymer sample. A solution of 15 g. of finely cut GR-S in 1500 ml. of benzene was prepared in a three liter stoppered separatory funnel maintained at 25°C in a constant temperature bath. All the components of the GR-S must have been soluble in benzene because the concentration of aliquots of the solution was found to be the same before and after filtration through sintered glass. A precipitant of 50% reagent grade methanol in benzene was added to the solution with vigorous stirring until the solution became so turbid that the stirrer shaft was not visible in the illumination of 100 watt light bulb held behind the bath. The temperature of the bath was very slowly increased, with stirring, until the cloudiness just disappeared at which point heating was stopped and the bath allowed to cool to 25°C. Stirring was then stopped, and the polymer phase allowed to precipitate for 24 hours. At the end of this period the precipitate was drawn off into a stoppered 100 ml. flask. If the precipitate was large, it was often necessary to leave the system another 24 hours after the first withdrawal and then remove the remainder of the fraction. To each precipitate 0.5 ml. of a 10% solution of antioxidant, B, in benzene was added, and the volume was made up to 100 ml. by the addition of more benzene. Exactly 30 ml. of this last solution were diluted to give a solution with the concentration suitable for viscosity measurements. To obtain the weight of each fraction, the solids content of 20 ml. of the viscosity solution was determined by a freeze drying technique. Twelve fractions were obtained in this manner.

Several partial fractionations were made to determine the quantity of precipitant necessary to assure that all fractions would be of about equal weight.

Cragg (78), used an almost identical method of fractionation, and found that none of the impurities came down with the precipitate, and that the initial 100 ml. solution of each fraction contained only 1.8% methanol.

Viscosity

A modified Ubbelohde viscometer, designed by Craig and Henderson (120) for a negligible kinetic energy correction was used to measure the intrinsic viscosity of each fraction. The instrument was clamped in a water bath maintained at 25 ± 0.05°C, and before each set of experiments the viscometer capillary was set exactly perpendicular with the aid of plumb lines in the bath. Dust was removed from the solvent, and the solution by filtration through sintered glass.

Exactly 20 ml. of solution were added to the viscometer for each set of viscosity determinations. The solution was first drawn into the capillary and allowed to efflux without timing three times, then the procedure was repeated five times with timing, or until the time fluctuated by no more than 0.02 seconds. An electric timer was used which measured to a tenth of a second. The same timing procedure was used for four serial dilutions of the sample prepared by addition of 10 ml. of benzene for each dilution. The validity of the method of dilution was established by determinations of the solids content after the final dilution. The initial concentration was such that the relative viscosity approached but never exceeded a value of two. This limitation on η_r insures that a plot of η_{sp}/c versus concentration gives a straight line.

To detect any dependence of viscosity on shear rate a four bulb viscometer was employed. It was a modified form of the suspended-level dilution capillary viscometer of Schurz and Immergut (121).

Sedimentation Velocity

Sedimentation velocity measurements were made in a Spinco Model E Ultracentrifuge equipped with Schlieren optics employing a Wölter phase plate as the opaque element. Throughout the experiments the rotor temperature was maintained at 25 ± 0.5°C, the rotor speed was 59,000 r.p.m. and the phase plate angle used was either 50° or 60°. In each sedimentation study about 12 photographs were taken at 16 minute intervals starting at some suitable time after the rotor had attained the desired angular velocity. Each fraction was examined at several concentrations between 0.7 and 0.1 g. per 100 ml. of solution. However, a few experiments were made at higher concentrations.

A double sector cell was normally employed in these experiments. This type of cell proved impractical in the studies of unfractionated polymer and of the low molecular weight fractions, since the boundary peak either took a very long time to leave the meniscus, or simply would not leave the meniscus. A synthetic boundary cell (122) was employed in these experiments. Preformed boundaries free of the meniscus are obtained by this technique. The breakthrough speed for the synthetic boundary cell employed was 2000 r.p.m. When the synthetic boundary cell was used for the low molecular weight polymer fractions reliable sedimentation coefficients could not be measured. With these fractions the preformed boundary peaks were so blurred that the position of the maximum ordinate could not be accurately determined.

RESULTS

Fractionation

The weight of polymer in each fraction is given in Table I. These results were obtained from the freeze drying experiments after correcting for the antioxident content and the volume to which the polymer was made up. The weights of fractions 2 to 11 vary between 1.385 g. and 0.765 g., but fractions 1 and 12 weigh 0.477 g. and 0.190 g., respectively. The sum of these weights is 11.76 grams. To this must be

TABLE I

Solution properties and molecular weights of the fractions and of the unfractionated polymer.

Fraction number	Weight g.	g.$^{-1}$dl.	k' g.dl.$^{-1}$	s_o x 10^{13}	$k_s/[\eta]$	$\bar{M}_v^c$x10^{-3}	$\bar{M}_v^h$x10^{-3}	$\bar{M}_{\eta s}$x10^{-3}
1	0.447	5.38	0.742	4.63	2.24	480	1,141	1,168
2	1.120	5.13	0.593	4.41	2.29	450	1,062	1,058
3	0.777	4.30	0.414	3.39	2.15	356	812	656
4	0.765	3.65	0.341	2.85	2.06	286	633	464
5	0.862	3.18	0.333	1.91	1.28	238	514	238
6	1.310	2.59	0.274	1.65	1.47	180	376	174
7	1.254	2.19	0.248	1.44	1.50	145	292	128
8	1.295	1.81	0.244	1.29	1.69	112	218	99.2
9	1.360	1.48	0.289	1.21	1.97	85.9	161	81.9
10	1.385	1.10	0.267	--	--	57.7	102	--
11	0.980	0.786	0.237	--	--	36.9	61.5	--
12	0.190	0.632	--	--	--	27.6	44.2	--
Unfractionated		2.31	0.415	1.29	0.96	165	339	106

added the impurities and a small amount of polymer remaining in solution after withdrawal of the last fraction, a total of 1.47 grams. Approximately 88% of the original material can be accounted for. The percentage of impurities in the unfractionated GR-S was found by the standard method (123) which will be discussed below. These impurities account for 6.73% of the sample, therefore about 3% of the polymer remains in solution. Since the moisture content of the GR-S was found to be negligible the loss in material must be related to adsorption of some of the polymer on the sides of the separatory funnel, and to errors in the pipette deliveries arising from the high viscosity of the polymer solutions.

Viscosity

The detailed viscosity data are given in Appendix I, Table IX. The η_{sp}/c versus c plots for all the fractions were straight lines. Fig. 7 shows the plot for fraction 4. No effect of shear rate on viscosity was found for even the highest molecular weight fraction. The results given in Table I show that intrinsic viscosity steadily decreases from fraction 1 to fraction 12. The same is true for k' for fractions 1 to 8, but the k' values for fractions 9 and 10 are between those for fractions 6 and 7. No value of k' was calculated for fraction 12 because of scatter in the plot of η_{sp}/c versus c.

Fig. 7

Plot of η_{sp}/c versus c for fraction 4.

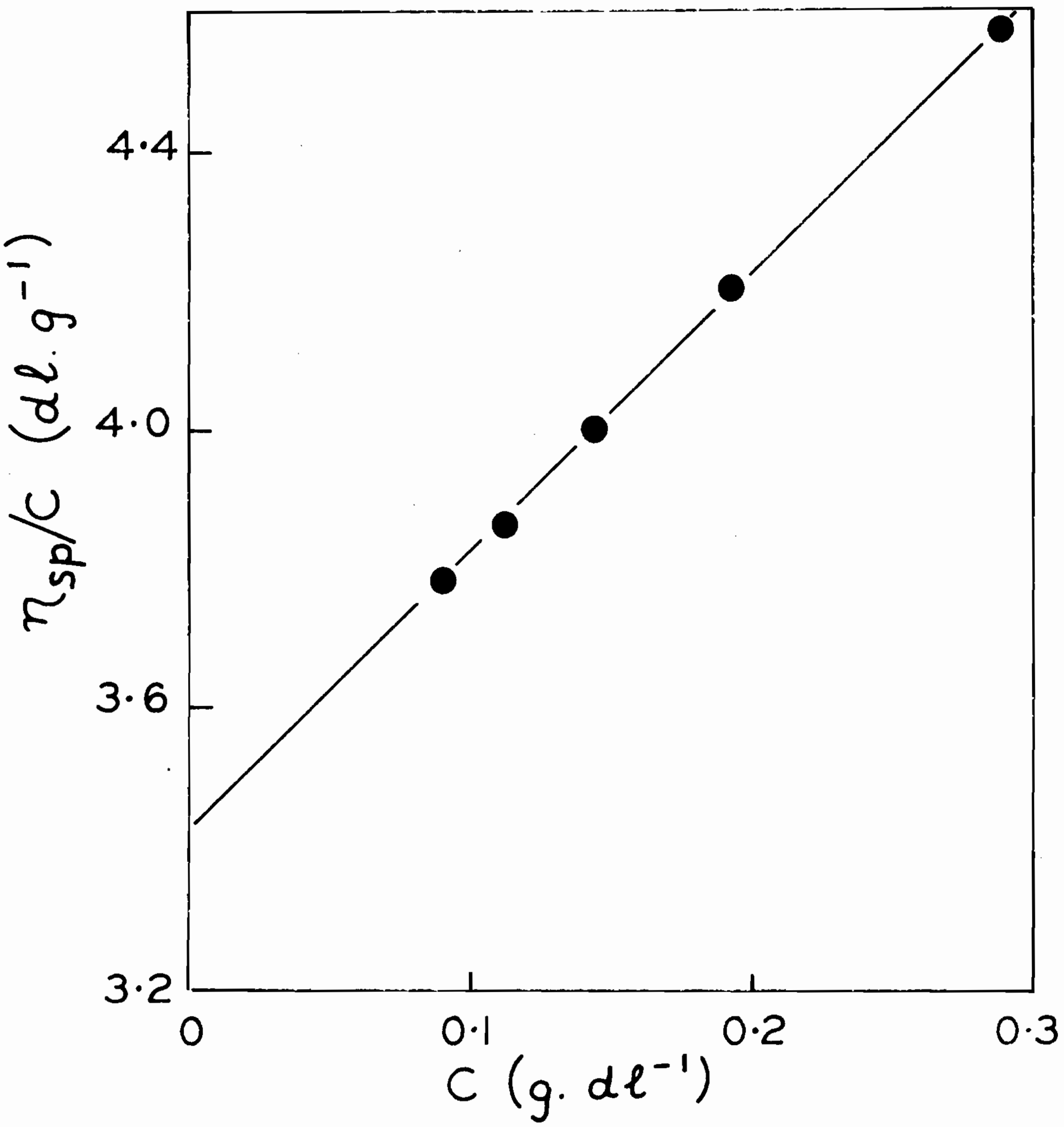

η_{sp}/C ($d\ell . g^{-1}$)
4·4
4·0
3·6
3·2
0
0·1
0·2
0·3
C ($g. d\ell^{-1}$)

For the fractions with high k' values plots of $\ln \eta_r/c$ versus c were non-linear, and on extrapolation to zero concentration higher values of the intrinsic viscosity were obtained than were found with plots of η_{sp}/c versus c. As mentioned in the introduction MacFarlene and McLeod (51) have given a reason for this discrepancy. According to these authors plots of η_{sp}/c versus c yield the correct values for intrinsic viscosity.

According to equation 7,

$$\frac{\eta_{sp}}{c} = [\eta] + k' [\eta]^2 c \qquad \text{..........} \quad (7)$$

the log of the slopes of plots of η_{sp}/c versus c versus the log of the corresponding intrinsic viscosities should give a straight line of slope two. In the plot of Fig. 8 a straight line of slope two can be drawn through the points for the five lowest intrinsic viscosity excluding fraction 12.

Sedimentation

Fig. 9 shows the single symmetrical peaks obtained using the double sector and the synthetic boundary cells. Peak movement could not be measured accurately for fractions 10, 11, and 12 because the peaks were too small and blurred.

The maximum-ordinate sedimentation coefficient, s, was found from the slope of linear plots of log X_m versus t,

<u>Fig. 8</u>

Dependence of intrinsic viscosity on the slope of η_{sp} versus c for the fractions.

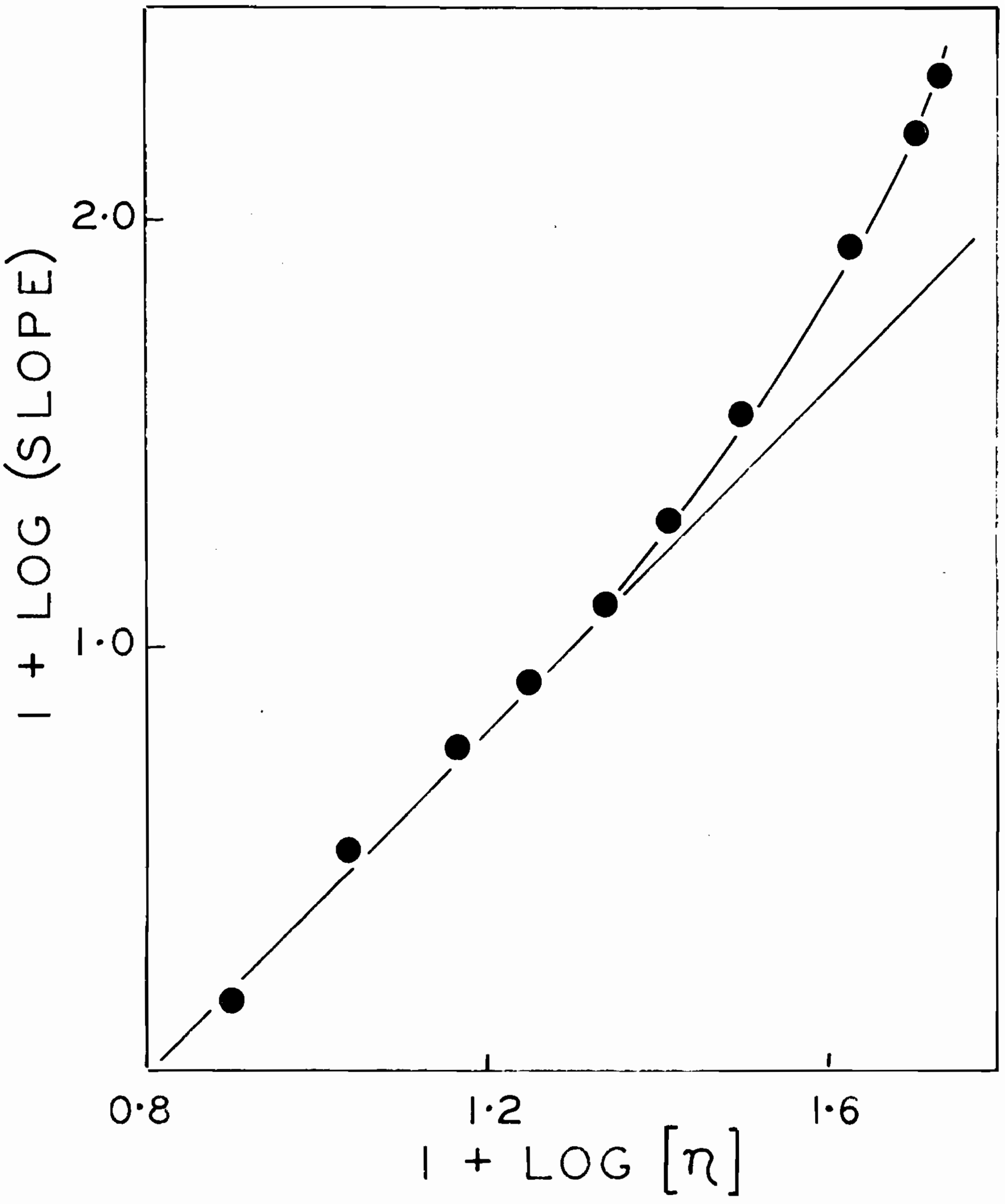
2·0
1·0
1 + LOG (SLOPE)
0·8
1·2
1·6
1 + LOG [η]

Fig. 9

Ultracentrifugation photographs.

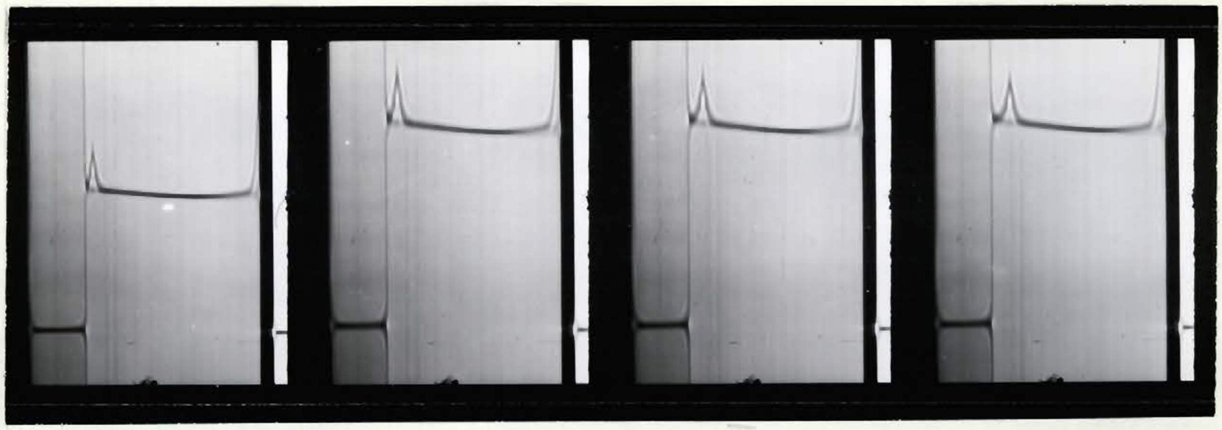

Fraction 4, Double Sector Cell

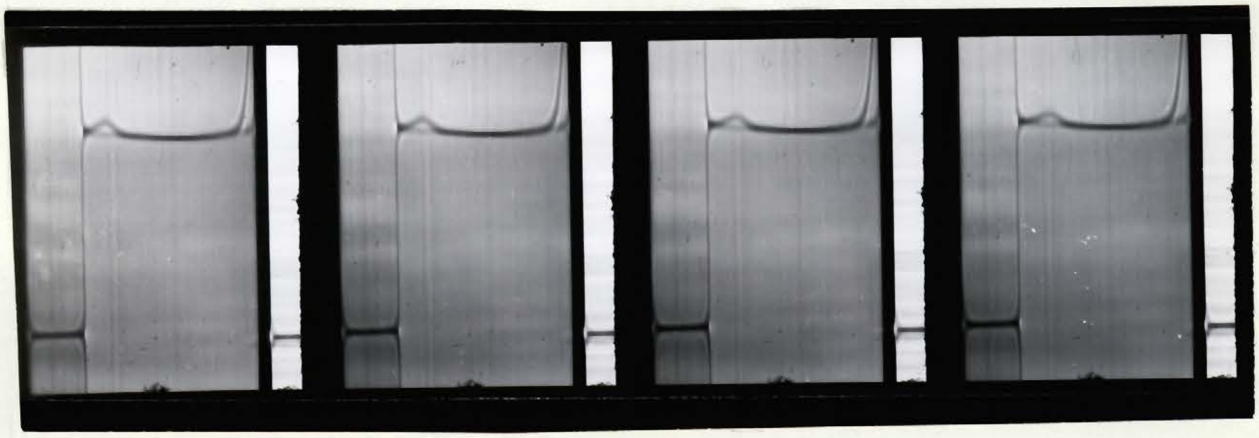

Unfractionated Polymer, Double Sector Cell

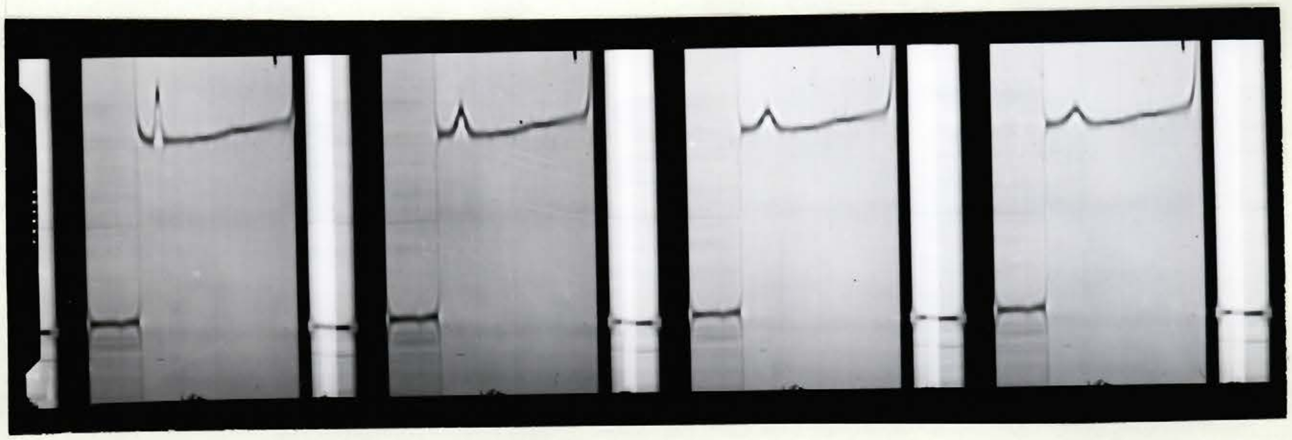

Unfractionated Polymer, Synthetic Boundary Cell where X_m is the distance of the maximum ordinate from the center of the rotor and t is the time (124). A typical plot is given in Fig. 10. Log X_m was calculated by the expression

$$\log X_m = \log \frac{(7.3 - X_1)}{2.19\ P} \quad \text{........} \quad (47)$$

where 7.3 is the distance in cm. from the bottom of the cell to the centre of the rotor, X_1 is the distance from the maximum ordinate to the centre of the rotor as measured on the photograph when viewed through an enlarger of magnification power P. The camera lens magnification power was 2.19. The value of the sedimentation coefficient, s, is obtained from the equation

$$s = \frac{1}{\omega^2} \frac{d \ln X_m}{dt} \quad \text{.........} \quad (48)$$

where ω is the angular velocity of the rotor in radians per second when t is in seconds.

The dependence of s on concentration, c, for fraction 4 is shown in Fig. 11. Similar plots were obtained for the other fractions. Extrapolation to zero concentration gives $1/s_o$. Values of s_o and $k_s/[\eta]$ are given in Table I, and detailed results are shown in Appendix I, Table X. The sedimentation coefficient steadily decreases on going from fraction 1 to 9, whereas $k_s/[\eta]$ decreases in an irregular

Fig. 10

Log X_m versus time for fraction 4 and a concentration of 0.29 $g.dl^{-1}$.

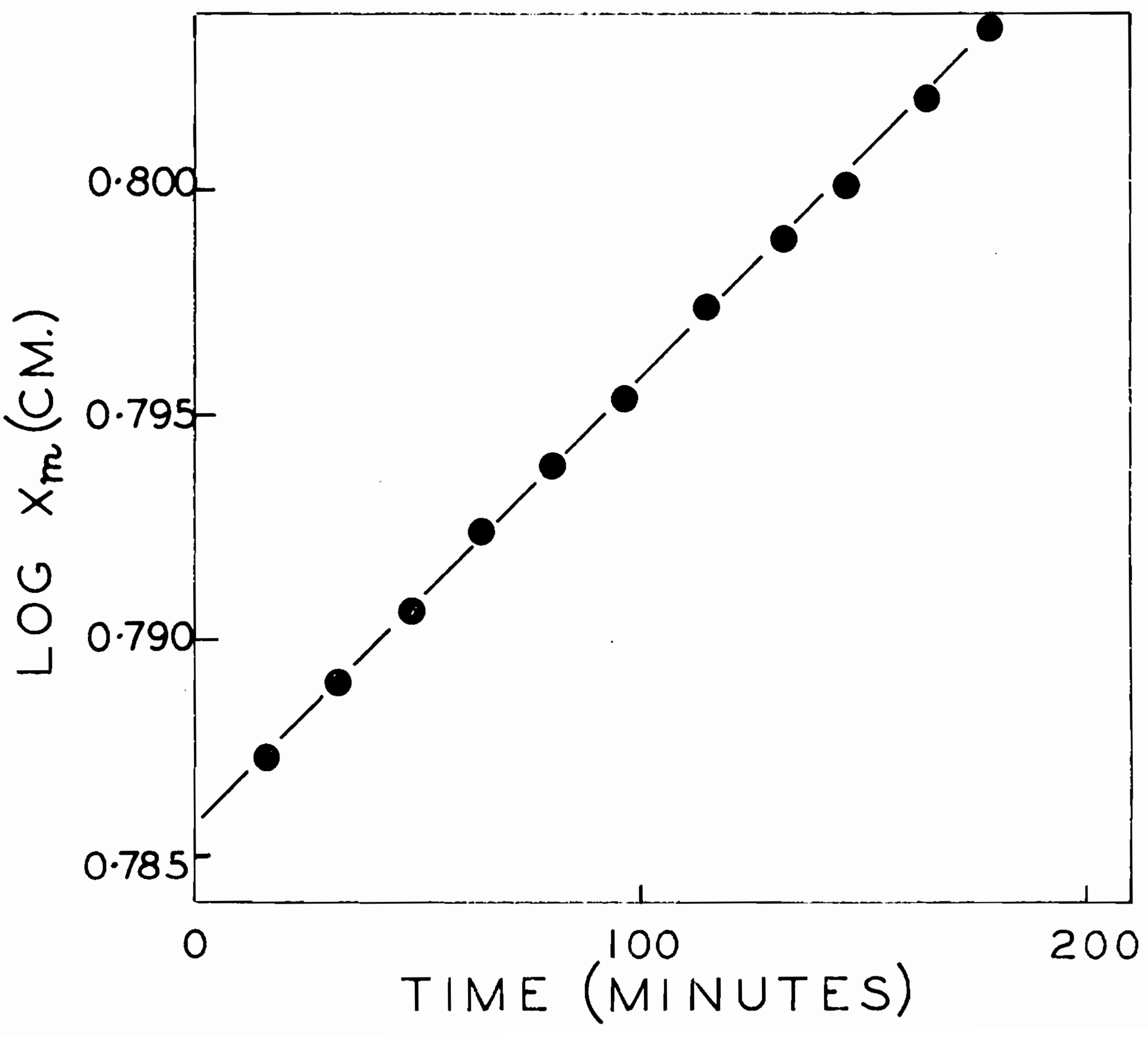
LOG X_m (CM.)
0·800
0·795
0·790
0·785
0
100
200
TIME (MINUTES)

Fig. 11

Dependence of the sedimentation coefficient on concentration for fraction 4.

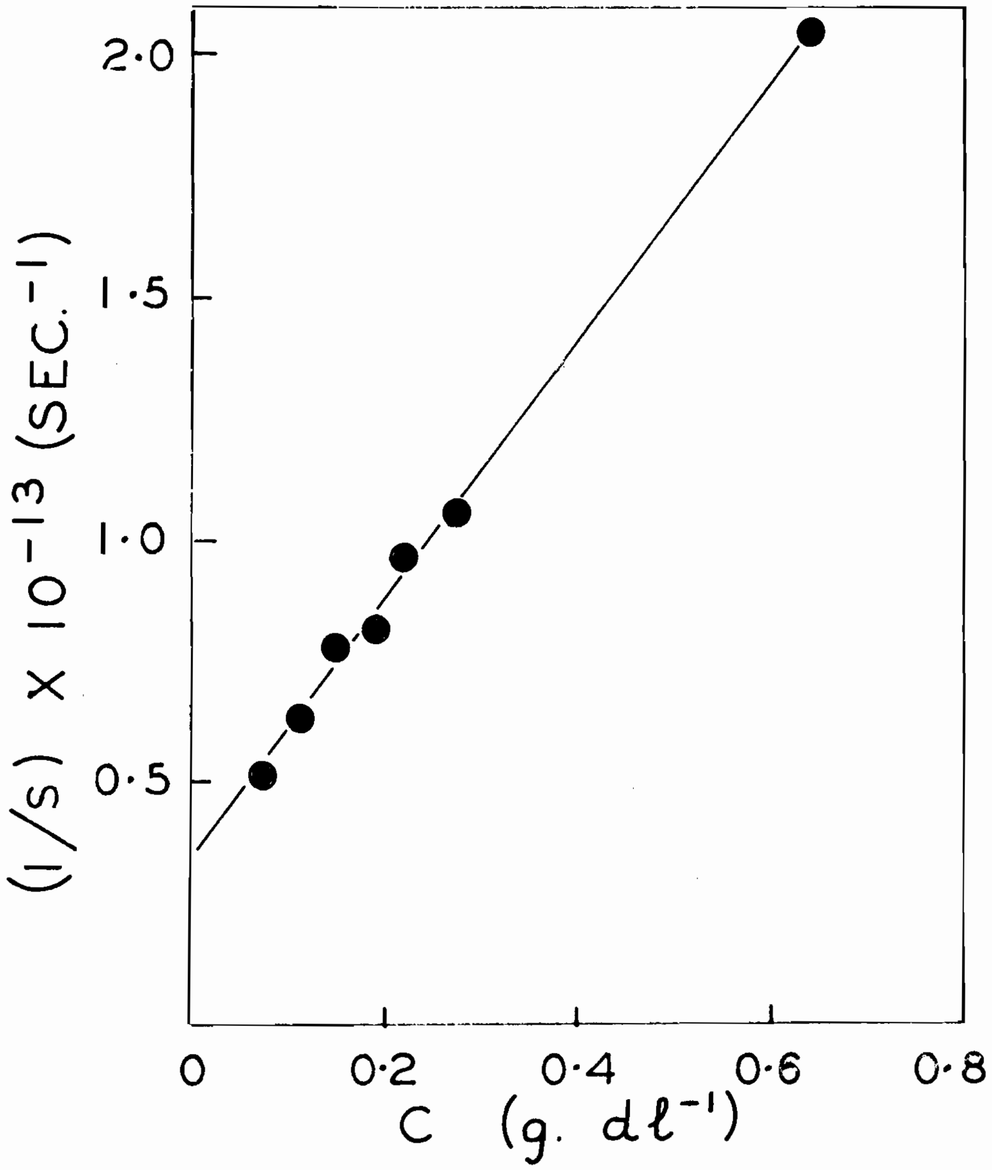

2·0
1·5
1·0
0·5
(1/s) X 10⁻¹³ (SEC.⁻¹)
0
0·2
0·4
0·6
0·8
C (g. dℓ⁻¹)

manner on going from fraction 1 to 5 and then begins to increase for the low molecular weight fractions. The errors of both $[\eta]$ and k_s are combined in this ratio, and so irregularity is not unexpected.

Because the density and viscosity of benzene are sensitive to pressure, the value of the sedimentation coefficient will depend on pressure. A correction for this effect has been proposed by Oth and Desreux (125) in the equation

$$s_p = s\,(1-\mu P_1) \qquad \text{.........} \; (49)$$

where s_p is the sedimentation coefficient uncorrected for pressure, s is the value at one atmosphere pressure, P_1 is the pressure at that point in the cell at which s_p was measured and

$$\mu = \gamma_p + \frac{\rho_o v_o\,(\Omega - \varphi)}{(1 - \rho_o v_o)} \qquad \text{.....} \; (50)$$

In this equation φ is the correction for changes in v and is generally assumed to be negligible, Ω and γ_p correct for changes in viscosity and density, respectively, and the zero subscripts denote values at 25°C and one atmosphere pressure. The values of Ω and γ_p for benzene are 0.85×10^{-9} cm^2/dyne and 0.083×10^{-9} cm^2/dyne, respectively (126). Upon completion of the calculation for several fractions it was found that s could be corrected for pressure effects satisfactorily by the approximation $(1 - \mu P_1) = 1.039$ for the double sector cell. The corresponding value for the synthetic boundary cell was 1.044.

Gralen's method (127) was used to estimate the polydispersity of each of the fractions and of the unfractionated material. The ratio of the area under the sedimentation curve to the value of the maximum ordinate was plotted against X_m for a particular concentration to give a straight line. The slope of this line was found to depend on the concentration. For all the fractions the slope increased slightly with decrease in concentration. But, in the case of the unfractionated polymer the slope decreased with decrease in concentration; this behavior is contrary to the results for other polymers (128, 129). Extrapolation of a plot of slope versus concentration gave the slope at zero concentration which is equal to (127)

$$(\gamma\beta)\ e^{(\gamma\beta)^2/4}\ \sqrt{\pi}$$

On solving for β , $\bar{M}_w/\bar{M}_n$ was obtained from the expression (127)

$$\bar{M}_w/\bar{M}_n \quad = \quad e^{\beta^2/2}$$

Using this method $\bar{M}_w/\bar{M}_n$ for all the fractions was found to be in the range 1.02 to 1.04. This is a much lower degree of polydispersity than that obtained by others (83) using $\bar{M}_w$ found by light scattering and $\bar{M}_n$ found from osmometry, and it is also low theoretically considering that only twelve fractions were obtained. For the unfractionated polymer $\bar{M}_w/\bar{M}_n$ was calculated to be 1.2 which is much lower than the minimum value it can have of approximately two (101).

There are three possible reasons why these results calculated using Gralen's method are unreliable. Gralen assumed that no diffusion occurred, but Eriksson (130) showed that a correction must be made for diffusion. Jullander (131) claims that the sedimentation peak must not have a positive skewness for the method to work. Although the photographs of Fig. 9 indicate no skewness, the molecular weight distribution curve of Fig. 13 shows a positive rather than negative, skewness. This skewness could only be noticed in the sedimentation photograph for the unfractionated polymer if the concentration was greater than 2 g./dl. According to several experiments using other polymers (128,129) the dependence of slope on concentration increases with decreasing concentration. Therefore, by failing to go to sufficiently low concentrations the value of the slope at zero concentration would be too small and therefore β and $\bar{M}_w/\bar{M}_n$ would be less than the true values.

Molecular Weight

Equation 5 on rearrangement gives

$$\bar{M}_{\eta s} = \left[\frac{N\ 10^{-13}\ \eta_o}{(\phi)^{1/3}\ P^{-1}\ (1-v_o\ \rho_o)} \right]^{3/2} s_o^{\ 3/2}\ [\eta]^{1/2} \quad \ldots (5a)$$

Fig. 12

Specific volume of the polymer solution, v,
as a function of the product vc.

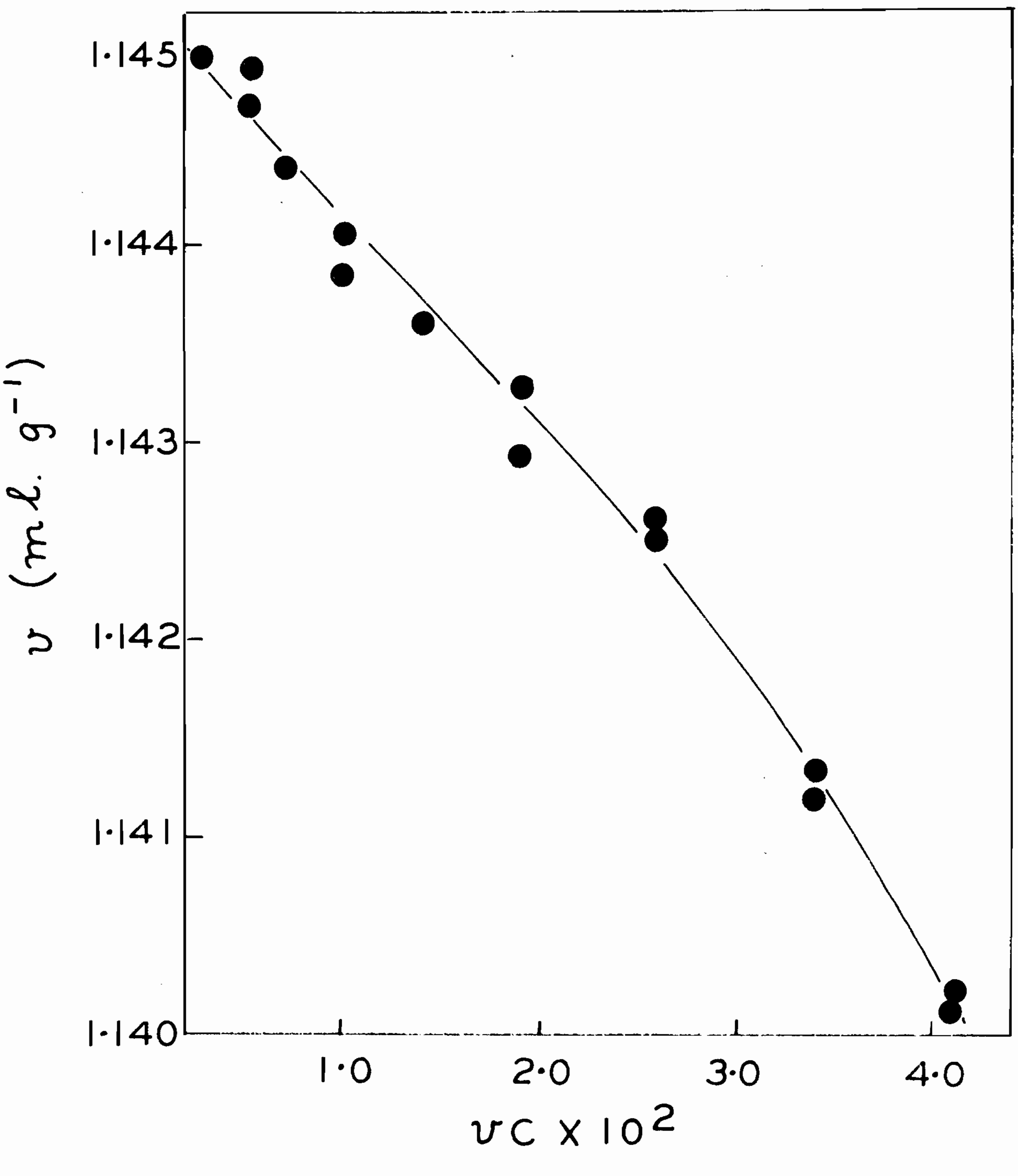

1·145
1·144
1·143
1·142
1·141
1·140
v (mℓ. g⁻¹)
1·0
2·0
3·0
4·0
$vc \times 10^2$

Fig. 13

Molecular weight distribution curves.

○ integral

● differential

— — — theoretical curve for $\bar{M}_n$ = 89,000, random distribution, and linear molecules.

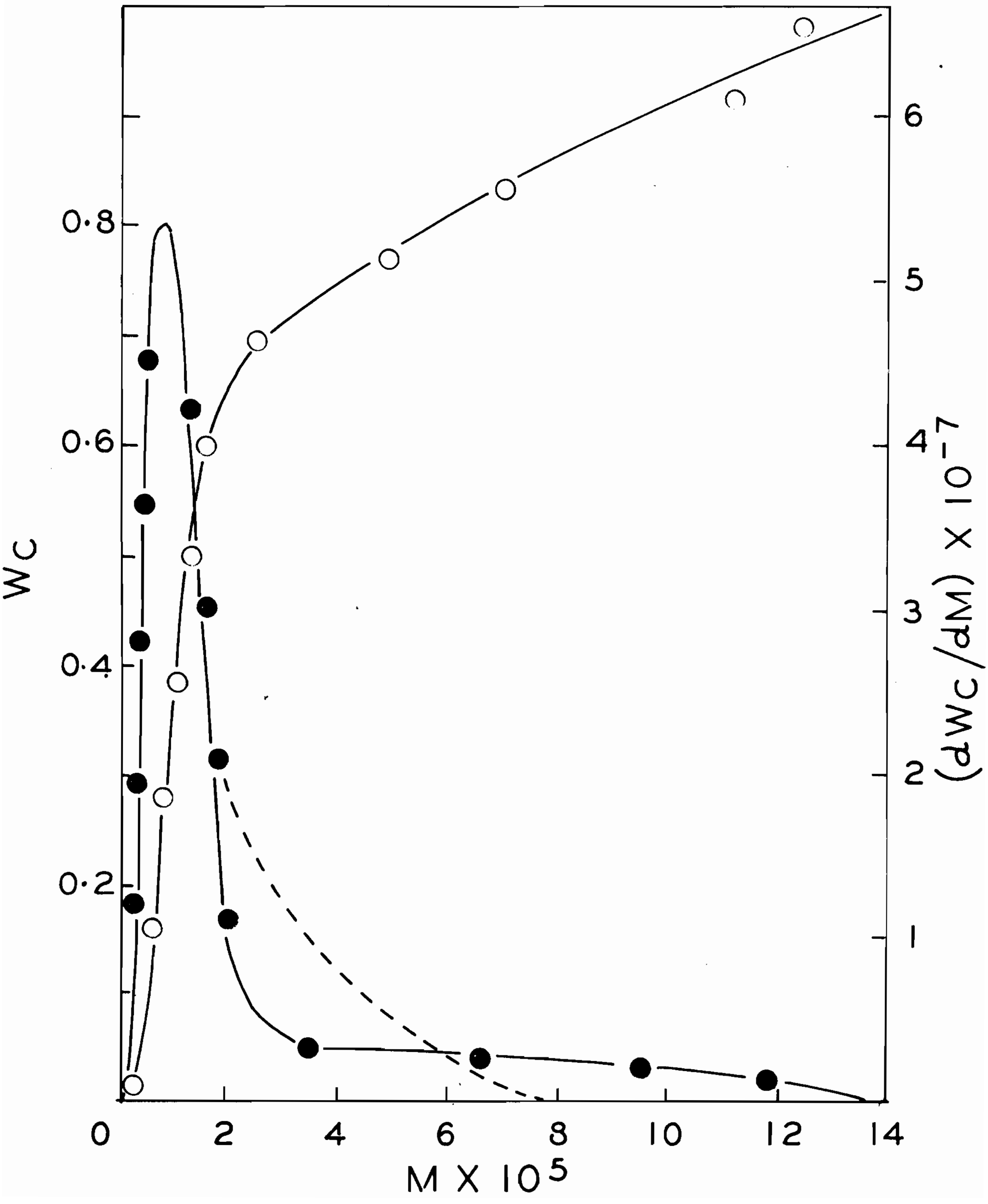
Wc
0·2
0·4
0·6
0·8
(dWc/dM) X 10⁻⁷
1
2
3
4
5
6
0
2
4
6
8
10
12
14
M X 10⁵

where η_o, the viscosity of the solvent, is 6.024 millepoises and ρ_o, the density of the solvent, is 0.8735 grams per ml. (132). The partial specific volume at any concentration is given by (133)

$$v = v_s\ (1 - v_s c)\ \frac{dv_s}{d(v_s c)} \qquad \text{.......}\ (51)$$

where v_s is the specific volume of the solution obtained by pycnometry. From the plot of the specific volume of the solute against $v_s c$ given in Fig. 12, $dv_s/d(v_s c)$ was found to have a constant value of 0.1253. Using this value in equation 51 for different values of c and v_s indicated that v changes a negligible amount with concentration, and therefore $(1 - v_o \rho_o)$ is a constant of 0.107. Values of $\bar{M}_{\eta s}$ were calculated using equation 5a with values of s_o and $[\eta]$ from Table I, and are listed in Table I.

The $\bar{M}_v^{\,c}$ and $\bar{M}_v^{\,h}$ values given in Table I were calculated from

$$[\eta] = 5.4 \times 10^{-4}\ (\bar{M}_v^{\,h})^{0.66} \qquad \text{.......}\ (52)$$

$$[\eta] = 2.95 \times 10^{-4}\ (\bar{M}_v^{\,c})^{0.71} \qquad \text{.......}\ (53)$$

The first equation is valid for a polymerization temperature of about 50°C, therefore h for "hot" is used and $\bar{M}_v^{\,h}$ is obtained (134). The second equation is for polymerization at about 5°C, therefore $\underline{c}$ for "cold" is used and $\bar{M}_v^c$ is obtained (135). The results of Table I show that $\bar{M}_{\eta s}$ is always less than $\bar{M}_v^h$, but is only less than $\bar{M}_v^c$ for the low molecular weight fractions. For the high molecular weight fractions $\bar{M}_{\eta s}$ becomes greater than $\bar{M}_v^h$.

Using $\bar{M}_{\eta s}$ from equation 5a for the high molecular weight fractions and $\bar{M}_v^c$ from equation 53 for the low molecular weight fractions, the molecular weight distribution curve shown in Fig. 13 was constructed. The integral distribution curve was obtained by plotting the molecular weight of the i th fraction against the cumulative weight fraction of the first (i-1) fractions plus half that of the i th fraction. The differential distribution curve was obtained by graphical differentiation of the integral curve. This involved drawing the integral curve on a scale four times that shown in Fig. 13 and finding the slope of the enlarged curve at several values of molecular weight.

Degree of Crosslinking

Fig. 14 shows the plot of log s_o versus log $[\eta]$ for the nine fractions examined and for the unfractionated polymer. The five lowest molecular weight fractions can be fitted to a

Fig. 14

Log sedimentation coefficient at zero concentration versus log intrinsic viscosity.

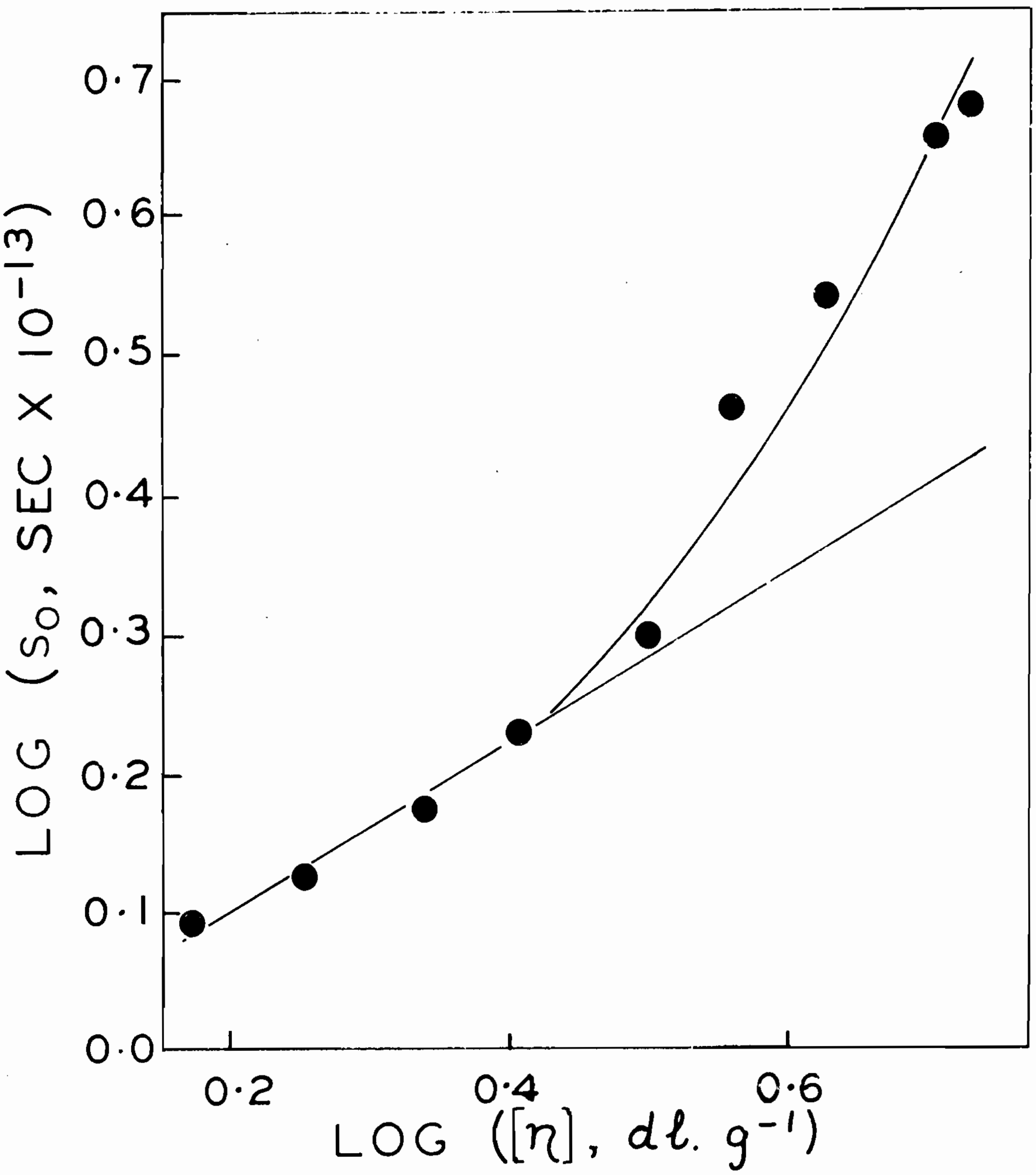
LOG $(s_0$, SEC X $10^{-13})$
0·0
0·1
0·2
0·3
0·4
0·5
0·6
0·7
0·2
0·4
0·6
LOG ([η], dl. g^{-1})

straight line described by the equation

$$s_o = 0.944 \ [\eta]^{0.61} \qquad \ldots\ldots\ldots (54)$$

The unfractionated material falls well below the line. This might be because the low and long tail of high molecular weight material shown in Fig. 13 has no effect on s_o but does increase the intrinsic viscosity. This explanation also accounts for the low values of $k_s/[\eta]$ and $\tilde{M}_{\eta s}$ given in Table I.

Using equation 20

$$(s_o) \ [\eta]_1^{(3\gamma + 1)/3} = (s_o)_b \ [\eta]_b^{1/3} \qquad \ldots\ldots (20)$$

and equation 54 and the $[\eta]_b$ and s_{ob} values for the first four fractions, $[\eta]_b / [\eta]_1$ values were obtained. Then from Fig. 1 the number of crosslinks per molecule, m, was found and m_w was then calculated. Finally δ_o was found from equation 23,

$$m_w = \frac{\delta_o}{1 - \delta_o} \qquad \ldots\ldots\ldots (23)$$

The results are given in Tables II and III. The three theories show an increase in nonlinearity with the molecular weight. The degree of nonlinearity calculated using the Zimm-Kilb theory (73) is about six times that based on equation 14 and

TABLE II

Degree of crosslinking in each fraction.

Fract.	$[\eta]_b / [\eta]_l$	m Zimm-Kilb	m Stockmayer-Fixman	m equation 14
1	0.544	21.3	6.4	2.7
2	0.558	19.0	5.9	2.5
3	0.661	8.4	3.8	1.7
4	0.712	5.4	2.9	1.3
5	1.000	0	0	0
.	.	.	.	.
.	.	.	.	.
.	.	.	.	.
	m_w	3.58	1.26	0.55

TABLE III

Values of δ_o using several theories.

Theory	from $[\eta]$ and $\bar{M}_{noo}$		from $\bar{M}_{wo}/\bar{M}_{no}$	from results
	equation 52 used	equation 53 used	equal 2.84	for fractions
Zimm-Kilb	--	--	--	0.78
Stockmayer-Fixman	--	--	--	0.56
equation 14	--	--	--	0.38
Kilb	0.80	0.30	0.36	--
Schultz	--	0.30	--	--
Katsuura	0.92	0.66	--	--

three times that according to the Stockmayer-Fixman theory (72).

Assuming each fraction is monodisperse, $\bar{M}_{wo}/\bar{M}_{no}$ was found by substituting values from Fig. 13 in the following expression (136).

$$\frac{\bar{M}_{wo}}{\bar{M}_{no}} = \frac{\Sigma (dW_c/dM)M \quad \Sigma (dW_c/dM)/M}{\Sigma (dW_c/dM)^2} \quad \ldots\ldots\ldots (55)$$

where W_c is the cumulative weight. This method gave $\bar{M}_{wo}/\bar{M}_{no}$ = 2.84. Substituting this value into equation 22,

$$\frac{\bar{M}_{wo}}{\bar{M}_{no}} = \frac{2 - \delta_o/2}{1 - \delta_o} \quad \ldots\ldots\ldots (22)$$

gave δ_o = 0.36. The value of $\bar{M}_{no}$ was found by osmometry to be 89,9000.[x] Therefore, $\bar{M}_{wo}$ according to equation 55 is 305,000.

Although the theories of Zimm and Kilb, Stockmayer and Fixman, and that represented by equation 14 are strictly valid only for results obtained at the theta temperature, results obtained by others (71) show only a negligible temperature effect.

---

[x] The osmotic pressure data were supplied by the Pulp and Paper Research Institute of Canada.

An assumed value for δ_o was used in equation 25 with $\bar{M}_{no}$ = 89,000 to give a value for the number average molecular weight of the primary linear molecules, $\bar{M}_{noo}$.

$$\bar{M}_{no} = \frac{\bar{M}_{noo}}{(1 - \delta_o/4)} \quad \text{........ (25)}$$

Substituting this value of $\bar{M}_{noo}$ in equation 26 with K and a from either equation 52 or 53 led to a value for the intrinsic viscosity of the primary molecules.

$$[\eta] = K\ \Gamma(2 + a)\ \bar{M}_{noo}^{a} \quad \text{...... (26)}$$

The ratio of this value to the experimentally obtained intrinsic viscosity of the nonlinear polymer was employed in Figs. 2, 3, or 4 to give a value for δ_o. Although Figs, 2, 3, and 4 are plots of $[\eta]_R/[\eta]_o$ versus R/R_g, it was shown in the introduction to this thesis that under the present circumstances $R/R_g = \delta_o$ and $[\eta]_R/[\eta]_o$ equals the ratio of the intrinsic viscosities of the nonlinear and primary linear molecules. If the value of δ_o obtained by this method was not the same as that assumed, a new value was assumed and the procedure repeated until agreement was reached. The results of this third method of finding δ_o are given in Table III. No value of δ_o is given for Schultz's theory (90) in the case of equation 52 because the value of

$[\eta]_R/[\eta]_o$ calculated lies above the maximum value for $[\eta]_R/[\eta]_o$ in the theoretical curve of Fig. 1.

DISCUSSION

Before discussing the results in detail it is necessary to determine whether the molecular weight distribution, M.W.D., before crosslinking is of the random type, and if the crosslinks are formed in a random manner. Bardwell's analysis (101) reveals that for poly(butadiene-co-styrene) the primary distribution is very close to the random type even at high conversions. Flory (137) claims that a small degree of nonrandom crosslinking probably occurs at high conversions. Because the degree of conversion of the polymer studied was not known, this factor must be considered in interpreting some of the results. There is a possibility that trifunctional branching occurs (137), but Morton (138) suggests that his experiments indicate that crosslinking occurs much more than branching. Experimentally (139), and theoretically (140) branching has been shown to broaden the M.W.D., but no detailed analysis has been made.

Because the slope of the plot

$$\log \frac{\eta_{sp} - [\eta]}{c} \quad \text{versus} \log [\eta]$$

shown in Fig. 8 is found to be two for the low intrinsic viscosity fractions it can be concluded that k' in equation 8 is a constant for these fractions.

$$\frac{\eta_{sp}}{c} = [\eta] + k'[\eta]^2 c \qquad \ldots\ldots\ (8)$$

However, the slope becomes increasingly greater on going to higher $[\eta]$ fractions. This means that k' in equation 8 is no longer a constant but is increasing with increasing $[\eta]$. The k' values shown in Table I indicate the extent of this increase. Cragg (78) obtained the same results using the same polymer. Because a change in shear rate had no effect on k' the increasing k' is not caused by orientation. Benzene is a good solvent for this polymer. Therefore its solvent power will not decrease sufficiently with increasing molecular weight to cause an increase in k'. An increase in polydispersity cannot explain the rise in k', because k' for the unfractionated polymer was less than k' for the high molecular weight fractions. An increase in the nonlinearity of the molecules must be responsible for the increase in k'. A further indication that increasing k' means increasing nonlinearity is that as k' increases so also does m_w, the weight average number of cross-links per molecule.

Because a nonlinear molecule is more compact and dense than a linear molecule, its shape parameters will tend to approximate those of a sphere more closely than would those of a linear molecule. The value of $\Phi^{1/3}P^{-1}$ is lower for a solid sphere than it is for a linear molecule (46). Equation 11 indicates that the ratio of $k_s/[\eta]$ is inversely proportional to $(\Phi^{1/3}P^{-1})^3$. The results in Table I show that $k_s/[\eta]$ tends to increase with increasing intrinsic viscosity. Therefore, $(\Phi^{1/3}P^{-1})$ is decreasing with increasing intrinsic viscosity which in turn means that the molecules are becoming more spherical and hence more nonlinear as the intrinsic viscosity increases. Wales (58) predicts that decreasing the polydispersity of a sample will increase the ratio of $k_s/[\eta]$. Therefore the increase in $k_s/[\eta]$ might be caused by the high intrinsic viscosity fractions having a lower degree of polydispersity than the low molecular weight fractions.

The molecular weight distribution, M.W.D., shown in Fig. 13 is accurate provided that the values of molecular weight and fraction weight were accurate, that the fractions were almost monodisperse, and that the differentiation of the integral curve was accurate. Errors in the weights of the fractions would have a negligible effect on the M.W.D. because these weights have a possible error of only one per cent. Although it was not possible to estimate the error for the differentiation of the integral curve, this error is probably small because a large diagram was used and many measurements were taken. The values of the molecular weights for the high molecular weight fractions were calculated using equation 5a, whereas those for the three lowest molecular fractions were obtained from equation 52. It was shown in the introduction that the values of molecular weight found from equation 5a are not affected by the nonlinearity of the molecules. Even though the molecular weight as calculated from equation 52 is reduced by nonlinearity, it can be assumed that the degree of nonlinearity of the molecules of the three lowest molecular weight fractions is negligible. The fractions are probably rather polydisperse because only nine fractions were collected and because a nonlinear molecule will precipitate with a linear molecule of greater molecular weight. For a polymer composed of only linear molecules corrections for the effect of polydispersity of the fractions on the experimentally determined M.W.D. have been proposed and tested experimentally (136, 141). But no correction has been suggested for a polymer containing both linear and nonlinear molecules; furthermore, there is no experimental evidence which indicates the importance of this correction for such a polymer. Therefore, the M.W.D. obtained in this work might be inaccurate and hence the values of $\bar{M}_{wo}/\bar{M}_{no} = 2.54$ and $\delta_o = 0.38$ might be in error.

The differences in the values of δ_o in Table III obtained using the intrinsic viscosity and the number average molecular weight of the unfractionated polymer indicate the great importance of the parameters K and a. The values calculated using equation 53 for the "cold" polymer are probably more accurate than those obtained using equation 52 for "hot" polymer because the structure of the polymer as revealed by infrared analysis indicated that it was indeed polymerized at a low temperature. Another indication that equation 53 is the more reliable is that the molecular weight results in Table I show that the ratio of $\bar{M}_{\eta s}$ to $\bar{M}_v^c$ is generally greater than unity, whereas the ratio of $\bar{M}_{\eta s}$ to $\bar{M}_v^h$ is less than unity. But $\bar{M}_{\eta s}$ should always be greater than $\bar{M}_v$ because s_o as obtained in this work is nearer to a weight average than is intrinsic viscosity (142). Therefore the $\bar{M}_v^c$ values are more reasonable than the $\bar{M}_v^h$ values. The increase in the ratio of $\bar{M}_{\eta s}$ to $\bar{M}_v^c$ with increasing molecular weight shown in Table I is a result of the fact that $\bar{M}_{\eta s}$ is unaffected by nonlinearity whereas $\bar{M}_v$ decreases with increasing nonlinearity for a constant molecular weight. For the low molecular weight fractions $\bar{M}_v^c$ is actually greater than $\bar{M}_{\eta s}$. A possible explanation for this is that the M.W.D. of these fractions might have long high molecular weight tails which are not accounted for in the measurement of s_o but are accounted for in the measurement of $[\eta]$. The unfractionated polymer does have such a tail and as the result in Table I shows the ratio of $\bar{M}_{\eta s}$ to $\bar{M}_v^c$ is very much less than one.

The hydrodynamic properties studied in this work depend on both the degree of nonlinearity and the M.W.D. The previous theories used to calculate δ_o must take into account both these effects. But, in calculating the degree of nonlinearity in monodisperse fractions the effect of M.W.D. need not be considered. For this reason the values of δ_o based on the values of m for the fractions are probably more accurate; furthermore, δ_o in this case is based on many more experiments and therefore is statistically more valid. Theoretical reports cited in the introduction to this thesis support the Zimm and Kilb theory, rather than the Stockmayer and Fixman theory or the theory represented by equation 14. Recent experimental evidence using monodisperse polystyrene also supports the Zimm and Kilb theory. Therefore, the most reliable value of δ_o obtained from the present data is probably that calculated from the application of the Zimm and Kilb (73) theory which gives the value $\delta_o = 0.78$. One of the assumptions made by these authors is that the sample is monodisperse. Consequently, polydispersity of the fractions and the possible errors in K_s and a in equation 20 imply that 0.78 has a large possible error.

If the true value of δ_o is 0.78 and if equation 53 relating intrinsic viscosity to $\bar{M}_v$ is also correct for the polymer being studied, then the low values for δ_o obtained using the intrinsic viscosity and the number average molecular weight of the unfractionated material indicate that the theories of Kilb (91), Schultz (90) and Katsuura (92) underestimate the effect of nonlinearity on the intrinsic viscosity. The value of δ_o obtained from the experimentally determined molecular weight distribution was 0.36, and therefore if the correct value is 0.78 the M.W.D. obtained is narrower than the true M.W.D. and the value of $\bar{M}_w$ calculated using $\delta_o = 0.36$ is too low.

RADIATION INDUCED CHANGES IN SOLUTION PROPERTIES

EXPERIMENTAL

Sample Preparation

The fatty acid, fatty acid soap and the antioxidant present in the GR-S were separated from the poly(butadiene-co-styrene) by precipitating the polymer from a dilute solution of GR-S in benzene. Methanol was the precipitant and its concentration needed for complete precipitation of the polymer was low enough that all the impurities remained soluble. To 5000 ml. of benzene 15 grams of rubber were added and dissolved. A 250 ml. volume of methanol was then added very slowly. The precipitate was allowed to settle for 24 hours, and the supernatant liquid was removed by using nitrogen pressure to force it out of a glass tube. The entire purification was accomplished in a nitrogen atmosphere to avoid oxidation. After the removal of nearly all the supernatant liquid the polymer was again dissolved in 500 ml. of benzene, reprecipitated, left for 24 hours, and the supernatant liquid withdrawn. Finally, the polymer was washed several times with methanol. The pure polymer was dissolved in 200 ml. of benzene and the solution transferred to a 250 ml. beaker, and a known quantity of antioxidant, B, added. The solution was frozen, placed in a vacuum desiccator and freeze dried. From the weight of the dry polymer and the known weight of B the per cent of B in the polymer was calculated. The sample was stored in a vacuum at 0 °C in the dark.

Irradiation Technique

The polymer sample to be irradiated was cut into small pieces and placed in the sealed end of a glass tube of 10 mm. width and 12 cm. length. About 9 cm. from the sample the tube was narrowed to an inner diameter of roughly 2 mm. The tube was connected to a high vacuum system by a ground glass joint and evacuated to a pressure of one micron for at least two days to assure the removal of all the benzene. Finally, at a pressure of one tenth of a micron, the tube was sealed at the narrow point.

While a sample was being evacuated the system could not be tested for leaks with a spark coil because the electric discharge and the ozone seriously affected the polymer. The application of the discharge for only a few seconds caused the formation of some insoluble polymer.

The sample was irradiated in a cobalt-60 gamma-cell model 220 manufactured by Atomic Energy of Canada Limited. The intensity of the radiation within the cavity of the cell where the sample was placed varied from one place to another in a manner described by the makers. This variation was always taken into account in calculating the dose received by the sample. The intensity variation within a sample was about 2% for a 0.3 gram sample and 8% for a 1.8 gram sample.

On September 25, 1959 the intensity of the radiation at the point in the cell where the intensity is greatest was found by the manufacturers to be 9.74×10^{4} roentgens per hour. Using this value and the value of 5.2 years (144) for the half life of cobalt-60 the intensity could be calculated at any time. To calculate the dose in rads received by the polymer the electron density of the polymer was determined from the percentages of carbon and hydrogen, and the number of electrons per gram for these elements (145). The electron density is 3.322×10^{-23} compared to 3.337×10^{-23} electrons per gram for water. If

W for air is taken as 34 e.v. then according to Chapiro (145), the ergs absorbed per gram of water from one roentgen is 97.0 and therefore, the corresponding value for the polymer is 96.7. Since by definition one rad is equal to 100 ergs absorbed per gram, the dose in rads can be calculated. The electron density of antioxidant, B, is 3.195×10^{-23} electrons per gram and therefore 96.0 ergs per gram were absorbed from one roentgen. To calculate the dose for a mixture of polymer and B the values 96.7 and 96.0 must be multiplied by the weight fractions of polymer and B, respectively.

Determination of the Gel Point

A relatively large error was inherent in the technique employed for measuring R_g, the radiation dose required to initiate gel formation. This error arose from the difficulty in detecting very small quantities of gel. Visual detection of gel was either direct or by noting the appearance of small bubbles of gas trapped in an otherwise invisible gel. However, this technique was applicable only after a fairly large quantity of gel had formed. Consequently the accuracy with which R_g could be determined by the visual technique is poor.

R_g was determined in the present study by noting the radiation dose required to cause a benzene solution of the irradiated polymer to block a sintered glass filter. This method was subject to several possible sources of error. A small quantity of gel would block such a small fraction of the area of the sintered glass filter that the presence of the gel would not be detected. The further possibility of the gel passing through the pores of the filter had always to be considered. The gel point determination was highly sensitive to the solvent employed. A small quantity of gel could block the filter to the passage of benzene, but on the addition of a small amount of methanol to the benzene the gel would contract and passage of the solvent through the filter was again possible. Close to the gel point the intrinsic viscosity for some of the molecules could be very high (81). This factor further complicated gel point determination since difficulty of filtration could be caused by either high viscosity or gel formation. Because of these many possible sources of error the precision with which R_g could be determined was only five per cent, as a conservative estimate.

Viscosity

The intrinsic viscosities of samples irradiated to doses less than R_g were determined as described in the first experimental part of this thesis. The pure polymer was irradiated in vacuo and the polymer mixed with antioxidant, B, was irradiated both in air and in vacuo.

The effect of radiation on oxidized polymer was determined by irradiating polymer previously exposed to air. The amount of oxygen in these exposed polymer samples was determined microanalytically.[x]

The filtration characteristics of solutions of samples which had been irradiated to doses near but less than R_g were also studied. These samples were also analyzed for microgel (146) by shaking the solutions with finally divided calcium sulphate (147).

Solubility

Solubility determinations were made on pure polymer and polymer containing B, when irradiated in air and in vacuo.

The determination of the percentage of irradiated polymer soluble in benzene was simple and accurate. A known weight of small pieces of polymer, generally about 0.3 grams, was placed in benzene for 24 hours. The solution was then decanted into a 100 ml. volumetric flask. The procedure was repeated three times, and the gel was then washed with small amounts of benzene and the final solution made up to 100 ml. A very dilute solution of B in benzene was used in the extraction of the pure polymer to prevent oxidation.

---

[x] Alfred Bernhardt, Max Planck Institute.

The solids content of 25 or 50 ml. of the final benzene solution was found by freeze drying. In calculating the per cent soluble polymer a correction was made for any B initially present in the polymer, assuming that B was completely soluble in benzene.

The gel content at less that 50% gel was difficult to measure because the gel would tend to break into small pieces and pass over into the solution phase during decantation. A copper 100 mesh filter was used in many experiments to minimize this loss in gel, but the mesh failed to improve the reproducibility of the technique which remained poor.

The ratio p_o/q_o was determined by the method of Baskett (148). A sample containing B was irradiated to a high dose, extracted, and the gel divided into several portions. The irradiation to high dose and extraction process were then repeated on each of these portions.

Swelling

After separating the gel from the sol the degree to which the gel swelled in benzene was determined. The benzene not incorporated into the gel was decanted off. The particles of swollen gel were rolled on a paper towel for about one minute to remove any surface benzene. They were then quickly transferred to a weighed stoppered bottle and their weight determined. Because the weight of the dry gel was known from solubility experiments, the benzene associated with the gel could be found.

This very practical technique was subject to two obvious sources of error. If the drying process was too prolonged some of the benzene contributing to the swelling might be lost during the drying of the gel. If too rapid a drying process was employed all of the excess benzene would not be removed. To determine the importance of these possible errors in the drying technique, Flory's method (149) of determining the extent of swelling in a saturated benzene atmosphere was applied to several samples of widely differing degrees of swelling. His rather complex method gave the same result as the paper towel method. Table IV gives the data from the two methods.

In preliminary experiments the degree of subdivision of the sample and the time of extraction had no effect on the extent of swelling. Bardwell (101) made a thorough study of these effects and reached the same conclusion. In the light of his results no further study was deemed necessary.

RESULTS AND TREATMENT OF DATA

Only irradiation in vacuo will be considered here. A detailed presentation and discussion of the results of irradiation in air is given in a following section.

TABLE IV

Comparison between the paper towel method and Flory's method for determining the weight of the swollen gel.

Paper towel method weight of swollen gel grams	Flory's method weight of swollen gel grams
7.9366	8.3761
7.0906	7.0345
5.5448	5.6736
2.3577	2.2261
1.7329	1.7662

Viscosity and Gel Point

The values of R_g listed in Table V were obtained by the filtration technique. Table V also gives G_x values which were calculated from equation 32 using $\bar{M}_{wo}$ of 3.05×10^5, 2.4×10^6 and 4.7×10^6. The value of $\bar{M}_{wo} = 305{,}000$ was calculated from the value of $\bar{M}_{no} = 89{,}900$ as determined by osmometry and the molecular weight distribution curve given in Fig. 13. From equation 22 using $\bar{M}_{no} = 89{,}900$ the values of $\bar{M}_{wo} = 2.4 \times 10^6$ and 4.7×10^6 were computed assuming $\delta_o = 0.8$ and 0.9, respectively.

$$\frac{\bar{M}_{wo}}{\bar{M}_{no}} = \frac{2 - \delta_o/2}{1 - \delta_o} \qquad \text{........(22)}$$

$$R_g = \frac{0.48 \times 10^6}{G_x \bar{M}_{wo}} \qquad \text{........(32)}$$

It is important to realize that in calculating G_x using equation 32 it is not necessary to correct the experimentally determined values of R_g and $\bar{M}_{wo}$ for the effect of nonlinearity in the unirradiated polymer. Although the values of R_g and $\bar{M}_{wo}$ depend on the value of δ_o, the product $R_g \bar{M}_{wo}$ does not. The weight average molecular weight of the primary molecules, $\bar{M}_{woo}$, is obtained from

$$\bar{M}_{wo} = \frac{\bar{M}_{woo}}{(1 - \delta_o)} \qquad \text{........(25a)}$$

and the dose to produce incipient gelation if the primary molecules are irradiated, $R_o + R_g$, is related to δ_o by

$$\frac{R_o}{R_o + R_g} = \delta_o \qquad \text{.........} (33)$$

Therefore the product of the weight average molecular weight of the primary molecules, $\bar{M}_{woo}$, and the dose to initiate gelation is

$$\bar{M}_{wo} \frac{1 - R_o}{R_o + R_g} (R_o + R_g)$$

which reduces to $\bar{M}_{wo} R_g$.

Fig. 15 shows the effect of radiation on the intrinsic viscosity for doses up to the gel point assuming $\delta_o = 0$ and for comparison the theoretical curves of Kilb (91) and Katsuura (92). The Schultz curve of Fig. 2 obviously does not agree with the experimental curves and is therefore not shown. Fig. 16 gives the same curves as Fig. 15 assuming δ_o to be 0.8; the deviation from theory in this plot is even greater than in Fig. 15. Table XI of Appendix II gives the data used in calculating $[\eta]_R$ for one of the samples. The plots of η_{sp}/c versus c were similar to that shown in Fig. 7 for one of the fractions. The values of $[\eta]_R$ and $[\eta]_o$ for all the

Fig. 15

Comparison between the theoretical and experimental dependence of intrinsic viscosity on R for δ_o equal to zero.

— — —	Kilb's theory,	$\underline{a} = 0.68$, $p_o/q_o = 0$
......	Katsuura's theory,	$\underline{a} = 0.70$, $p_o/q_o = 0$
———	experimental	

○	0% B
●	0.5% B
□	2.1, 5.3, 7.1, and 11.3% B
△	2.7% B irradiated in the presence of air.

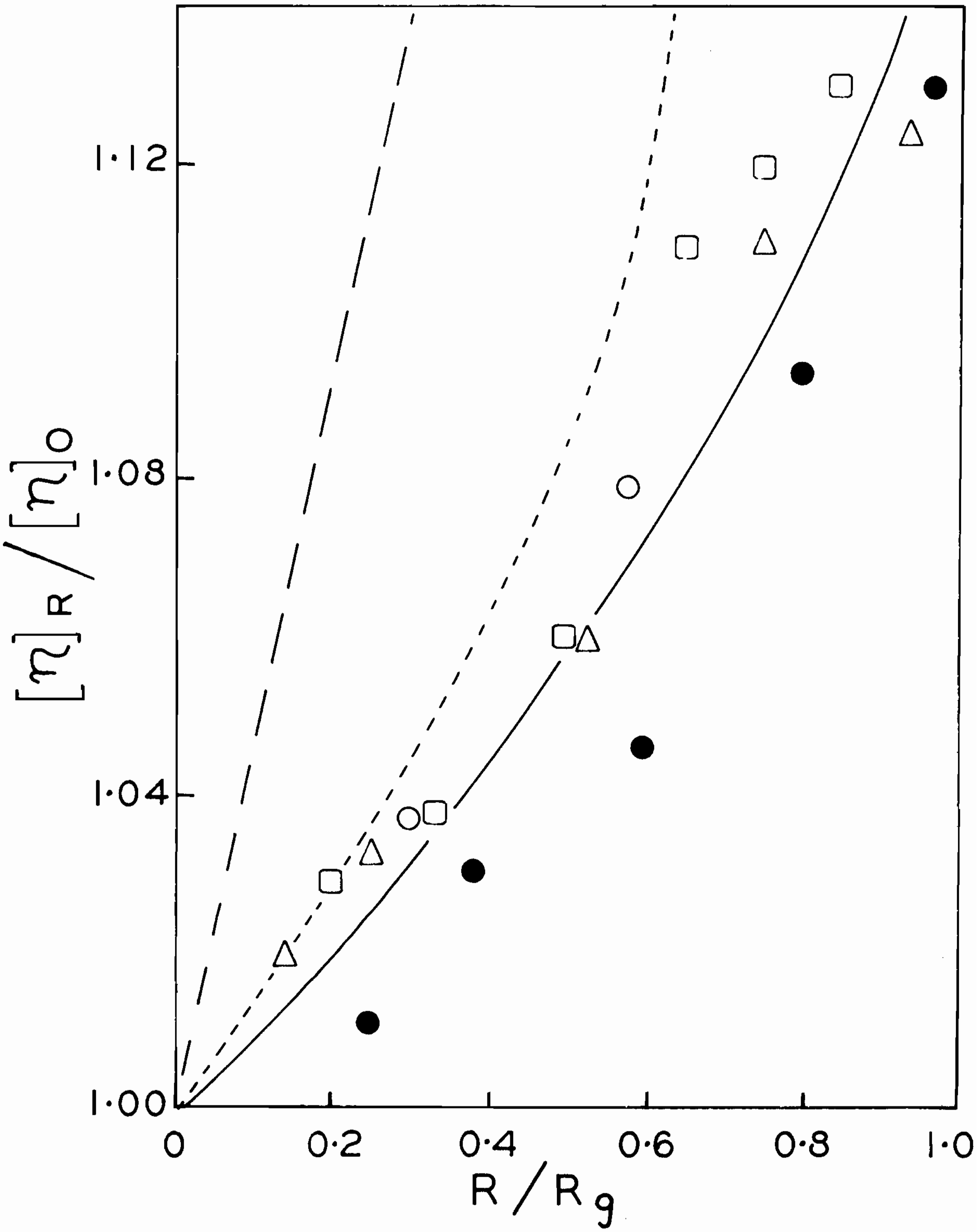

$[\eta]_R / [\eta]_0$
1·00
1·04
1·08
1·12
0
0·2
0·4
0·6
0·8
1·0
R / R_g

samples are given in Table XII of Appendix II. The log of the slopes of the η_{sp}/c versus c plots are plotted against log $[\eta]$ in Fig. 17. The straight line obtained can be fitted to the equation

$$\frac{\eta_{sp}}{c} = [\eta] + k'[\eta]^2 c$$

where k' has the value

$$k' = 0.223\,([\eta])^{0.75} \qquad \text{........} \quad (56)$$

An increase in the oxygen content of the polymer from 0.12% to 0.46% had no effect on the change in viscosity with irradiation. It required one week of exposure to air at room temperature to oxidize the polymer to an oxygen content of 0.46%. Therefore, the deviation from theory shown in Figs. 15 and 16 is not caused by oxidation because the samples were never exposed to air for longer than an hour.

No microgel was found in any of the samples. Filtering the polymer solutions reduced k' and the intrinsic viscosity by a very small amount if the dose was close to R_g but had no effect at lower doses. Therefore, neither the filtration of the sample, which was carried out to remove dust, nor the presence of microgel, caused the deviation from the theoretical manner in which $[\eta]_R$ increases with dose.

Fig. 16

Comparison between the theortical and experimental dependence of intrinsic viscosity on R for δ_o equal to 0.8.

— — —	Kilb's theory,	a = 0.68, $p_o/q_o = 0$
······	Katsuura's theory,	a = 0.70, $p_o/q_o = 0$
———	experimental	

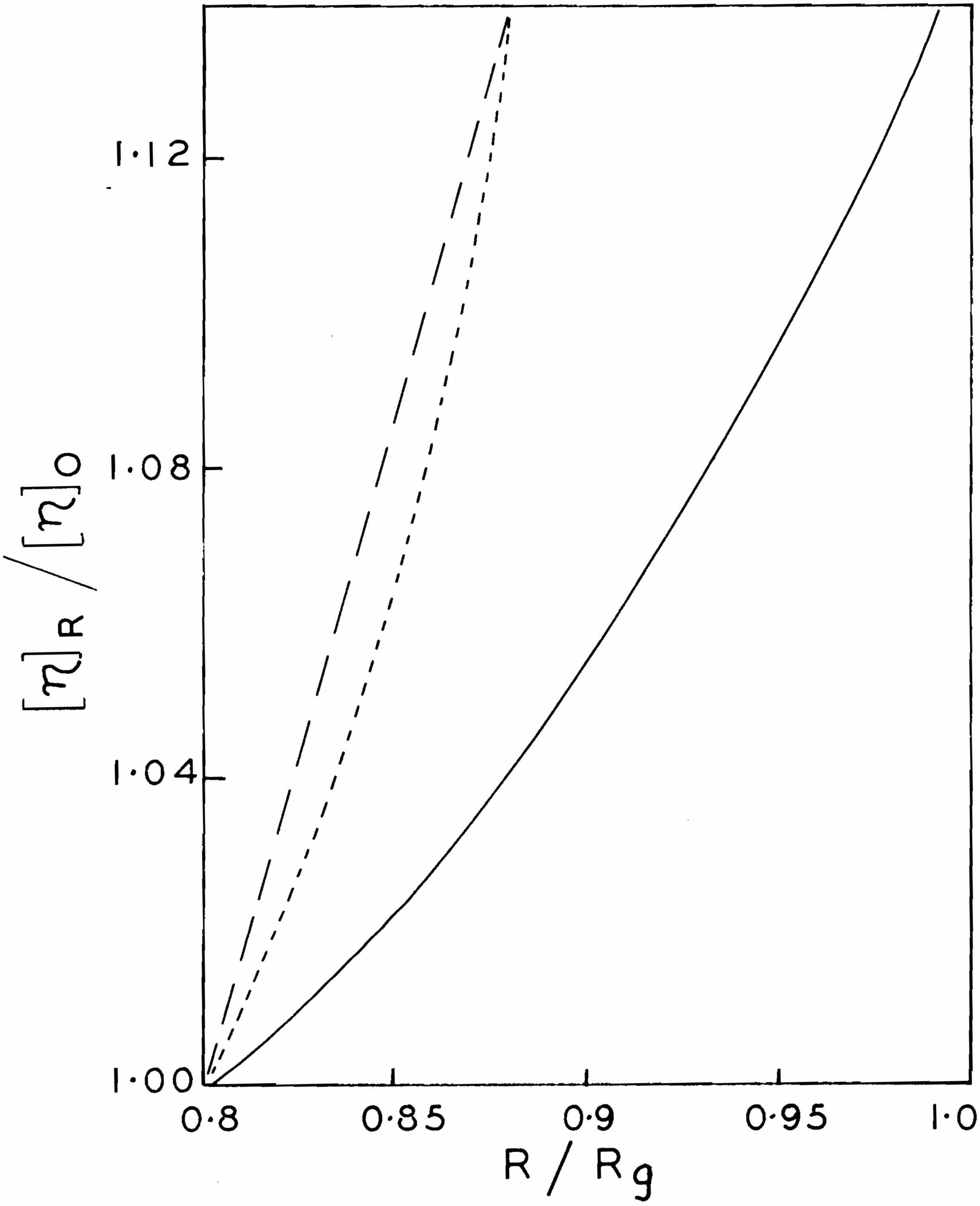

$[\eta]_R / [\eta]_0$
1·12
1·08
1·04
1·00
0·8
0·85
0·9
0·95
1·0
R / R_g

Fig. 17

Dependence of intrinsic viscosity on the slope of η_{sp}/c versus c for the irradiated polymer.

○ 0% B

● 0.5% B

□ 2.1, 5.3, 7.1, and 11.3% B

△ 2.7% B irradiated in the presence of air.

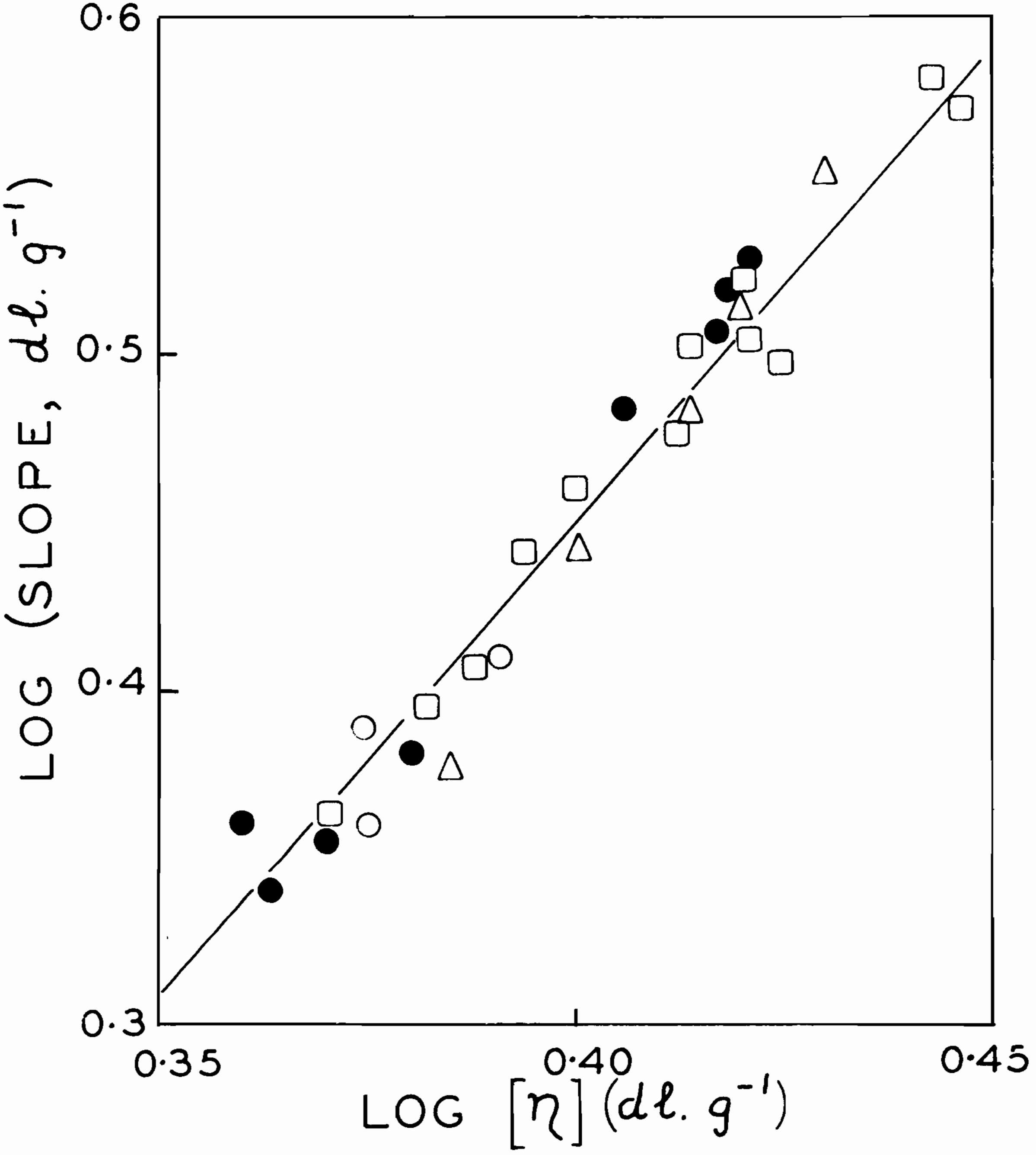
0·6
0·5
0·4
0·3
0·35
0·40
0·45
LOG (SLOPE, dℓ. g⁻¹)
LOG [η] (dℓ. g⁻¹)

Solubility

Fig. 18 shows the manner in which the sol fraction decreases with dose for several different radiation conditions. Complete results are given in Table XIII Appendix II. If each dose is divided by R_g the curves of Fig. 19 result. This is the type of plot shown and explained in the introduction to this thesis. Theoretical curves for random crosslinking imposed on a random M.W.D. are given in Fig. 19 for δ_o of 0.4, 0.7, and 0.9. These theoretical curves were obtained by plotting values of % sol for given values of R/R_g obtained from the curve for $\delta_o = 0$ against $\frac{(R/R_g) - \delta_o}{1 - \delta_o}$. R_g is equal to the experimental value for R_g minus R_o, therefore $\delta_o = \frac{R_o}{R_g}$. This means that $\frac{(R/R_g) - \delta_o}{1 - \delta_o} = \frac{R - R_o}{R_g - R_o}$. The experimental curve is seen to approximate the theoretical curve for δ_o equal to 0.9.

A second method of plotting sol data is presented in Fig. 20 where 1/R is plotted against $S + \sqrt{S}$. This plot emphasizes the change in solubility at high doses whereas Fig. 19 emphasizes solubility behavior at low doses. This is the type of plot shown in Fig. 6 in the introduction to this thesis. From the slopes of the curves at infinite dose shown

Fig. 18

Sol fraction as a function of radiation dose.

○	0% B
●	0.5% B
□	2.1, 5.3, 7.1, and 11.3% B
■	60.0% B
▲	0% B irradiated in the presence of air.
△	2.7% B irradiated in the presence of air.

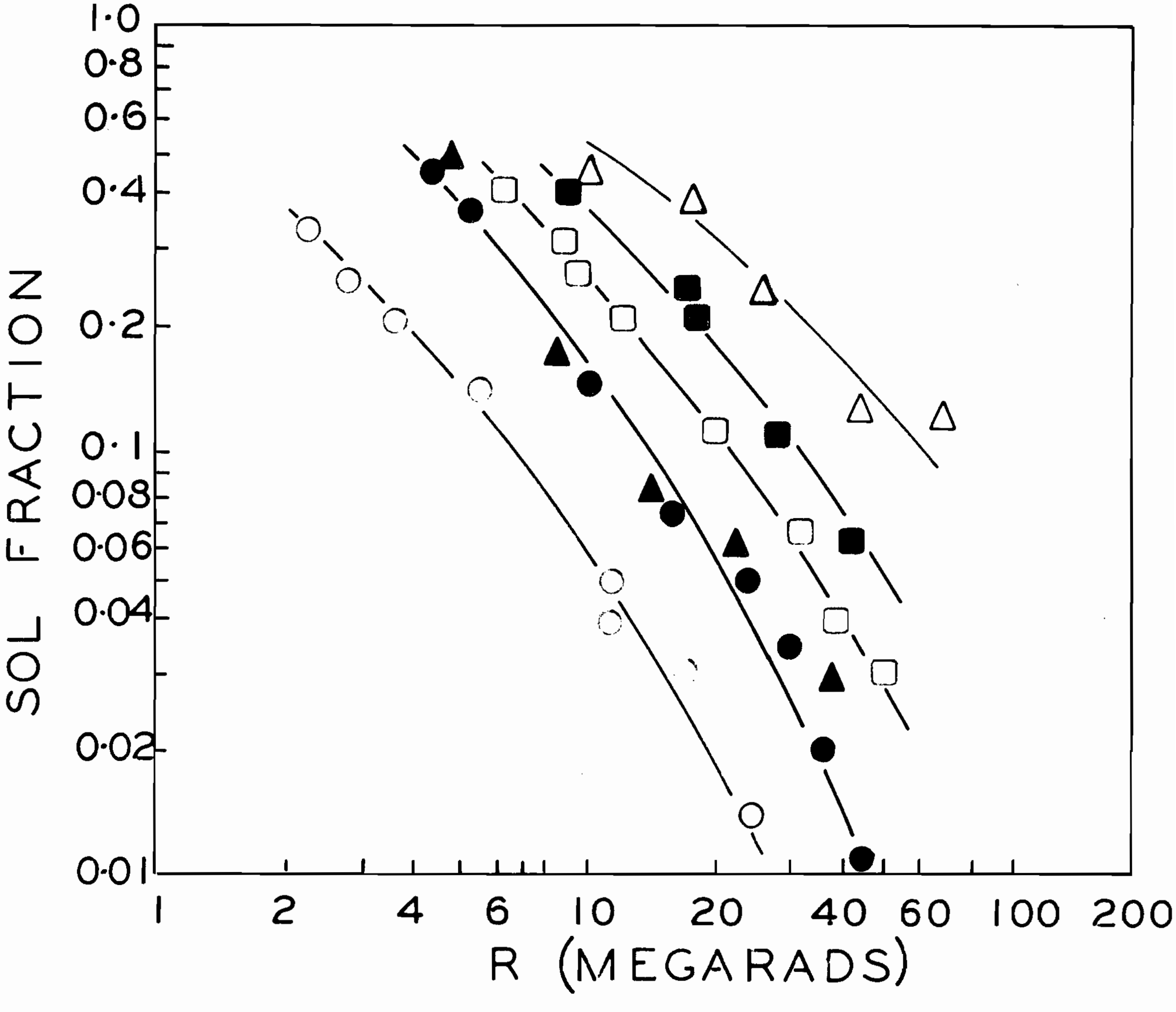
1·0
0·8
0·6
0·4
0·2
0·1
0·08
0·06
0·04
0·02
0·01
SOL FRACTION
1
2
4
6
10
20
40
60
100
200
R (MEGARADS)

Fig. 19

Comparison between theoretical and experimental dependence of sol fraction on R/R_g.

— — — theoretical, random distribution initially

——— experimental

● 0.5% B

○ 0, 2.1, 5.3, 7.1, and 11.3% B

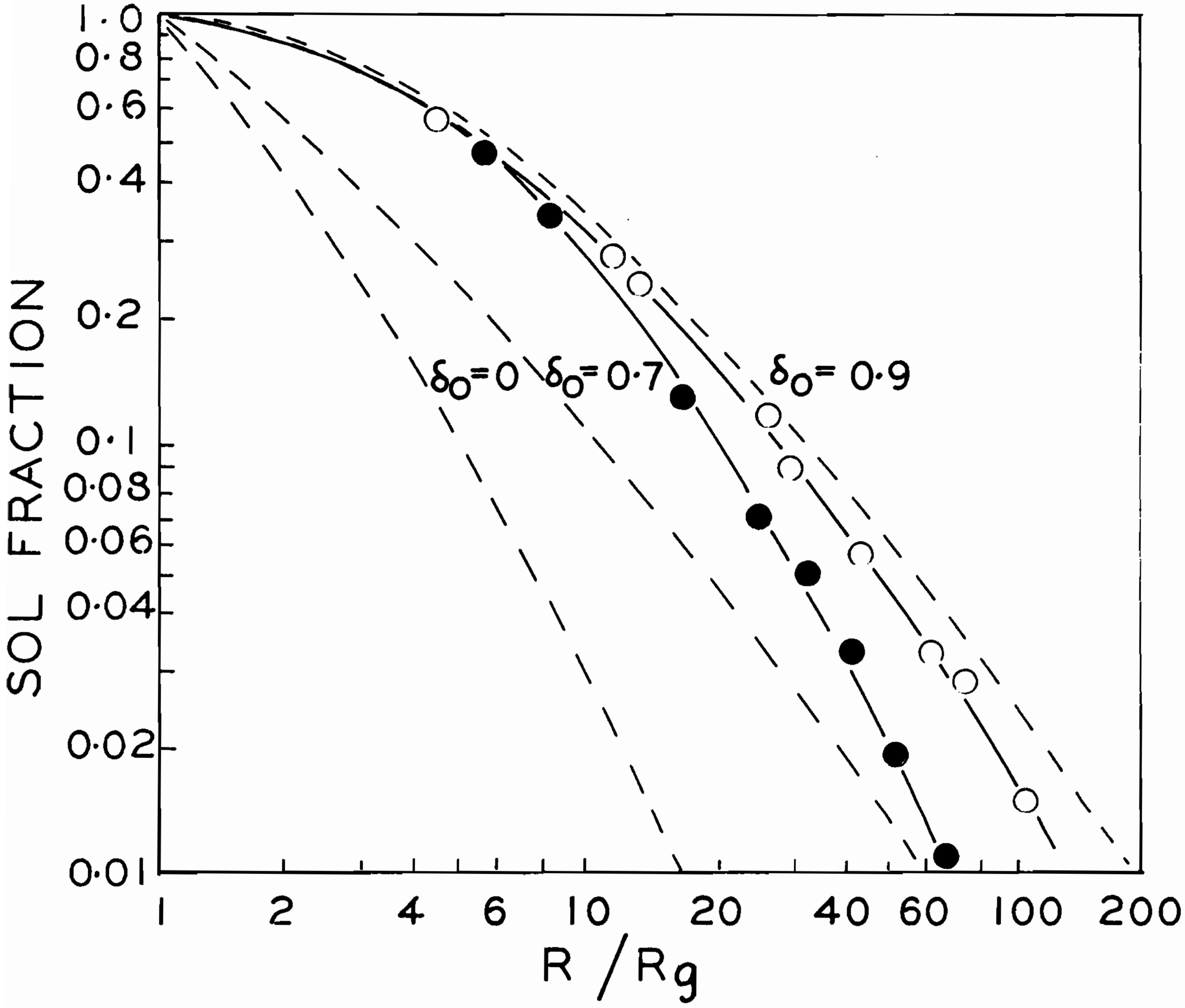

SOL FRACTION
1·0
0·8
0·6
0·4
0·2
0·1
0·08
0·06
0·04
0·02
0·01
1
2
4
6
10
20
40
60
100
200
R / Rg
δ_0=0
δ_0=0·7
δ_0= 0·9

in Fig. 20, and the values of $\overline{M}_{no}$ = 89,900 and w, the monomer unit weight, of 68.4, G_x values in Table V were calculated using equations 25, 29 and 34. These G_x values have been calculated assuming δ_o values of zero and 0.8. Unlike the value of G_x calculated using equation 32, the value of G_x calculated by the present method is affected by the value of δ_o, but only slightly. To correct for the effect of nonlinearity in the unirradiated polymer $(R + R_o)$, rather than R, is used in equation 34.

$$\overline{M}_{no} = \frac{\overline{M}_{noo}}{(1 - \delta_o/4)} \quad \ldots\ldots\ldots (25)$$

$$G_x = 0.48 \times 10^6 \left(\frac{q_o}{w}\right) \quad \ldots\ldots\ldots (29)$$

$$S + \sqrt{S} = \frac{p_o}{q_o} + \frac{1}{q_o \overline{u}_{noo}(R + R_o)} \quad \ldots\ldots (34)$$

In Fig. 21 the solubility data is presented in a plot of log S against R. This type of plot is used to determine whether a chain reaction is occurring. The average slope between 20 and 80% solubility, $\frac{d \log S}{dR}$, is 3.42×10^{-2}. Substituting this value into equation 37, and combining equations 37 and 36

$$\frac{d(\log S)}{dR} = 0.45 \times 10^{-6} \; \frac{G_x \overline{M}_{no}}{i} \quad \ldots\ldots (37)$$

$$R_g = \frac{0.5 \times 10^6}{G_x \overline{M}_{wo}} \quad \ldots\ldots (36)$$

Fig. 20

Plot of $S + \sqrt{S}$ versus 1/R.

○ 0% B
● 0.5% B
□ 2.1, 5.3, 7.1, and 11.3% B
■ 60.0% B
▲ 0% B irradiated in the presence of air
△ 2.7% B irradiated in the presence of air

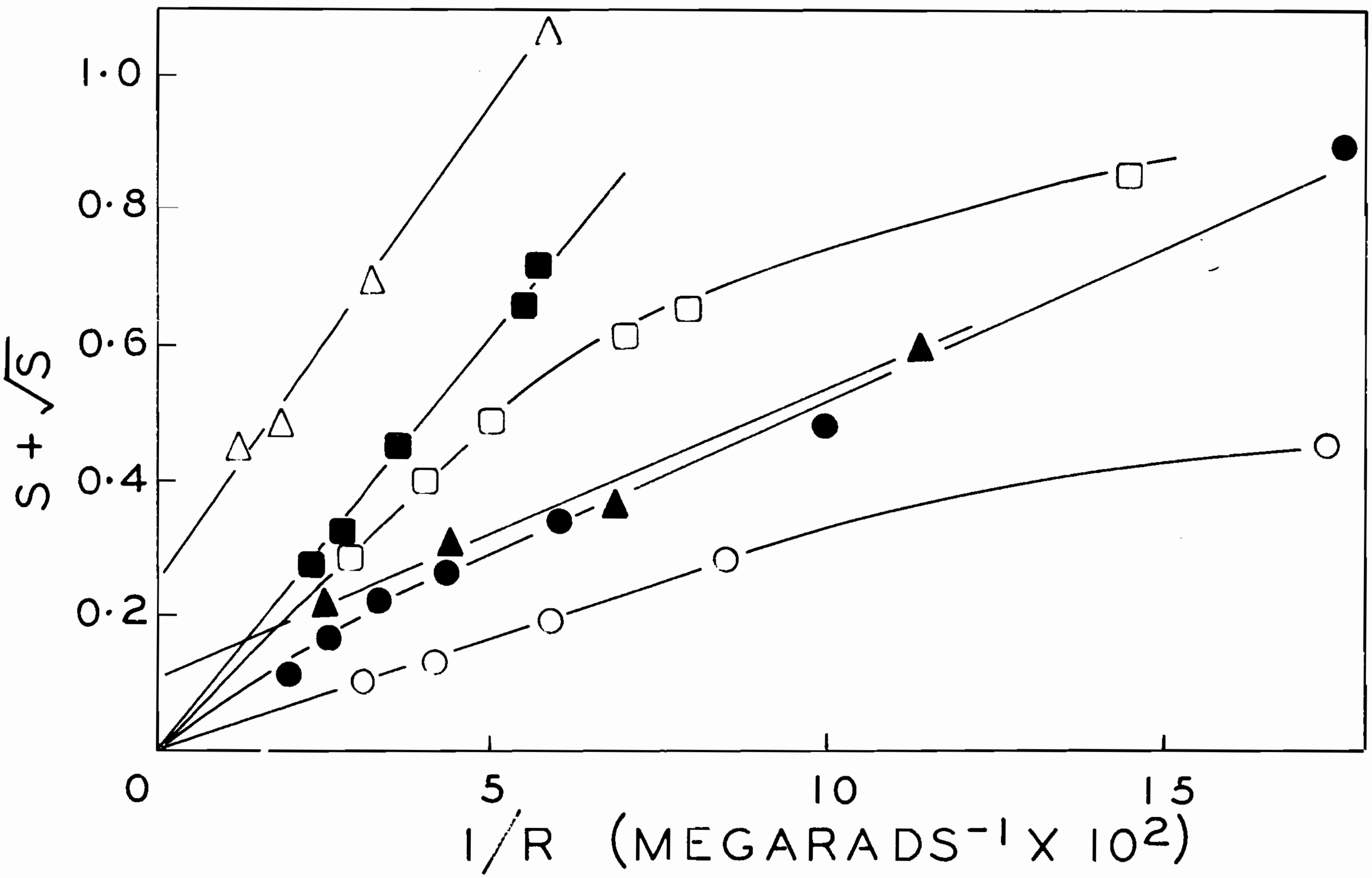

S + √S
1·0
0·8
0·6
0·4
0·2
0
5
10
15
1/R (MEGARADS⁻¹ X 10²)

TABLE V

Values of R_g and G_x for several concentrations of B and for several values for $\bar{M}_{wo}$ and δ_o.

% B	R_g megarads	G_x calculated using equation 32 crosslinks per 100 e.v. absorbed by sample			G_x calculated using equation 34 crosslinks per 100 e.v. absorbed by sample	
		$\bar{M}_{wo}=3.0\times10^5$	$\bar{M}_{wo}=2.4\times10^6$	$\bar{M}_{wo}=4.7\times10^6$	$\delta_o = 0$	$\delta_o = 0.8$
0	0.20	9.41	3.33	1.72	1.62	1.59
0.5	0.54	3.49	1.24	0.64	0.97	0.94
2.1, 5.3 7.1, 11.3	0.69	2.73	0.96	0.50	0.59	0.56
60.0	1.00	1.88	0.67	0.35	0.46	0.43
0*	1.69	3.18	1.13	0.59	1.16	1.10
2.7*	0.53	1.00	0.36	0.18	0.41	0.39

* Irradiated in air.

<u>Fig. 21</u>

Log S versus R for samples with
2.1, 5.3, 7.1, and 11.3% B.

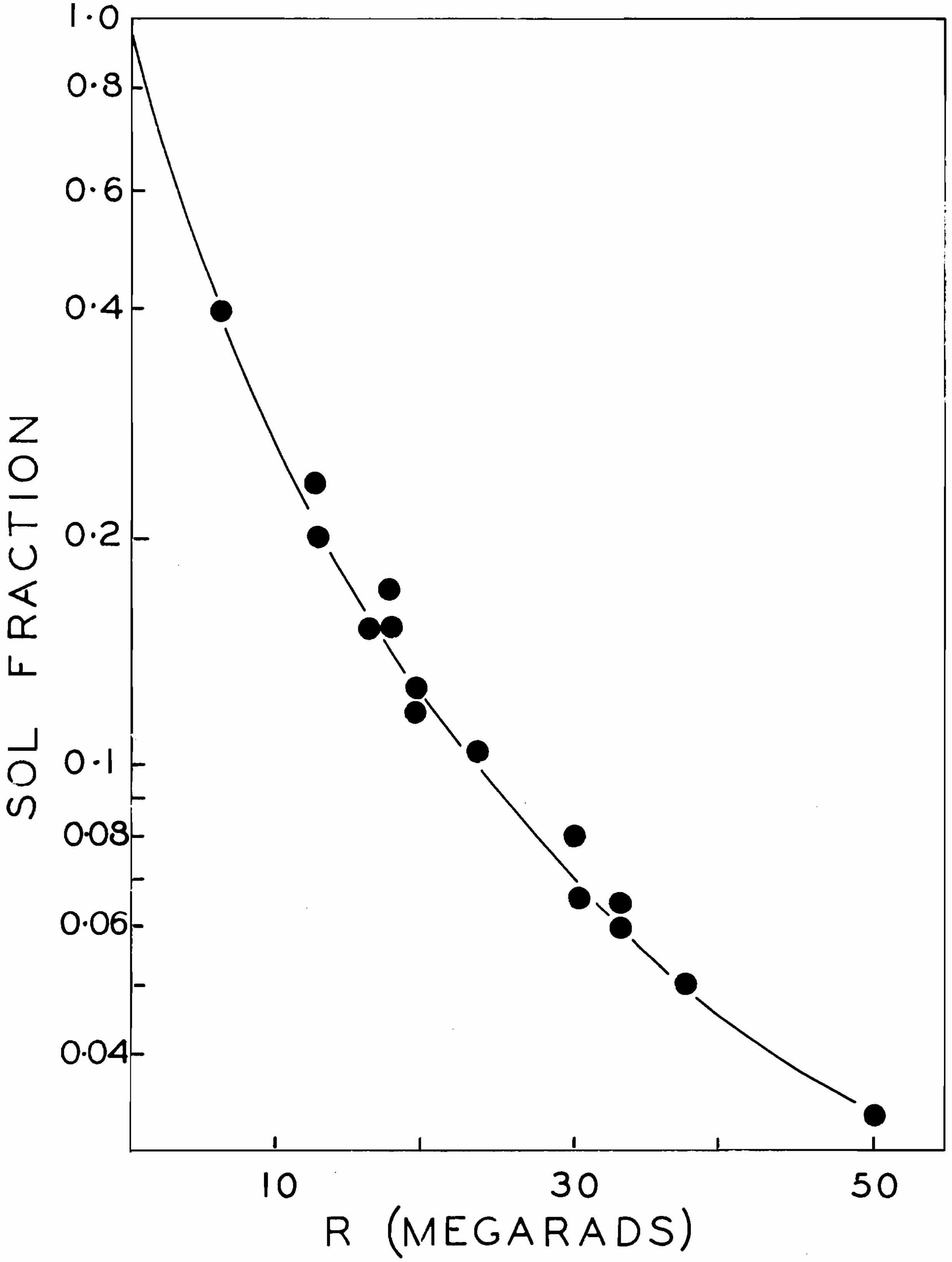
1·0
0·8
0·6
0·4
0·2
0·1
0·08
0·06
0·04
SOL FRACTION
10
30
50
R (MEGARADS)

leads to

$$i = \frac{d(\log S)}{dR} \quad R_g \frac{\bar{M}_{wo}}{\bar{M}_{no}} \quad = \quad 0.203 \frac{\bar{M}_{wo}}{\bar{M}_{no}}$$

The average number of links per chain is $(1 - i)/i$. The ratio of weight average to number average molecular weight according to the molecular weight distribution, M.W.D., of Fig. 13 and also theory (101) is at least two, and therefore, i is close to 0.5 and the number of links per chain is close to one. If a correction is made for δ_o then i will be increased because $d(\log S)/dR$ is uneffected by R_o, $R_g\bar{M}_{wo} = (R_g + R_o)\bar{M}_{woo}$, and $\bar{M}_{noo}$ is less than $\bar{M}_{no}$. These results suggest that crosslinking is not the result of a chain reaction mechanism.

Table VI gives the necessary data for obtaining p_o/q_o by Baskett's method (148). $S + \sqrt{S}$ should become constant after a certain dose. Its value at this point is $S + \sqrt{S} = p_o/q_o$. Table VI shows that except for the lowest dose $S + \sqrt{S}$ increases with dose. Doses sufficiently high to give a constant value of $S + \sqrt{S}$ were not used and the value of p_o/q_o could not be calculated. The results in Table VI indicate that p_o/q_o is greater than 0.013.

TABLE VI

Solubility following irradiation, extraction and irradiation.

Sample	R megarads	% S	$S + \sqrt{S}$
1	5.8	0.819	0.0170
2	25.2	0.280	0.0081
3	42.2	0.315	0.0087
4	122.0	0.568	0.0132

Initial solubility was 5 ± 0.5%.

Swelling

The volume fraction of polymer in the swollen gel was calculated from the equation

$$v_2 = \frac{W_g / \rho_p}{W_b / \rho_o + W_g / \rho_p} \quad \text{.......} \; (57)$$

where W_g and W_b are the weights of dry gel and benzene, respectively, and ρ_o and ρ_p are the corresponding densities. The value of ρ_o is 0.8739 g./ml. (130) and that of ρ_p is 0.941 g./cm^3 (150). The dependence of v_2 on sol fraction is depicted in Fig. 22. The detailed results are given in Appendix II, Table XIII.

Rather than calculate the density of crosslinking, q, for every sample, the values of q corresponding to seven points from the main curve of Fig. 22 were calculated. These points cover a wide range of degrees of crosslinking. The values of R corresponding to these points were obtained from Fig. 18 using the curve for samples containing 2.1, 5.3, 7.1, and 11.3 per cent antioxidant, B.

By definition F is equal to the right side of equation 38.

$$F = \frac{-\rho_p V_1 \left(v_2^{1/3} - v_2 / f_n\right)}{\chi v_2^2 + \ln(1 - v_2) + v_2}$$

Fig. 22

Degree of swelling as a function of S.

○	0% B
●	0.5% B
□	2.1, 5.3, 7.1, and 11.3% B
■	60.0% B
▲	0% B irradiated in the presence of air
△	2.7% B irradiated in the presence of air.

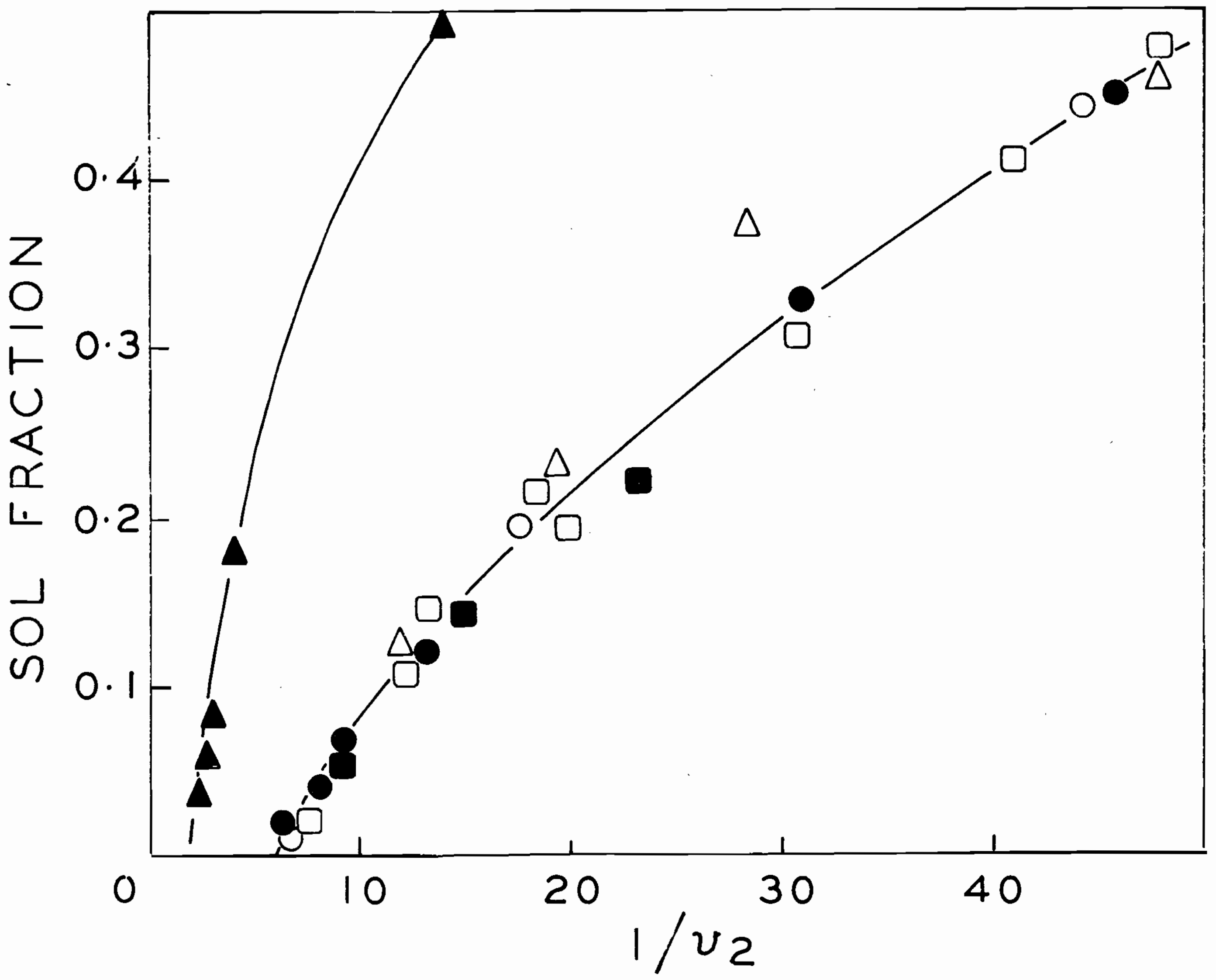
SOL FRACTION
0·1
0·2
0·3
0·4
0
10
20
30
40
$1/v_2$

A value of 0.38 was used for χ, the interaction coefficient between polymer and solvent. This value is the average of the values 0.36 and 0.40 obtained by French and Ewart (134) and Bristow (151), respectively. The values of F given in Table VII were calculated assuming only crosslinking occurred, $f_n = 4$. If endlinking, $f_n = 3$, is assumed the value of F corresponding to a low dose is reduced by approximately 1% and the value corresponding to a very high dose is reduced by approximately 4%. The values of $\bar{M}_{cg}$ uncorrected for chain entanglements were calculated from equation 39

$$F = \frac{\bar{M}_{cg}}{(1 - 2\bar{M}_{cg}/\bar{M}_{nog})} \quad \ldots\ldots\ldots (39)$$

and the values of $\bar{M}_{cg}$ corrected for chain entanglements were calculated from equation 40 using the same correction factors as were found by Blanchard and Wooton for natural rubber.

$$\bar{M}_{cg} = (1 - 4.14 \times 10^{-5}\ \bar{M}_{cg})\ F\ (1 - 2\bar{M}_{cg}/\bar{M}_{nog}) \quad \ldots\ldots (40a)$$

The values of $\bar{M}_{nog}$ used in these equations were calculated from equation 44.

$$\bar{M}_{nog} = \bar{M}_{noo}\ (1 + \sqrt{S}) \quad \ldots\ldots\ldots (44)$$

Equation 25 was employed in calculating $\bar{M}_{noo}$ assuming $\delta_o = 0$ and $\delta_o = 0.8$. Table VII gives the four series of $\bar{M}_{cg}$ values.

TABLE VII

Swelling and crosslinking density data

R megarads	$1/v_2$	% S	$\bar{M}_{nog}\mathrm{x}10^{-4}$ $\delta_o = 0$	$\mathrm{Fx}10^{-4}$	$\bar{M}_{cg}\mathrm{x}10^{-4}$ $\sigma = 0$ $\delta_o = 0$	$\bar{M}_{cg}\mathrm{x}10^{-4}$ $\sigma = 4.1\mathrm{x}10^{-5}$ $\delta_o = 0$	$\mathrm{qx}10^{4}$ $\sigma = 0$ $\delta_o = 0$	$\mathrm{qx}10^{+4}$ $\sigma = 4.1\mathrm{x}10^{-5}$ $\delta_o = 0$
4.6	52	48.0	15.2	46.2	6.5	7.4	4.0	3.0
6.4	36	38.0	14.5	23.7	5.6	6.7	5.5	4.0
10.7	22	24.0	13.4	9.85	4.0	5.6	10.0	6.0
22.5	12	10.0	11.8	3.06	2.0	3.2	25.5	14.5
42.0	8	4.0	10.7	1.39	1.1	1.6	53.5	35.0
50.0	7.2	3.0	10.5	1.12	0.92	1.3	65.0	45.0
62.0	6.5	2.0	10.2	0.89	0.87	1.0	81.5	60.0

$R + R_o$ $\delta_o=0.8$ megarads	$1/v_2$	% S	$\bar{M}_{nog}\mathrm{x}10^{-4}$ $\delta_o = 0.8$	$\mathrm{Fx}10^{-4}$	$\bar{M}_{cg}\mathrm{x}10^{-4}$ $\sigma = 0$ $\delta_o = 0.8$	$\bar{M}_{cg}\mathrm{x}10^{-4}$ $\sigma = 4.1\mathrm{x}10^{-5}$ $\delta_o = 0.8$	$\mathrm{qx}10^{4}$ $\sigma = 0$ $\delta_o = 0.8$	$\mathrm{qx}10^{+4}$ $\sigma = 4.1\mathrm{x}10^{-5}$ $\delta_o = 0.8$
7.36	52	48.0	12.16	46.2	5.37	5.86	4.80	4.10
9.16	36	38.0	11.61	23.7	4.67	5.40	6.38	4.90
13.46	22	24.0	10.71	9.85	3.58	4.01	10.2	8.60
25.26	12	10.0	9.50	3.06	1.86	2.91	26.9	14.80
44.76	8	4.0	8.63	1.39	1.03	1.48	56.2	36.80
52.76	7.2	3.0	8.43	1.12	0.886	1.21	66.4	47.00
64.76	6.5	2.0	8.20	0.89	0.725	0.94	84.2	63.20

The corresponding q values were obtained from equation 45.

$$q = \frac{(1 - \bar{M}_{cg}/\bar{M}_{nog})}{(1 + S)\,\bar{M}_{cg}} \qquad \ldots\ldots (45)$$

Fig. 23 shows the dependence of q on R for q calculated from equation 45, for q calculated using solubility results, and for q calculated from $\bar{M}_{wo} = 203{,}000$ and $R_g = 0.69$ Mrads. The values of q calculated using $\delta_o = 0.8$ were plotted against $(R + R_o)$ where the value of R_o is obtained from equation 33.

$$\frac{R_o}{R_o + R_g} = \delta_o \qquad \ldots\ldots (33)$$

DISCUSSION

Viscosity

A serious deviation from the theoretical curves of the results of the present work is evident in both Figs. 15 and 16. The agreement with Katsuura's theory (92) is fairly satisfactory for low doses if δ_o is 0.36 or zero, but at higher doses or for $\delta_o = 0.8$ the agreement is poor with both theories. The experimental results whether δ_o is 0.8 or zero deviate markedly from the more reliable theory of Kilb (91).

Fig. 23

Crosslinking density calculated from swelling data as a function of R.

— — —	solubility data
———	from swelling data
●	uncorrected for both δ_o and chain entanglements.
○	$\delta_o = 0.8$, uncorrected for chain entanglements.
△	$\delta_o = 0.8$, corrected for chain entanglements.

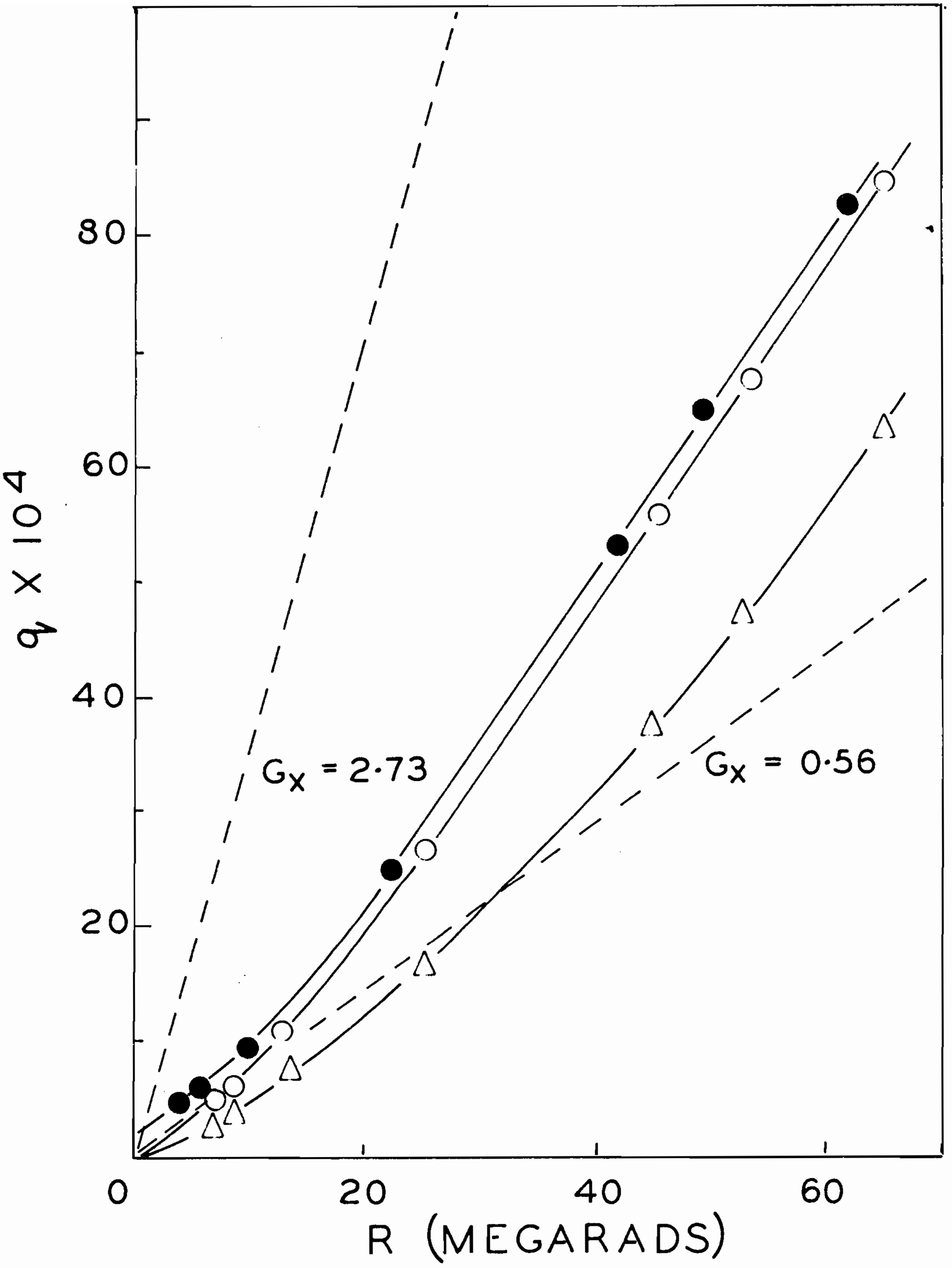
$q \times 10^4$
80
60
40
20
0
20
40
60
R (MEGARADS)
$G_X = 2{\cdot}73$
$G_X = 0{\cdot}56$

The disagreement between theory and experiment might be attributed to many possible sources of error, but the results show that the cause cannot be related to the filtration technique, microgel formation, oxidation, or incomplete evacuation. An unfiltered sample had the same intrinsic viscosity as a filtered sample, and microgel was never detected under any conditions. An irradiated oxidized sample had the same intrinsic viscosity as an irradiated unoxidized sample. The plot of $[\eta]_R/[\eta]_o$ versus R/R_g for a sample irradiated in air was the same as that for a sample irradiated in a vacuum (Fig. 15).

The deviation of experiment from theory might result if chain reaction crosslinking, endlinking, or cyclization occurred, instead of crosslinking, on irradiation of the polymer. The same structural nonlinearity mechanisms which occur on irradiation probably apply to both polybutadiene and poly(butadiene-co-styrene) because G_x for polystyrene (90) is about 0.04, whereas for polybutadiene G_x is about 3.6 (27). Therefore almost all the structural nonlinearity in poly(butadiene-co-styrene) must involve the butadiene units. The change in intrinsic viscosity obtained by Vaughan et al. (152) using monodisperse linear polybutadiene does follow Kilb's theoretical curve. Therefore, the deviation from theory in the experimental data is probably not due to the processes mentioned above.

A basic assumption of the theoretical work is that crosslinking occurs at random. The results of others indicate that crosslinking occurs at random in irradiated polystyrene (153) and polybutadiene (27). The possibility that in a copolymer of styrene and butadiene radiation induced crosslinking is non-random must be considered. Styrene units are distributed at random in the chains of poly(butadiene-co-styrene) (154), and therefore crosslinking probably occurs at random even though the styrene units are much more resistant to radiation than the butadiene units. Styrene protects the butadiene units, but this protective effect probably does not contribute to non-random crosslinking. Witt's results (27) show no change in the shape of the solubility curves with increasing styrene content of GR-S. This is a further indication that the presence of styrene is not causing non-random nonlinearity.

The experimental results can only be compared to the two theories predicting the change in intrinsic viscosity with dose if radiation induced crosslinking is imposed upon either a polymer composed of linear molecules with a random M.W.D. or upon a polymer composed of a mixture of linear and nonlinear molecules where the nonlinearity is caused by randomly distributed tetrafunctional units, and the primary M.W.D. is of the random type. According to the experimental results of Morton (138) almost all the nonlinearity in poly(butadiene-co-styrene) is caused by tetrafunctional units. Bardwell (101) has shown that the primary M.W.D. for this polymer is the random type or slightly broader. According to the theory of Kotliar and Podgar (75) even if the primary M.W.D. is broader than the random type the theoretical curves will be altered in a manner which increases the disagreement between theory and the experimental results of Fig. 15. Flory (137) suggested that a small amount of non-random crosslinking occurs in butadiene polymers if the degree of conversion of monomer to polymer is sufficiently high. There is a possibility that the degree of conversion of the polymer being studied was sufficiently high to cause non-random crosslinking which might be the cause of the disagreement between theory and experiment.

If p_o/q_o is greater than zero, the deviation of experiment from theory will be significantly reduced. Figs. 3 and 4 show the extent to which the value of this ratio affects the theoretical curves. The solubility data presented in Fig. 20 indicate that p_o/q_o is tending to zero and therefore that nonlinear units formed by the irradiation process are not subsequently degraded. There is still the possibility that p_o/q_o is significantly greater than zero at low doses because the value of this ratio when determined by solubility measurements is valid only for high doses. Possibly the nonlinear units in the polymer before irradiation undergo degradation during the early stages of irradiation. Trifunctional units present in polyethylene before irradiation were found to degrade when the polymer was irradiated (155); once these units were destroyed degradation stopped. There is no evidence in the literature for degradation of the tetrafunctional units of any polymer. Although, according to Morton (138) these units rather than trifunctional units produce most of the nonlinearity in poly(butadiene-co-styrene), the possibility that they cause degradation cannot be dismissed.

The deviation of the experimental curves from the theoretical curves might be explained by experimental errors. If the true R_g values are greater than those used in Figs. 15 and 16, and if a is lower than the value used in equation 52 or 53, then there would be a closer agreement between theory and experiment. Figs. 3 and 4 show the important influence of the value of a on the theoretical plots. Neither of these possible errors alone can account for the extent of the disagreement between experiment and theory. To obtain a reasonable agreement the true R_g would have to be twice the experimental value, or a would have to be lower than 0.5. Cleverdon (136) claims that the true a is lower than a as determined by the method used in obtaining equation 52, but judging from his analysis it is unlikely that a could be in error by more than 0.2.

It can be concluded that the deviation from the theories, assuming that the theories are correct, is related either to errors in both R_g and a, or to degradation at low doses or to non-random crosslinking in the unirradiated polymer. The theories might be incorrect in that they underestimate the effect of nonlinearity on intrinsic viscosity when nonlinearity is imposed upon a polydisperse sample. It has already been shown in this thesis that these same theories give a value of δ_o which is lower than the more reliable value bases on the Zimm and Kilb theory (73). This disagreement also indicates that the theories of Kilb (81) and Katsuura (92) underestimate the effect of nonlinearity.

The results of Table V show that R_g is increased by the presence of B in the polymer. This increase in R_g is apparently not caused by an increase in p_o because the dependence of $[\eta]_R / [\eta]_o$ on R/R_g for a sample containing B is approximately the same as for pure polymer.

Equation 56 shows the extent to which k' increases with dose. The variation in k' is probably related to increasing nonlinearity, but not exclusively since increasing polydispersity would also result in a similar variation in k'.

Solubility

Even though Baskett's method (148) for finding p_o/q_o indicates that this ratio is greater than zero, the solubility data as presented in Fig. 20 show that p_o/q_o is almost zero. Therefore the experimental curves in Fig. 19 can be compared to the theoretical curve for $p_o/q_o = 0$. The further conditions for the validity of this comparison are that any nonlinearity in the unirradiated polymer must have been the result of crosslinking randomly imposed on a random primary M.W.D. and the radiation has produced random crosslinking or endlinking. It has already been shown that these conditions are fulfilled, except possibly that of random crosslinking in the unirradiated polymer. However, the extent of non-random crosslinking in the unirradiated polymer is probably small (137); its effect is also probably small because large doses of radiation were used.

An examination of the graph of sol fraction versus R/R_g presented in Fig. 19 shows that the plots for the samples containing 2.1, 5.3, 7.1, and 11.3% B coincide with that for the pure polymer. This indicates that the presence of B does not increase p_o. Fig. 20 giving $S + \sqrt{S}$ versus $1/R$ also shows that for both pure polymer and a mixture of B and polymer $p_o/q_o = 0$. Therefore the increase in R_g shown in Table V must be due to a reduction in q_o caused by B. Furthermore, if the protective effect of B for these samples is not constant the same plot of sol fraction versus R/R_g would not be obtained for both pure polymer and that containing more than 2.1% B. However, for the sample containing 0.52% B the sol fraction tends to decrease more rapidly with R/R_g that for the other samples. This must be because the protective effect of B in this sample is decreasing with increasing dose and hence R_g is decreasing and q_o is increasing with dose. Because the theories to be examined in this section are valid only for a constant value of q_o the results for the sample containing 0.52% B will not be examined here.

If the true values of R_g are greater than those used in Fig. 19, the curve gives a value of δ_o which is too high. A lower δ_o would agree better with $\delta_o = 0.78$ obtained from fractionation data. As previously mentioned, if the value of R_g is increased the viscosity results will agree more closely with theory. Therefore, it is likely that all the R_g values of Table V are lower than the true values.

The solubility results when plotted as in Fig. 21 and analyzed as already described, indicate that a chain reaction is unlikely. If R_g is increased the possibility of a chain reaction becomes even less likely.

If cyclization occurs solubility data would give a value for δ_o which is too high. According to Saito (89), the importance of cylization will increase with increasing dose. Therefore, curves of the shape shown in Fig. 5 for p_o/q_o greater than zero would be obtained. The curve of Fig. 19 shows little resemblance to these curves, consequently the possibility of cyclization is very small.

Table V shows a marked difference between the values of G_x obtained using the slopes of Fig. 20 with $\bar{M}_{noo}$ and those calculated from R_g and $\bar{M}_{wo}$. $\bar{M}_{wo}$ was obtained using $\bar{M}_{no}$ equal to 89,000 and $\bar{M}_{wo}/\bar{M}_{no}$ equal to 2.84 as calculated from the molecular weight distribution curve of Fig. 13. This value for $\bar{M}_{wo}/\bar{M}_{no}$ substituted into equation 22 gives $\delta_o = 0.36$. If values of δ_o of 0.8 and 0.9 are used in equation 22, $\bar{M}_{wo}/\bar{M}_{no}$ values of 8 and 15.5, and $\bar{M}_{wo}$ values of 2,400,000 and 4,700,000, respectively, are obtained. These molecular weight values are approximately an order of magnitude greater than the value of 305,000 based on $\delta_o = 0.36$. Light scattering can be used as an independent measure of $\bar{M}_{wo}$ but was not used in this work because of the extreme sensitivity of this method to small amounts of gel (83). The results of Table V show that when G_x is calculated by equation 32 using these higher values of $\bar{M}_{wo}$ the agreement between the two methods of calculating G_x becomes very good. Charlesby (156) claims that the G_x values of the slope calculation are more accurate since they are obtained by a method relatively insensitive to the molecular weight distribution. This analysis of the solubility data has provided further evidence that δ_o is about 0.8, not 0.36, and therefore the molecular weight distribution curve of Fig. 13 is narrower than the true distribution curve. Moreover, the solubility results support the viscosity theory of Zimm and Kilb (73) which gave $\delta_o = 0.78$, rather than the viscosity theories of Kilb (81), Schultz (90), Katsuura (92), Stockmayer and Fixman (72), and that represented by equation 14 which gave values of δ_o shown in Table II which are considerably less than 0.8. The theory of Kotliar and Podgar (75) predicts an even greater increase in intrinsic viscosity with increasing dose than does Kilb's theory, therefore their theory also underestimates the effect of nonlinearity when the solubility and viscosity results of the present work are considered.

Swelling

Fig. 22 which is a plot of sol fraction versus $1/v_2$ shows one curve for pure polymer irradiated in air and another curve for all the other samples. The significance of the former curve will be discussed in another section.

In obtaining the plot of q versus R presented in Fig. 23 the main solubility curve of Fig. 19 was used. Therefore, any errors in the solubility results will be added to swelling errors. For this reason, and because the correction for chain entanglements has been assumed to be the same as for natural rubber, these results are not as reliable as solubility results.

The plots of q, the density of crosslinking, versus R in Fig. 23 are concave towards the q axis when q is based on swelling data but linear when q is based on solubility data, as would be expected if the degree of nonlinearity is directly proportional to dose. In calculating q from swelling data it was assumed that χ, the interaction coefficient for solvent with polymer, remained constant. Substituting $\bar{M}_{cg}$ from equations 38 into 45 indicates that q is reduced by an increase in χ. Therefore if χ tended to increase with a decrease in the degree of swelling, the plots of Fig. 23 would approach linearity. There is evidence that χ does indeed increase with decreasing degree of swelling for poly(butadiene-co-styrene); French and Ewart (134) found $\chi = 0.36$ for a completely soluble sample, whereas Bristow (151) found $\chi = 0.40$ when v_2, the volume fraction of polymer in the swollen gel, was 0.181. Charlesby (157) has shown that to a good approximation q is directly proportional to $(0.5-\chi)$. Using this approximation it can be calculated that χ must increase from 0.36 at $v_2 = 0$ to approximately 0.43 at v_2 = 0.154 if the plot of q versus R, where q is uncorrected for chain entanglements, is to be linear and agree with q values based on solubility data alone. When q is corrected for chain entanglement the corresponding value of χ is 0.40 at v_2 = 0.154. Applying Flory's (117) equation 46

$$\chi = \chi_1 + \chi_2 v_2 + \chi_3 v_2^2 \qquad \ldots\ldots (46)$$

using the maximum values for χ_1, χ_2, and χ_3 shows that the greatest value χ can have at v_2 = 0.154 is 0.41. The fact that χ for the case of no correction for chain entanglement is greater than the theoretical maximum value, whereas when a correction is made for chain entanglement the value of χ is smaller than this maximum, indicates the importance of chain entanglement.

Turner (158) showed that if p_0/q_0 is a constant greater than zero and no correction is made for chain entanglements, degradation, or changes in χ , a plot of q versus R will result in a curve which is concave towards the R axis. The curve in Fig. 23 does not show this characteristic. Therefore this curve can be taken as further evidence of the absence of any significant amount of degradation occurring in the polymer on irradiation.

After correcting for degradation Turner's (158) plot of q against R for natural rubber is slightly concave towards the R axis. According to his results this type of concavity is indicative of chain entanglements. The absence of such concavity in Fig. 23 might mean that chain entanglements are less important for poly(butadiene-co-styrene) than for natural rubber. If this is true then the assumption that the correction for chain entanglements is the same for both materials is incorrect.

Fig. 23 shows that q values calculated from swelling data are much closer to q values calculated from solubility data than to q values based on $G_x = 2.73$. The value 2.73 for G_x is calculated from equation 32 using $\bar{M}_{wo} = 302{,}000$. This value for $\bar{M}_{wo}$ is based on the assumption that $\delta_o = 0.36$. Therefore swelling data provide further evidence that $G_x = 0.56$, not 2.37, and δ_o and $\bar{M}_{wo}$ are approximately 0.8 and 2,400,000, respectively, not 0.36 and 302,000.

CONCLUSIONS

The following conclusions pertain to samples irradiated in a vacuum. The swelling and particularly the solubility results suggest that p_o/q_o is approximately zero, that $G_x = 1.6$ for pure polymer, and that δ_o is between 0.8 and 0.9. This value for δ_o indicates that the experimentally determined M.W.D. is much narrower than the true M.W.D. and also that of the many theories examined which predict the effect of nonlinearity on viscosity for either a monodisperse or polydisperse sample only the theory of Zimm and Kilb (73) gives an accurate value for δ_o. All the other viscosity theories underestimate the effect of nonlinearity on intrinsic viscosity. This tendency to underestimate in three of the theories, Kilb (81), Schultz (90) and Katsuura (92). is also shown by the manner in which the experimentally determined dependence of intrinsic viscosity on dose deviates from theoretical predictions. But, this deviation might also be caused by non-random crosslinking or endlinking in the unirradiated polymer, by a value of p_o/q_o greater than zero at low doses, or by very large errors in both R_g and a.

All the results indicate that the presence of B in the polymer lowers q_o but does not increase p_o. Furthermore, for samples containing more than 2.1% B the protective effect remains constant over the dose range examined. Solubility results show that the protective effect decreases with increasing dose for a sample containing 0.52% B.

The swelling results indicate that the correction for chain entanglements for poly(butadiene-co-styrene) is probably not the same as for natural rubber. The disagreement between q values from swelling results and those from solubility results are probably related to either chain entanglements or to both chain entanglements and changes in χ.

An analysis of the solubility data reveals that neither cyclization nor crosslinking by a chain reaction is the cause of nonlinearity in the irradiated polymer. Therefore, radiation induced nonlinearity is probably caused by either endlinking or crosslinking, or both these processes.

RADIATION INDUCED CHEMICAL CHANGES

EXPERIMENTAL

Destruction of Antioxidant

The destruction of the antioxidant, B, was studied by extracting an irradiated sample with a solvent which dissolves B, but not polymer, and determining the concentration of B in the solvent by ultraviolet spectroscopy.

Exactly 1.8 grams of polymer containing 0.52% B were cut into pieces of about 1 x 1 x 2 mm. These pieces were placed in a 150 ml. electrically heated flask equipped with a condenser. The polymer was refluxed in 50 ml. of ethanol - toluene azeotrope, E.T.A., containing 7 parts of ethanol to 3 parts of toluene. After four hours of refluxing the solution was cooled and the supernatant decanted into a 250 ml. volumetric flask. This extraction was repeated four times. The volume of the combined supernatants was made up to 250 ml. by washing the extracted polymer with small portions of E.T.A. A 4 ml. sample of this solution was transferred by pipette to a 100 ml. flask, 21 ml. of pure E.T.A. added and the solution made up to 100 ml. with anhydrous ethanol. The absorbance of the solution was determined using a Beckman Model DK-1 spectrophotometer. The peak at 308 millimicrons was attributed to B. This technique is essentially the same as the standard method for the determination of the antioxidant content of GR-S (159).

The sample containing 5.46% B was treated in the same manner as the 0.52% sample, with appropriate modification for the higher B content. Only 0.3 grams were extracted and the collective supernatants made up to 250 ml. A 10 ml., rather than 4 ml., aliquot was transferred to the 100 ml. flask. To make the concentration of E.T.A. in the final solution the same as for the 0.52% B sample, 15 ml. of the azeotrope were added.

Several irradiated samples which initially contained 5.46% B were divided into two portions. One portion was extracted as already described; the other portion was extracted using cold E.T.A. In the cold extraction process the sample was extracted in E.T.A. at room temperature for two days instead of being refluxed for four hours.

The absorbancy index of B was determined from the analysis of several solutions of known B content. These solutions were made by dissolving a known weight of B in E.T.A. and increasing the volume with ethanol until 25% of the final solution was E.T.A.

Infra-red and Ultraviolet Spectra

A solution technique could not be used to obtain the infra-red spectrum of the insoluble irradiated polymer. A thin film of unirradiated polymer was formed between two sodium chloride plates by evaporating the benzene from a small amount of solution spread on the plates. The film, held between the plates, was dried in a high vacuum and its spectrum measured on a Perkin - Elmer Model 21 spectrophotometer. The sample was placed in a glass tube which was evacuated to 0.1 micron for at least a day and then sealed under vacuum. The sample was irradiated and the infra-red spectrum was again measured.

The infra-red spectra used to determine the composition of the unirradiated polymer were obtained by measuring the spectra of the solutions of the polymer in carbon disulphide of known polymer concentration (160).

Evans' method (161) was employed to obtain the ultraviolet spectrum. A concentrated solution of polymer in benzene was placed in a glass ring floating on mercury. On evaporation of the benzene a thin circular film of polymer remained attached to the sides of the ring. Because very thin films were desired rings of about one cm. diameter were used. When larger rings were used the film would break during or shortly after, removal from the mercury surface. The ultraviolet spectrum was examined for polymer irradiated both in air and in vacuum.

The high sensitivity of sodium chloride crystals to moisture made it necessary to employ the glass ring method to prepare the sample when the infra-red spectrum of polymer irradiated in air was to be obtained.

The ultraviolet spectrum of B was found from a dilute solution of B in iso-octane. The potassium bromide pellet method (162) was used to obtain the infra-red spectrum of B.

Gas Evolution

Gas evolution associated with irradiation was measured in a calibrated manifold. The sealed tube containing the irradiated sample was placed in a vertical tube attached to a manifold containing a McLeod gauge. The system was pumped to a high vacuum, then the pumping system was isolated from the manifold. The pressure in the manifold was monitored for 15 minutes to assure the absence of leaks. A small metal ball suspended at the top of the vertical tube was then dropped on the tip of the glass sample tube causing it to break. After waiting 10 minutes for the gas released from the tube to distribute itself uniformly throughout the system, the change in pressure was determined. From the volume of the entire system, and the volume and constants of the McLeod gauge, the moles of gas released from the tube were calculated.

The composition of the gas evolved during the irradiation of pure polymer and pure B was determined mass spectrometrically.

RESULTS

Destruction of Antioxidant

From an examination of the experimental results given in Fig. 25 it is evident that the temperature of extraction, room temperature or reflux temperature, does not affect the data.

The Beer-Lambert law may be expressed as

$$A = \log(I_o/I) = a,bc$$

where A is the absorbancy; I_o and I are the intensities of the light transmitted through solvent and solution, respectively; c is the concentration of the solute, in grams per ml., of solution; a, is the absorbancy index, in ml./g.cm., and b is the length, in cm., of the path the light travels in passing through the solution. b was one cm. in all the experiments. a, was found to be 103×10^3 ml./cm.g. Then

$$c = \frac{A \times 10^{-3}}{103} \qquad \ldots\ldots\ldots (58)$$

If Q is the weight fraction of soluble B in the sample, then,

$$Q = c\left(\frac{250}{W}\right)\left(\frac{V_3}{V_2}\right) \qquad \ldots\ldots\ldots (59)$$

where W is the weight in grams of the sample extracted, V_2 is the volume in ml. taken from the original 250 ml. of solution made up in turn to V_3. The variation of Q with radiation dose is given in Fig. 24 and 25.

The material balance for the effect of radiation on a mixture of polymer and antioxidant is

$$B_o + P_o = B_R + B_D + B_{DG} + P_R + P_{DG} \qquad \ldots. (60)$$

Fig. 24

Antioxidant content as a function of dose. 0.52% B before irradiation. Q is the weight fraction of soluble antioxidant.

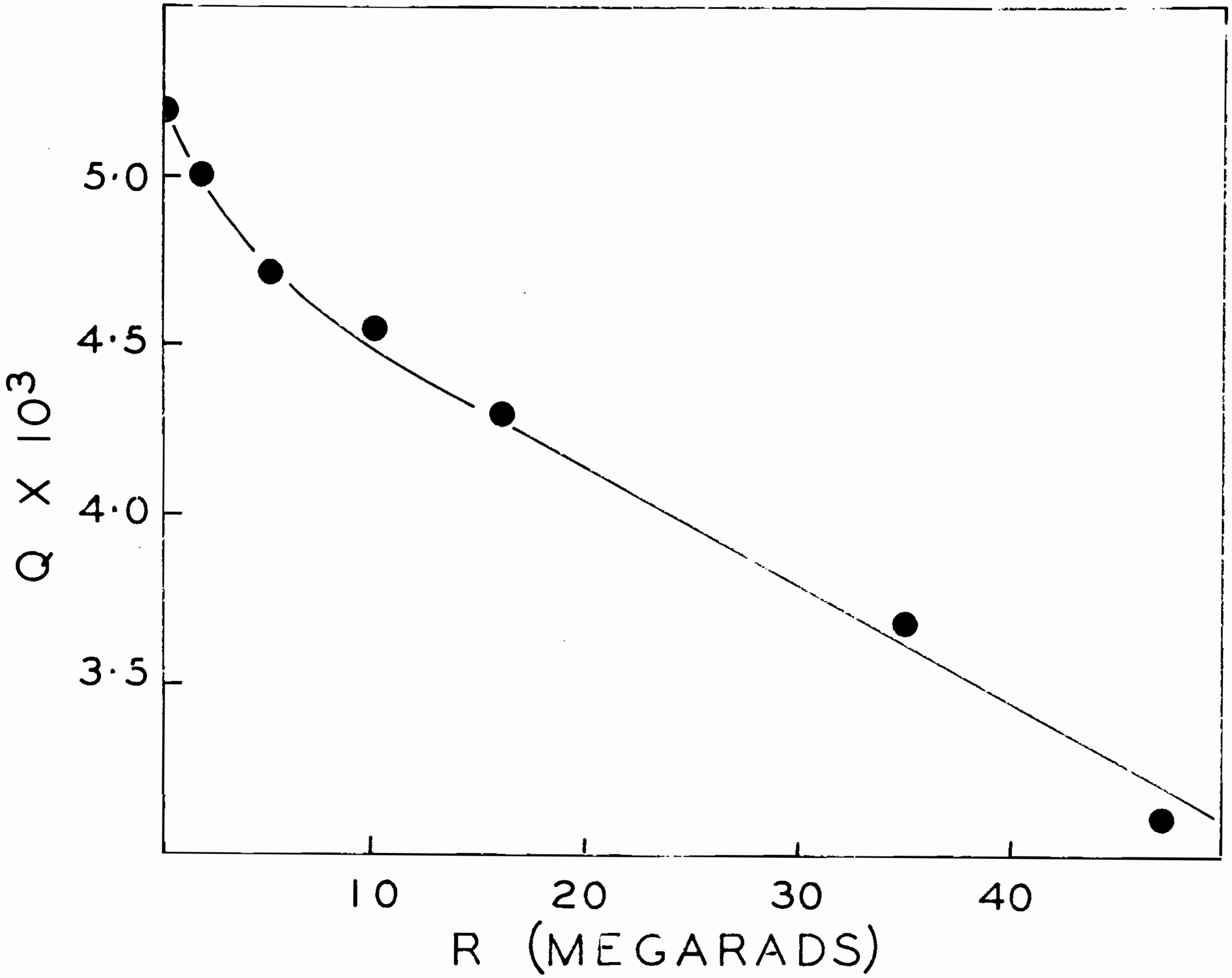
5·0
4·5
4·0
3·5
Q X 10^3
10
20
30
40
R (MEGARADS)

Fig. 25

Antioxidant content as a function of dose. 5.46% B before irradiation. Q is the weight fraction of soluble antioxidant.

○ reflux temperature extraction

● room temperature extraction

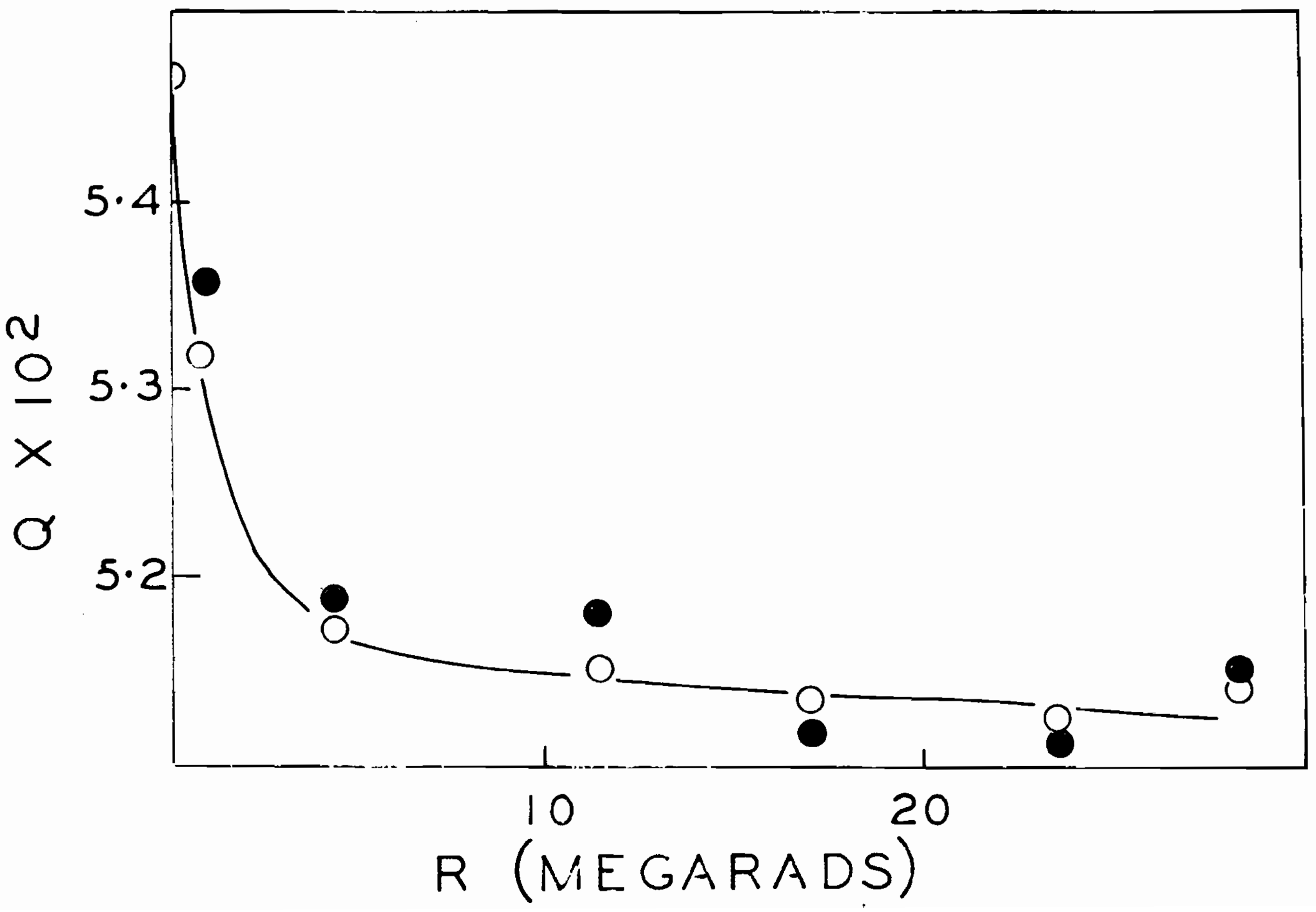
Q X 10²
5·4
5·3
5·2
10
20
R (MEGARADS)

B_o and P_o are the weights of antioxidant and polymer, respectively, in the unirradiated sample. All the symbols of the right hand side of this equation represent weights in the irradiated sample. B_R is the weight of antioxidant which is soluble in E.T.A., B_D is the weight of antioxidant attached to the polymer, and B_{DG} the weight of antioxidant decomposed to gas or to fragments which do not absorb in the same ultraviolet region as the pure antioxidant. P_R and P_{DG} are the weights of polymer extracted and decomposed to gas, respectively.

The number of molecules of antioxidant which are destroyed or become attached to the polymer per weight average primary molecule is

$$D = \left[(B_D + B_{DG}) \frac{N}{217} \right] \left[\frac{\bar{M}_{woo}}{P_o \; N} \right] \qquad \ldots\ldots (61)$$

where 217 is the molecular weight of the antioxidant and N is Avogadro's number. The value of Q before irradiation is

$$Q_o = \frac{B_o}{B_o + P_o} \qquad \ldots\ldots (62)$$

whereas after irradiation

$$Q_R = \frac{B_R}{B_R + P_R + B_D} \qquad \ldots\ldots (63)$$

Substituting the relation $B_D + B_{DG} = B_o - B_R$ and equations 62 and

63 into equation 61 leads to

$$D = \frac{\bar{M}_{woo}}{217}\left[\frac{1}{1 - \frac{1}{Q_o}} - Q_R(B_R + P_R + B_D)\right] \qquad ..... (64)$$

If it is assumed that $P_R = P_o$ and $B_D = 0$ then

$$D = \frac{\bar{M}_{woo}}{217}\left[\frac{1}{(1 - 1/Q_o)} - \frac{1}{(1 - 1/Q_R)}\right] \qquad ...... (65)$$

This can be simplified to

$$D = \frac{\bar{M}_{woo}}{217}\left[\frac{Q_R - Q_o}{(1 - Q_o)\,(1- Q_R)}\right] \qquad .... (65a)$$

Because of the assumptions, D calculated by this equation will be greater than the true value.

It has already been concluded in another section of this thesis that δ_o is approximately 0.8. If $\delta_o = 0.80$ is used in equations 25a and 22, $\bar{M}_{woo}$ is found to be 143,800. Using this value of $\bar{M}_{woo}$ in equation 65a together with Q values from Fig. 24 for the sample containing 0.52% B gives D = 1.32 for a dose of 50 Mrad. Because of the assumptions made in deriving equation 65a this value for D is probably greater than the true value. Even if $\delta_o = 0.4$, rather than 0.80, is used, D is only increased to 1.48; therefore, the effect of an error in the value of δ_o on the calculated value of D is small.

Changes in the Spectra

Fig. 26 gives the infra-red spectrum of pure polymer before and after irradiating in a vacuum to a dose of 150 Mrads. The decrease in the peaks at 912, 995, and 1642 $cm.^{-1}$ indicates the destruction of vinyl groups. A dose of 35 Mrads had no effect on the spectrum of a polymer containing 2.7% B.

The change in the infra-red spectrum on irradiating pure polymer in air to a dose of 10 Mrads is also given in Fig. 26. Pure polymer exposed to air for the same period as required for a dose of 20 Mrads showed only a small change in infrared spectrum. A sample containing 2.7 % B showed a detectable change in the spectrum on irradiation in air only after the dose exceeded 50 Mrads.

The spectra from the carbon disulphide solutions were analyzed by Hampton's method (160). Styrene, vinyl, and 1,4-trans units are represented by peaks at 700, 913, and 970 $cm.^{-1}$, respectively. The composition obtained in the present work was 31.5% styrene, 17.9% vinyl, 13.1% 1,4-cis, and 68.7% 1,4-trans, compared to values obtained by Polymer Corporation of 28.7%, 20%, 7% and 73%, respectively.

Ultraviolet spectra of pure polymer before and after irradiation are given in Fig. 27 for irradiation carried out in

Fig. 26

Radiation induced changes in the infra-red spectrum.

——— unirradiated

...... irradiated in vacuum, 150 Mrads

— — — irradiated in air, 10 Mrads

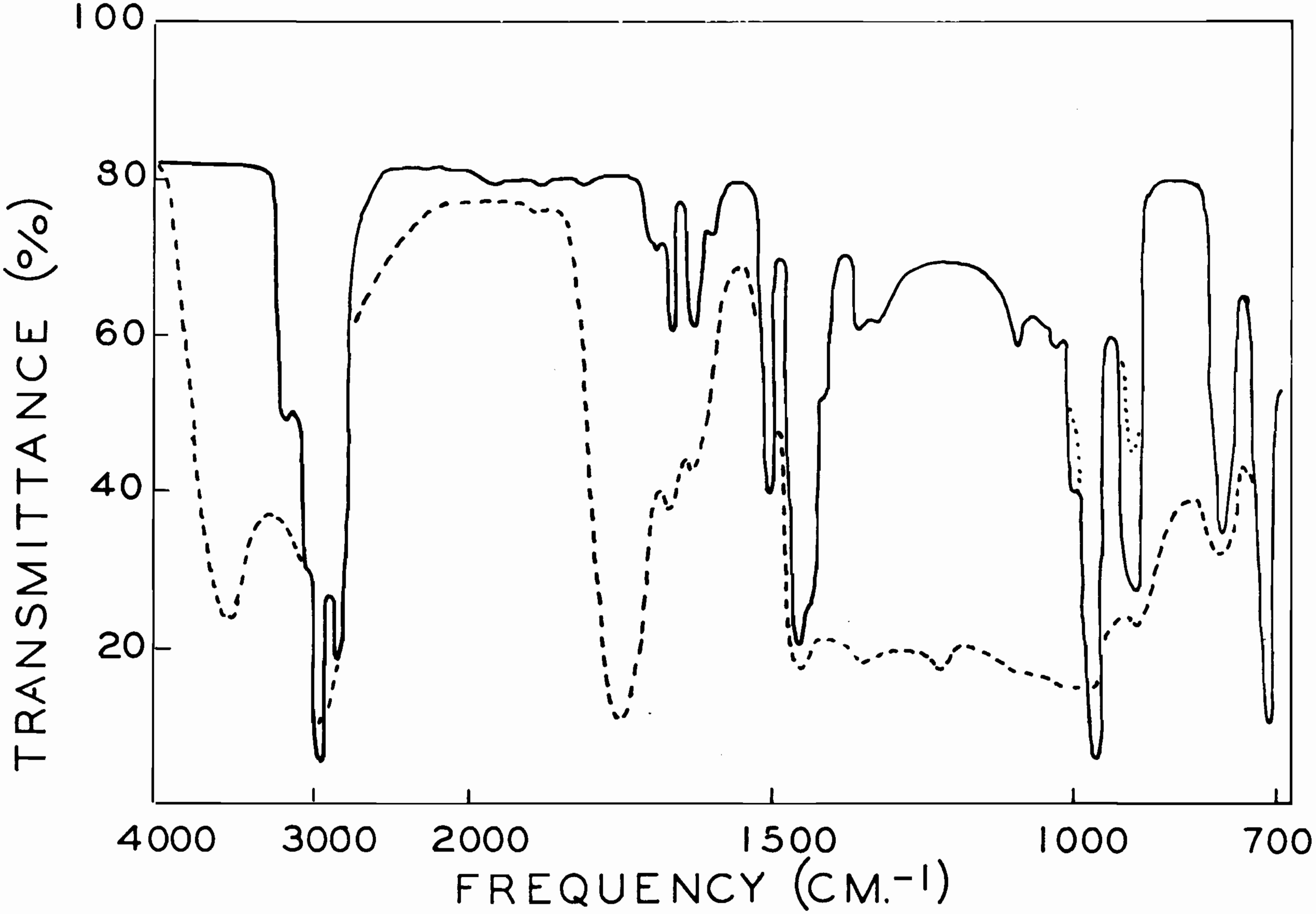
100
80
60
40
20
TRANSMITTANCE (%)
4000
3000
2000
1500
1000
700
FREQUENCY (CM.-1)

Fig. 27

Radiation induced changes in the ultraviolet spectrum.

――――	unirradiated
......	irradiated in vacuum, 100 Mrads
— — —	irradiated in air, 12 Mrads

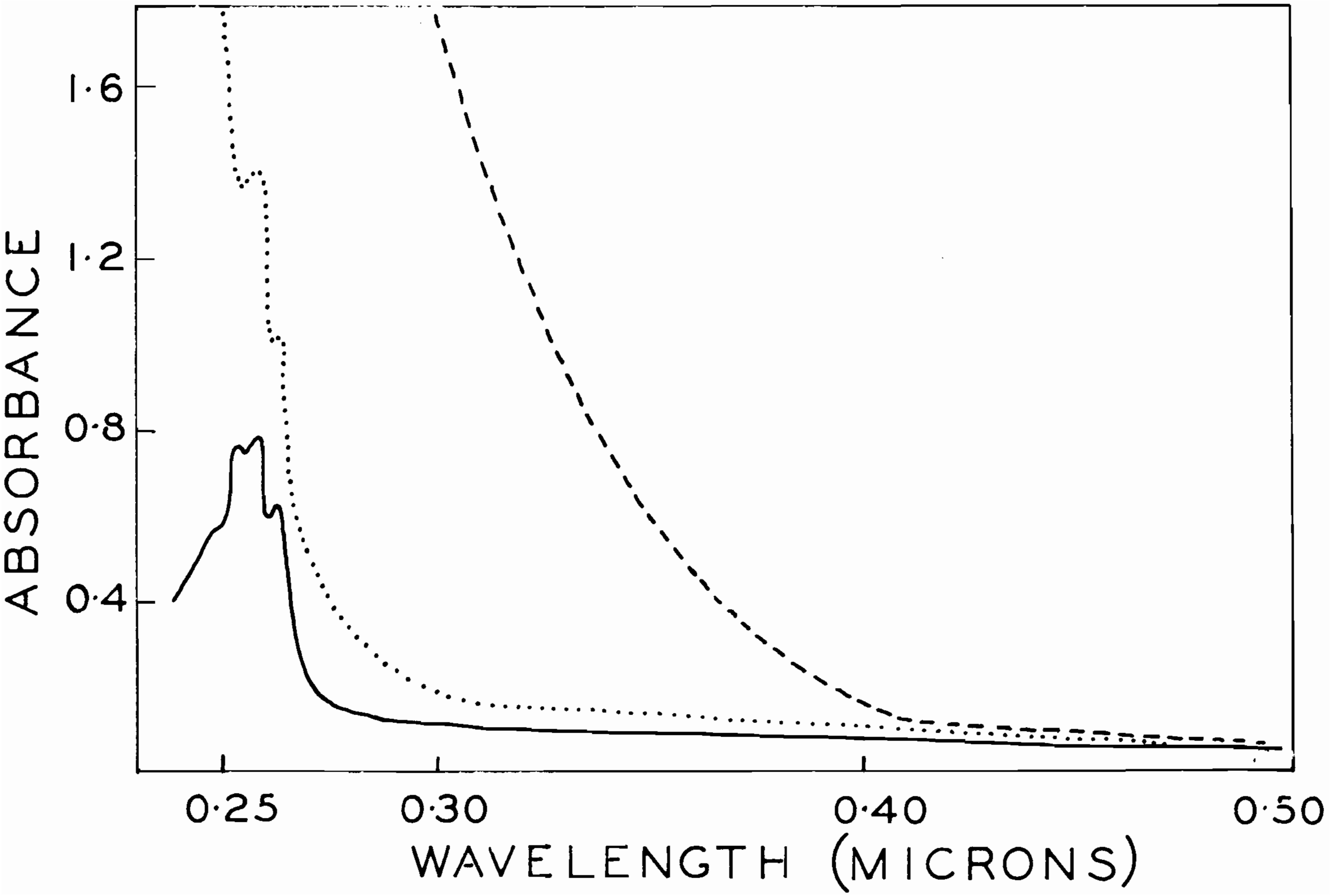
ABSORBANCE
1·6
1·2
0·8
0·4
0·25
0·30
0·40
0·50
WAVELENGTH (MICRONS)

air and in vacuo. The unirradiated spectrum is the same as that obtained by others (163).

Irradiating pure B in a vacuum to a dose of 25 megarads had no effect on either the infrared or ultraviolet spectra. The infrared spectrum was the same as that found by Angert (164), and the ultraviolet spectrum was identical to that obtained by Rehner (165).

Gas Evolution

The moles of gas per gram of sample, Y, was calculated from

$$Y = \frac{1.99 \times 10^{-4} (h_2^2 - h_1^2)\, C_c\, V_s}{R^1 T\, W} \qquad \ldots\ldots (66)$$

where 1.99×10^{-4} is the McLeod gauge constant; h_1 and h_2 are the initial and final mercury column heights, in cm., C_c is the compression correction and is 1.135; V_s, the volume of the system, is 480 ml.; T the temperature (room) in °K; R^1 the gas constant; and W the sample weight in grams.

The data obtained for the dependence of Y on the dose are plotted in Fig. 28. From the slopes of the plots the molecules of gas per 100 e.v. absorbed, G_g, was calculated using the equation

$$G_g = \left(\frac{dY}{dR}\right)\left(\frac{N}{6.24 \times 10^{11}}\right) \qquad \ldots\ldots (67)$$

Fig. 28

Gas yield as a function of dose.

○	0% B
●	0.5% B
□	2.1, 5.3, 7.1, and 11.3% B
■	60.0% B

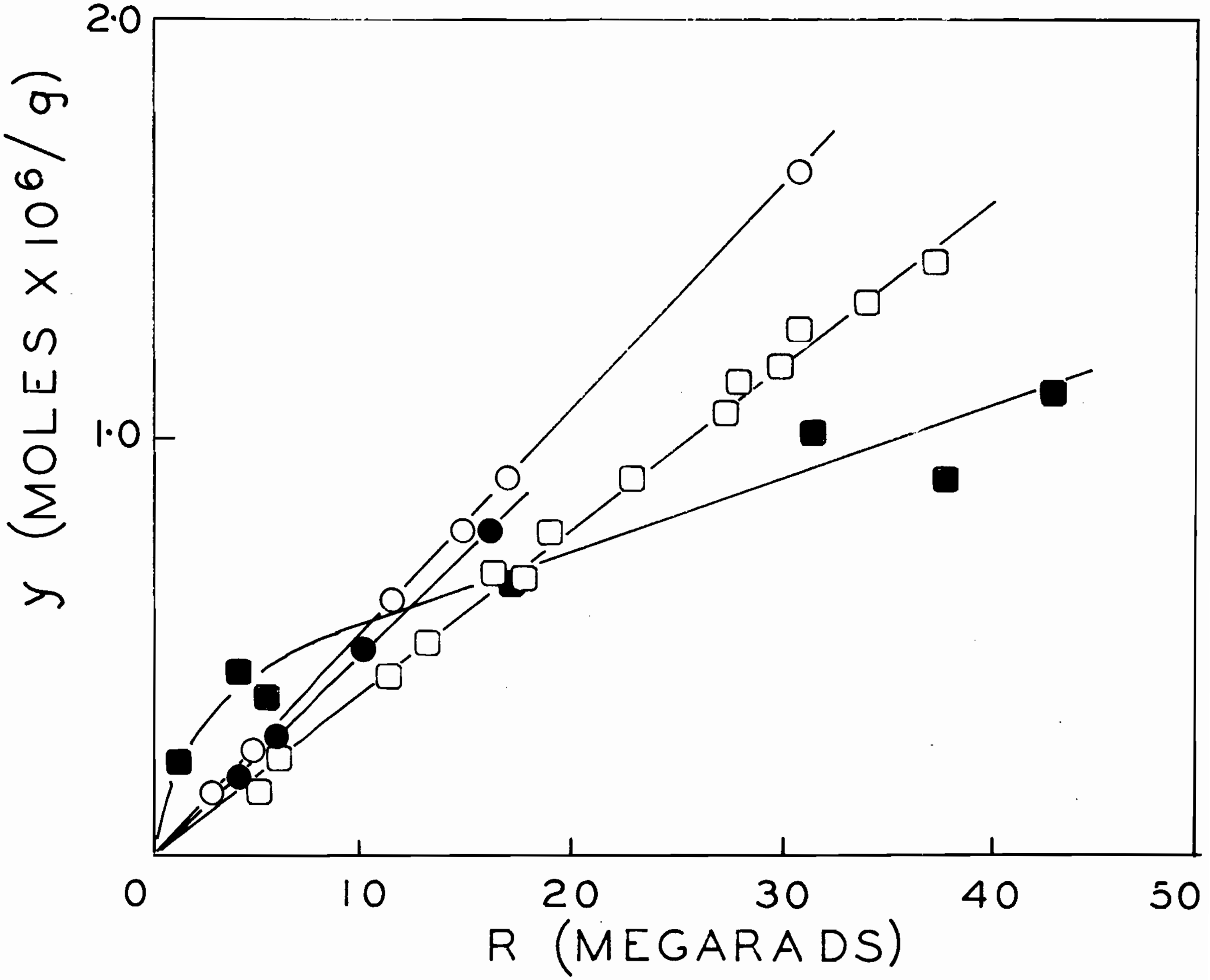
y (MOLES X 10⁶/ g)
2·0
1·0
0
10
20
30
40
50
R (MEGARADS)

In this equation N is Avogadro's number and 6.24×10^{11} is the number of 100 e.v. equal to one gram-rad. The values of G_g obtained by this method are given in Table VIII. Fig. 28 indicates that G_g for the sample containing 60% B decreases with increasing dose; the initial value of G_g is 1.8, whereas at a dose of 42 Mrads G_g is approximately 0.25.

The "mixture law" (166) states that, if the radiolysis of a material X gives a product M with a yield G_m then, in a mixture where the electron fraction of X is E_A, the yield of M is G_mX_A. This law may be expressed for the system studied here as

$$G_g = \left(\frac{PE_p}{PE_p+BE_b}\right) G_{gp} + \left(\frac{BE_b}{PE_p + BE_b}\right) G_{gb} \quad ..(68)$$

where E_p and E_b are the electron densities of polymer and antioxidant, respectively; P and B the weights of polymer and antioxidant, and G_{gp} and G_{gb} are the values of G_g for pure polymer and pure antioxidant, respectively. Because the value of E_p is approximately equal to that of E_b, ($E_p = 3.322 \times 10^{-23}$ and $E_b = 3.195 \times 10^{-23}$ electrons per gram), equation 66 may be simplified to

$$G_g = \left(\frac{P}{P + B}\right) G_{gp} + \left(\frac{B}{P + B}\right) G_{gb} \quad .... (68a)$$

The antioxidant does not contribute to the formation of nonlinear units and so the "mixture law" as applied to G_x

TABLE VIII

Dependence of G_g and G_x on concentration of B.

% B	G_g from plot of gas yield versus dose and from equation 70	G_x from equation 34 and $\delta_o = 0.8$
	molecules of gas per 100 e.v. absorbed by sample	crosslinks per 100 e.v. absorbed by sample
0	0.52	1.59
0.5	0.48	0.94
2.1, 5.3 7.1, 11.3	0.38	0.56
60.3	1.8 if R = 0 0.25 if R = 40 Mrads	0.43
100.0	0.04 if R = 6 Mrads 0.02 if R = 54 Mrads	0.00

becomes

$$G_x = \left(\frac{P}{P + B}\right) \quad G_{xp} \qquad \ldots\ldots\ldots (69)$$

where G_{xp} is the value of G_x for the pure polymer.

Values of G_g and G_x from experiment and G_g and G_x from equations 68a and 69 are plotted against % B in Fig. 29. G_g for the sample containing 60% B is not shown because it was very dose-dependent. This graph shows that at low B content G_g and G_x are much less than predicted by equations 68a and 69.

In Table XIV of Appendix III the values are given for G_g calculated from gas yield and dose according to the equation

$$G_g = \left(\frac{Y}{R}\right)\left(\frac{N}{6.24 \times 10^{11}}\right) \qquad \ldots\ldots (70)$$

G_g at low doses had to be calculated by this equation rather than from a plot of Y versus R because of the pronounced scatter of the points at these doses in a plot of Y versus R. Table XIV in Appendix III shows that G_g for samples irradiated to low doses is generally greater than G_g corresponding to high doses. This Table also gives G_g calculated by equation 70 for pure B irradiated to three doses. G_g for pure B decreased slightly with increasing dose, G_g = 0.039 at 6.31 Mrads and 0.021 at 54.2 Mrads, but not to the extent that G_g decreased for the sample containing 60% B.

Fig. 29

G_g and G_x as a function of B concentration.

– – – theoretical

——— experimental

○ G_g, molecules of gas per 100 e.v. absorbed

● G_x, crosslinks per 100 e.v. absorbed

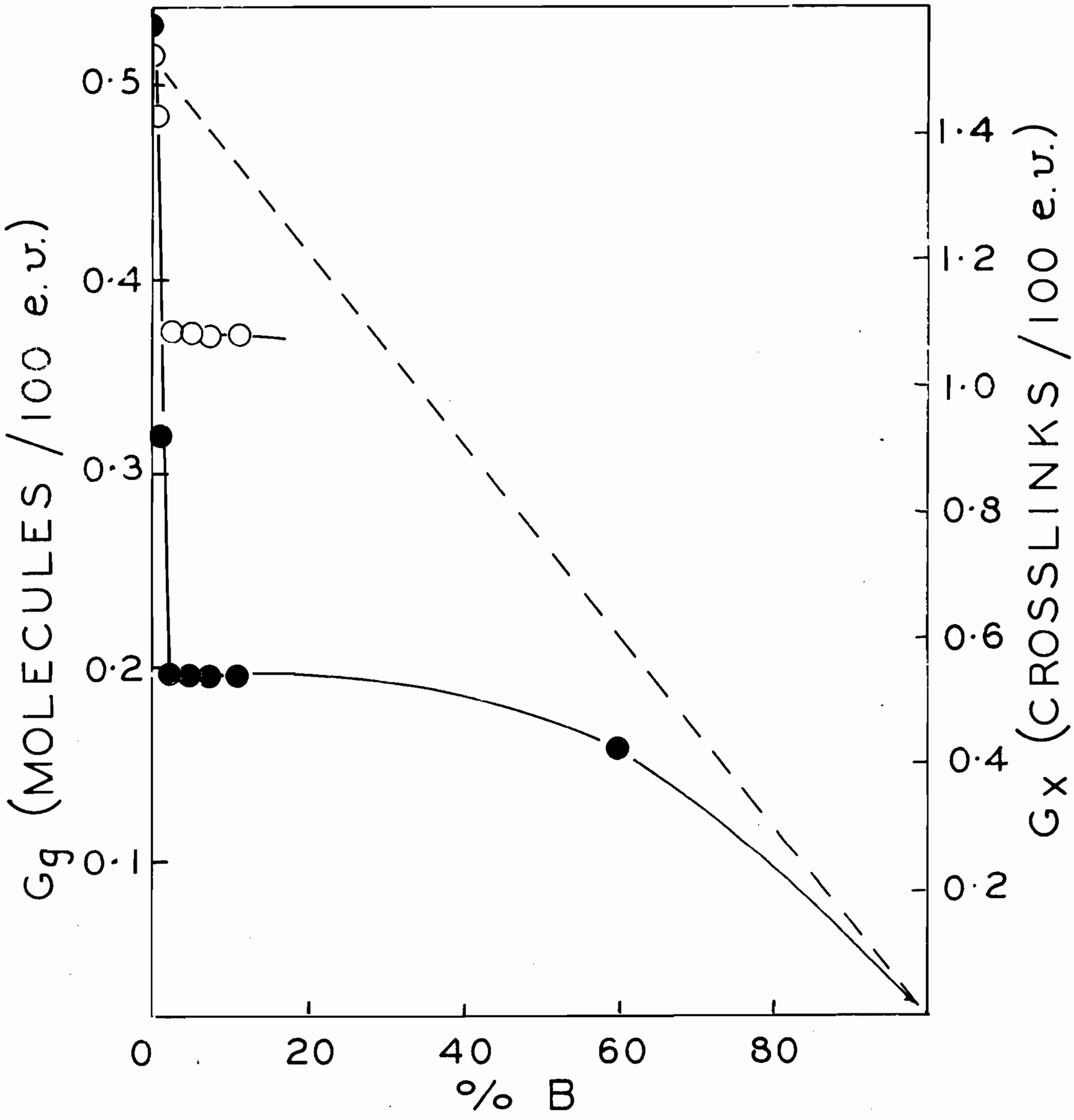
Gg (MOLECULES /100 e.v.)
0·5
0·4
0·3
0·2
0·1
Gx (CROSSLINKS /100 e.v.)
1·4
1·2
1·0
0·8
0·6
0·4
0·2
0
20
40
60
80
% B

The composition of the gas formed on irradiation of pure polymer to a dose of 31 Mrads was found by masspectrometry to be 87.1% hydrogen, 4.7% ethylene and 8.2% high mass number constituents. The composition of the gas produced when pure B was irradiated to a dose of 54 Mrads was found by the same technique to be 46.9% hydrogen and 53.1% CH_4, C_2H_4, C_2H_6 and higher mass number constituents.

DISCUSSION

Destruction of Antioxidant

From a critical consideration of the technique used to determine the role of antioxidant destruction during the irradiation process it seems probable that most of the possible sources of error will lead to values of D. which are high. D is the number of molecules of B which have become attached to polymer molecules or have been decomposed per weight average primary molecule of polymer.

In protecting the polymer from oxygen the antioxidant probably becomes attached to the polymer by a reaction of the type (164)

$$RO_2^{\bullet} + HN(Ar)_2 \longrightarrow RO_2H + {}^{\bullet}N(Ar)_2$$

$$RO_2^{\bullet} + {}^{\bullet}N(Ar)_2 \longrightarrow RO_2N(Ar)_2$$

If oxidation occurs during extraction, a hot solvent should increase the amount of oxidation. Experimentally, the results using hot solvent were the same as for cold solvent. This fact would tend to indicate that very little oxidation occurred.

A high value of D will be obtained if some of the polymer dissolves in the azeotrope. Bane and Eby (167) showed that the error introduced by this solubility factor is insignificant.

After irradiation, polystyrene contains many trapped radicals which react with oxygen (31) to form RO_2 radicals. If RO_2 radicals formed in poly(butadiene-co-styrene) they would react with B. Only a very small amount of post-irradiation oxidation has been observed in GR-S, however (31).

If the sample before irradiation is highly oxidized, D might be high particularly at low doses. Since precautions were taken to avoid oxidation this source of error is probably not significant. Traces of oxygen present as a result of incomplete evacuation might also lead to high values for D particularly at low doses.

Besides these possible experimental errors, D as calculated by equation 65a will be higher than the true value because of the assumptions made in deriving this equation.

The last source of experimental error mentioned above, incomplete evacuation, might account for the rapid decrease in Q, the weight fraction of soluble B in the polymer, with increase in dose as shown in Fig. 25 for the sample containing 5.46% B. Above a dose of 10 Mrads the slope of the Q versus R plot for this sample approximates that for the 0.52% B sample. This might mean that all the oxygen initially present as a result of incomplete evacuation has reacted with the polymer after a dose of 10 Mrads. There is also the possibility that above a certain concentration of B the rate at which B is decomposed or becomes attached to the polymer is very high, but no results have been reported by others to support this possibility.

The results for the 0.52% B sample alone will be discussed in detail. These results are more reliable than those for the 5.46% B samples because the samples were five times as large, and the B percentage was a tenth as great, hence the small changes in B content would be more easily detected. Fig. 18 which is a plot of sol fraction, S, versus dose gives S = 0.01 at R = 50 Mrads for the sample containing 0.52%B. The plot of sol fraction versus R/R_g shown in Fig. 19 indicates that $R/R_g = 70$ at sol fraction, S = 0.01 for this sample. But the effective value of R_g corresponding to R = 50 Mrads is not the value experimentally determined at low doses, since the protective action of the antioxidant decreases with increase in dose and therefore the instantaneous or effective R_g also decreases.

If the value of R/R_g for this sample is to agree with the value of R/R_g for pure polymer or polymer containing sufficient B to assure constant protection, R_g must be 0.454 for a sol fraction of 0.01. This is not the value of 0.54 found for R_g by the filtration technique as given in Table V. The total number of crosslink units per weight average primary molecule after a dose R will be

$$\delta = \frac{R + R_o}{R_g + R_o} \qquad \text{.........(71)}$$

If $\delta_o = 0.78$ then R_o from equation 35 with $R_g = 0.454$ will be 1.816 for the 0.52% B sample.

$$\delta_o = \frac{R_o}{R_o + R_g} \qquad \text{.........(35)}$$

Therefore $\delta = 22.9$ at a dose of 50 Mrads. For the pure polymer $R_g = 0.2$, $R_o = 0.8$ and therefore $\delta = 50.8$ at a dose of 50 Mrads. This indicates that after a dose of 50 Mrads, B has prevented the formation of 27.9 crosslink units per weight average primary molecule of polymer compared to 98.3 for $\delta_o = 0.36$. It has previously been shown that after a dose of 50 Mrads 1.32 molecules of B have become attached to the polymer or decomposed per weight average primary molecule. Therefore if $\delta_o = 0.78$, the ratio of crosslink units prevented to molecules of B decomposed or attached to the polymer, will be

$$\frac{27.9}{1.32} = 21.3$$

The true value of the ratio is probably less than 21.3 because the figure 1.32 in the denominator is probably an overestimation. When the less reliable value $\delta_o = 0.36$ is used the ratio becomes 66.4.

In the sample containing 0.52% B there are 5.5 molecules of B per weight average primary molecule of polymer. Thus a further indication that B is an efficient protector is that after a dose of 50 Mrads these 5.5 molecules of B have prevented the formation of 21.3 crosslink units.

Several possibilities must first be considered before it can definitely be concluded that B is as efficient a protector as the preceding calculations indicate. If the crosslinking mechanism is

$$R_1H \rightsquigarrow R_1\cdot + H\cdot$$
$$R_2H \rightsquigarrow R_2\cdot + H\cdot$$
$$R_1\cdot + R_2\cdot \longrightarrow R_1R_2$$

or

$$R_1H \rightsquigarrow R_1\cdot + H\cdot$$
$$R_1\cdot + R_2H \longrightarrow \cdot R_1R_2H$$

then B might prevent crosslink formation by the reaction

$$R\cdot + HN(Ar)_2 \longrightarrow RH + \cdot N(Ar)_2$$

If two antioxidant radicals joined to give $(Ar)_2NN(Ar)_2$ it would appear from the ultraviolet spectrophotometric results that none of the antioxidant had been destroyed because $(Ar)_2NN(Ar)_2$ would have the same effective ultraviolet absorbance as two molecules of B. If B does protect the polymer in this manner it would not affect the yield of hydrogen; however, Fig. 29 shows a decrease in G_g on the addition of B. This form of protection might account for part of the decrease in G_x because the percentage decrease in G_g is not as great as for G_x. According to this protective mechanism one molecule of B can only prevent one crosslink unit, but the experimental results show that only 5.5 molecules of B prevent 21.3 crosslink units.

B might prevent crosslinks by reactions such as

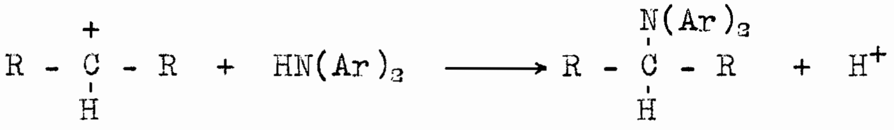

$$R - \underset{H}{\overset{+}{C}} - R \;+\; HN(Ar)_2 \longrightarrow R - \underset{H}{\overset{N(Ar)_2}{C}} - R \;+\; H^+$$

or

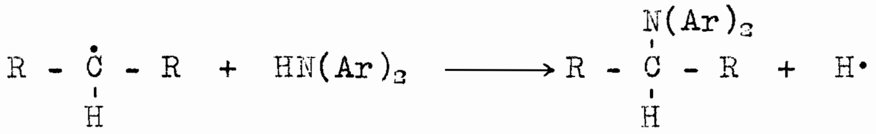

$$R - \underset{H}{\overset{\bullet}{C}} - R \;+\; HN(Ar)_2 \longrightarrow R - \underset{H}{\overset{N(Ar)_2}{C}} - R \;+\; H\cdot$$

During the extraction process $(Ar)_2NN(Ar)_2$ might be formed by the reaction

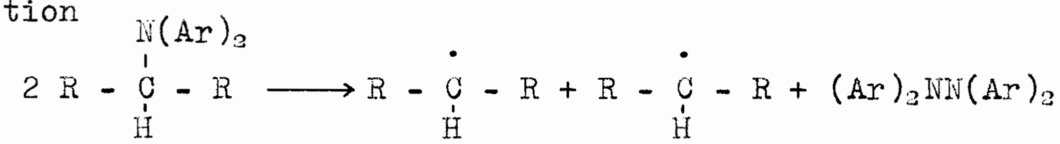

$$2\,R - \underset{H}{\overset{N(Ar)_2}{C}} - R \longrightarrow R - \underset{H}{\overset{\bullet}{C}} - R + R - \underset{H}{\overset{\bullet}{C}} - R + (Ar)_2NN(Ar)_2$$

These protective mechanisms cannot be valid because they result in an increase in gas yield. Even if $(Ar)_2NN(Ar)_2$ is formed, it is likely that the two $R - \underset{H}{\overset{\bullet}{C}} - R$ radicals would combine to form a crosslink. Neither of these mechanisms can account for the prevention of 21.3 crosslinks units by 5.5 molecules of B. It can be concluded that B is definitely a very efficient protector. This high efficiency can be explained by some form of excitation energy transfer, charge transfer, or even by quenching.

Changes in the Spectra

The composition of the poly(butadiene-co-styrene) obtained by Polymer Corporation was 28.7% styrene, 20% vinyl, 7% 1,4-cis, and 73% 1,4-trans, but the values obtained in the present work were 31.5%, 17.9%, 13.1% and 68.7%. The discrepancy between the two sets of results might be accounted for by a comparison of the extinction coefficients of the infra-red technique in the present work and at the Polymer Corporation, or by the possibility of the Polymer Corporation employing a refractive index method for the estimation of the polymer styrene content. The infra-red technique is known to give a higher value for the styrene content than the refractive index method (168). The present results suggest a slightly higher temperature of polymerization than the results of Polymer Corporation indicate, because as the temperature of polymerization increases so also does the ratio of cis to trans 1,4 units (119).

The peripheral thickness of the films used in the ultraviolet technique decreased progressively with time of irradiation. This physical change in film characteristic probably exaggerates the apparent changes in film composition observed as a function of irradiation dose. The central part of the film only was examined by the spectrophotometer. Therefore, if some of the polymer in the peripheral area of the film moved to the area being examined the effect would be to increase the absorption.

Evans et al. (161) in a study of the effect of radiation on natural rubber in vacuo found a small increase in the diene and triene content as measured by the ultraviolet peaks at 245 and 290 millimicrons, respectively. Fig. 27 shows absorption in the regions of these peaks for the polymer irradiated in vacuo. Diene and triene formation could result from a hydrogen radical of one carbon atom abstracting hydrogen from an adjacent carbon. This would tend to give G_g/G_x a value greater than unity, however in the present study

$$\frac{G_g}{G_x} = \frac{0.52}{1.59} = 0.33$$

The low value of this ratio would tend to favour diene formation according to the crosslinking reaction

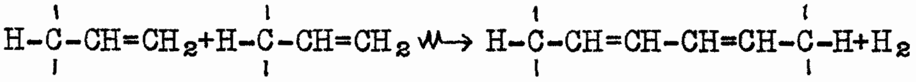

$$H-C-CH=CH_2+H-C-CH=CH_2 \rightsquigarrow H-C-CH=CH-CH=CH-C-H+H_2$$

The data of Fig. 26 indicate that no cis-trans isomerization has occurred as a result of irradiation in vacuo. This is to be expected since the cis to trans ratio of the unirradiated polymer is very close to the equilibrium value found by Golub (25) for polybutadiene.

Kuzminsky et al. (169) found that the unsaturation in GR-S had been reduced by 80% after a dose of 150 megarads. Turner (158) claims that the chemical method used by Kuzminsky et al. to measure the degree of unsaturation, overestimates the destruction of unsaturation. The present work tends to support Turner's criticism.

Charlesby (20) has reported the equilibrium ratio for straight chain olefins to be one double bond to twenty single bonds. If vinyl and styrene groups are ignored, the ratio in the unirradiated polymer studied in the present work is one to fifteen. Therefore, an increase in unsaturation might be expected; but styrene and vinyl groups might greatly affect the equilibrium ratio.

The results of Fig. 26 for pure polymer irradiated in vacuo show that the transmission peak at 911 cm.$^{-1}$ which represents the vinyl group, decreases from 44.0% at R = 0 to 27.5% at R = 150 Mrads. Therefore the absorbance decreases from 0.561 to 0.357. If the vinyl content of the polybutadiene portion of the unirradiated polymer is 20.0%, the vinyl content of the whole polymer is 15.5%. After a dose of 150 Mrads the number of vinyl groups destroyed per weight average primary molecule is

$$\frac{\bar{M}_{woo}}{68.4}\left[1 - \frac{0.357}{0.561}\right] 0.155 = 8.22 \times 10^{-4}\ \bar{M}_{woo}$$

assuming the validity of Beer's Law. This indicates that 36.3% of the vinyl groups present before irradiation have been destroyed.

If $\delta_o = 0.78$, $\bar{M}_{woo} = 143{,}800$ and $R_g = 0.20$ Mrads for the pure polymer, the number of crosslinks formed per weight average primary molecule after a dose of 150 Mrads is calculated from equations 71 and 35 to be $5.82 \times 10^{-4}\ \bar{M}_{woo}$. For every vinyl group destroyed 0.706 crosslinks or 1.41 crosslink units are formed. The implication of this result will be discussed after considering the gas yield and gas composition corresponding to a dose of 150 Mrads.

Because the vinyl group has a lower ionization and excitation potential than vinylene or paraffinic structures, charge transfer or excitation transfer to the vinyl group would be expected (170). This group would then protect the rest of the polymer, but might be destroyed in so doing. The experimental results for samples containing B suggest that B protects the vinyl groups since no decrease in vinyl content was noted after a dose of 35 Mrads. Apparently, even if the charge or excitation energy does go preferentially to the vinyl groups, these groups must be able to transfer the charge or excitation energy to B before bond cleavage occurs. However, the possibility exists that the vinyl content decreased but the decrease could not be detected after a dose of 35 Mrads.

Because the effect of air is dependent on sample thickness, air pressure and radiation intensity (171), the results of the present work must be considered semi-quantitative, particularly for thick samples. The solubility, viscosity and swelling results underestimate the effects of air. The results of the infra-red and ultraviolet analyses account accurately for the effects of air because thin polymer films were irradiated.

On irradiation in vacuo a pure or protected polymer remained colourless. On irradiation in air a pure polymer became yellow and a protected polymer became reddish-brown. The yellow colour is probably related to carbonyl groups in conjugation with double bonds (172). When large specimens of either pure or protected polymer were cut it was found that the colour change occurred only near the surface of the sample. The inner portions of the sample must represent polymer which had been irradiated essentially as if the polymer were in a vacuum.

Fig. 18 shows the decrease in solubility with dose for a pure polymer and one containing 2.7% B. The R_g values are given in Table V. The plot of $S + \sqrt{S}$ versus $1/R$ of Fig. 20 shows p_o/q_o greater than zero for both cases, 0.10 for pure polymer and 0.25 for polymer containing 2.7% B sample.

Viscosity results are shown in Fig. 15 for the 2.7% B sample. They indicate no degradation, but solubility results are a more reliable index of degradation.

The ratio of the gelation dose in the absence of degradation, R_{gc}, to that in the presence of degradation, R_{ga}, is given by the relation (90).

$$\frac{R_{gc}}{R_{ga}} = \frac{q_{oa} - p_{oa}/2}{q_o} \qquad \ldots(72)$$

In the present work R_{gc} and R_{ga} correspond to the gelation dose in the absence and in the presence of air, respectively. The subscript a denotes irradiation in the presence of air. If $q_{oa} = q_o$ then the ratio R_{gc}/R_{ga} should be 0.9 for the 2.7% B sample and 0.95 for the pure polymer, using q_{oa}/p_{oa} values obtained from Fig. 20. However, the experimental ratio of R_{gc}/R_{ga} is 0.41 for the protected polymer and 0.37 for the pure polymer. Therefore, on irradiating the polymer in air, crosslinking is retarded and degradation is initiated. Bauman and Born (173) came to the same conclusion when natural rubber was studied. If thinner samples had been employed in the present work air would have affected the sample to a greater extent and R_g and p_{oa}/q_{oa} would have been greater.

From swelling results Dogadkin (174) concluded that the rate of crosslinking in the presence of oxygen is about three times as great as in vacuo. An examination of the plot of Fig. 22 shows this conclusion to be of very doubtful validity.

For a given solubility the degree of swelling of a pure polymer irradiated in air is much less than for a sample containing B irradiated either in vacuum or in air. Apparently the pure polymer is oxidized to such an extent that it no longer swells as does the unoxidized pure polymer. Oxidation probably changes both the value of χ and the polymer density. Solubility and viscosity measurements on polymer irradiated in air at low doses before much oxidation has occurred will be less subject to error, but even these measurements will be influenced by the high rate of oxidation.

The results of ultraviolet analyses shown in Fig. 27 are not considered a reliable index of the effect of air because of the possibility of film shrinkage as mentioned earlier. Apart from film shrinkage, the large increase in absorption is probably caused by a variety of oxidation products.

The results of infra-red analyses shown in Fig. 26 indicate that oxidation is greatly accelerated by the irradiation of pure polymer, but if the polymer contains B, oxidation proceeds at about the same rate as for unirradiated pure polymer. The infra-red spectrum changed in the same way whether oxidation occurred in the absence or in the presence of radiation. According to Field et al. (175) and Miller et al. (172) acids, aldehydes, ketones, anhydrides and esters absorb in the region 1710 to 1760 cm.$^{-1}$; hydroperoxides from

3555 to 3620 cm.$^{-1}$ and from 830 to 1000 cm.$^{-1}$; peroxides, alcohols, and ethers absorb from 830 to 900 cm.$^{-1}$, and epoxides at about 1250 cm.$^{-1}$. Fig. 26 shows absorption in all these regions. Many of the radiation induced reactions which might produce these compounds are suggested by Dole (29).

Even in the absence of radiation oxidation and protection of butadiene polymers involve several complicated mechanisms (164, 175). In the presence of radiation the mechanisms must become very complicated indeed. A few of the large number of possible mechanisms are

$$\mathrm{RH} \rightsquigarrow \mathrm{R}\cdot + \mathrm{H}\cdot$$

$$\mathrm{R}\cdot + \mathrm{O_2} \longrightarrow \mathrm{RO_2}\cdot$$

$$\mathrm{RO_2}\cdot + \mathrm{RH} \longrightarrow \mathrm{ROOH} + \mathrm{R}\cdot$$

The last reaction is the propagation step of a chain reaction. Crosslinking and degradation can be produced by oxidation as follows:

$$\mathrm{RO_2}\cdot + \mathrm{RO_2}\cdot \longrightarrow \mathrm{ROOR} + \mathrm{O_2}$$

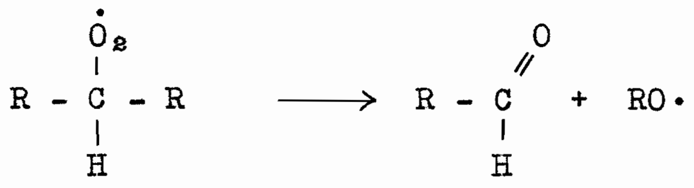

$$\mathrm{R-\underset{\displaystyle H}{\overset{\displaystyle \dot{O}_2}{C}}-R} \longrightarrow \mathrm{R-\underset{\displaystyle H}{C}{=}O} + \mathrm{RO}\cdot$$

Because oxygen is a good electron acceptor its presence will prolong the life of polymeric ions (28). It has been suggested by Alexander and Toms (30) that an oxygen ion can attack a polymer molecule and cause oxidation. Oxygen is probably a good quenching agent as well (28).

According to Bauman and Born (173), B protects the polymer from radiation induced oxidation not only by energy or charge transfer, but also by the reaction

$$RO_2\cdot \; + \; HN(Ar)_2 \longrightarrow RO_2H \; + \; \cdot N(Ar)_2$$

There are several other possible reactions

$$RO\cdot \; + \; HN(Ar)_2 \longrightarrow ROH \; + \; \cdot N(Ar)_2$$

$$RO_2\cdot \; + \; \cdot N(Ar)_2 \longrightarrow RO_2\,N(Ar)_2$$

$$RO\cdot \; + \; \cdot N(Ar)_2 \longrightarrow RO\,N(Ar)_2$$

In contrast to the present results, Field et al. (175) found that B sensitized ultraviolet radiation induced oxidation of poly(butadiene-co-styrene). Twice the amount of oxidation occurred when the polymer contained B.

Gas Evolution

The experimental fact that G_g, the number of molecules of gas evolved per 100 e.v. absorbed by the sample, was slightly greater at very low doses than at higher doses can be explained in a variety of ways. If the unirradiated polymer were oxidized the oxygen might have been evolved on irradiation. Experimentally, however, no change was observed in G_g even after increasing the degree of oxidation by a factor of four. Lawton et al. (176) have found that the gas first evolved when polyethylene is irradiated has a higher percentage of condensable components than the gas evolved at higher doses. This change in composition is probably caused by secondary reactions. When poly(butadiene-co-styrene) is irradiated secondary reactions might occur which reduce the gas yield. The nonlinear units created during polymerization might also be sensitive to radiation. Degradation might occur at these units resulting in gas production. Incomplete evacuation would cause G_g to be high at low doses. Oxygen adhering to the sides of the sample container might be released by the radiation. Small amounts of benzene, not completely removed by the drying process, might also be released during irradiation of the polymer. Measurements on the unirradiated sample suggest the absence of gas, but some benzene might adhere to the polymer and be vaporized by the radiation.

Except for the pure B sample and the sample containing 60% B, gas yields were directly proportional to dose for doses in excess of 0.5 Mrad. This supports the assumption that the degree of crosslinking is directly proportional to dose. The G_g values given in Table XIV of Appendix III for pure B indicate that G_g decreases from 0.039 at 6.31 Mrads to 0.021 at 54.20 Mrads. This dependence of G_g on dose suggests the presence of secondary reactions which reduce the gas yield. If some of the initially formed products are unsaturated these products might scavenge hydrogen and thereby reduce G_g. Dyne and Stone (177) have found a pronounced decrease in G_g for for low molecular weight organic molecules.

The results of Fig. 28 which gives the plot of Y versus R show that the dependence of G_g on dose for the sample containing 60% B is much greater than for pure B. The 60% B sample has $G_g = 1.8$ when R is extrapolated to zero and G_g decreases to approximately 0.25 at R = 40 Mrads. Secondary reactions probably cause this decrease. The scatter in the plot of Y versus R for the 60% B sample is much greater than for the other samples. This can be explained if the solubility limit of B in the polymer has been exceeded and B is not uniformly dispersed throughout the sample.

In the present study the value of 0.52 found for G_g with pure polymer is considerably greater than that obtained by Petrov et al. (178). These workers found G_g to vary from 0.26 to 0.29. Errors in dosimetry, gas measurement, or in the estimation of impurities, in either of the investigations could cause this discrepancy in the evaluation of G_g. The low value of $G_g = 0.02$ found for pure antioxidant B, supports the findings of other workers (27) that aromatic groups are good internal protectors.

The composition of the gas evolved during irradiation of pure polymer was determined at only one dose, 20 Mrads. If the gas composition is dose dependent it is likely that G_g would show a similar dose dependence. Except for the polymer sample containing 60% B, G_g was found to be independent of dose. However, the composition of the gas evolved from pure B is probably dependent on dose because G_g is dose dependent. The gas evolved from pure B after a dose of 31 Mrads was only 46.9% hydrogen. At lower doses the percentage of hydrogen is probably greater because unsaturated compounds, which would scavenge hydrogen, would be absent. Most of the hydrogen from B probably comes from N-H bond cleavage. Other workers (179) have found this bond to be more sensitive to radiation than any other bond in amines.

The presence of ethylene in the gas evolved from pure polymer might indicate the removal of vinyl groups by a reaction of the type

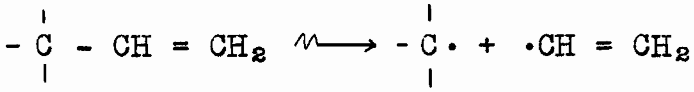

$$-\overset{|}{\underset{|}{C}} - CH = CH_2 \xrightarrow{\sim\sim} -\overset{|}{\underset{|}{C}}\cdot + \cdot CH = CH_2$$

where the radical $\cdot CH = CH_2$ ultimately abstracts a hydrogen atom from a polymer molecule or combines with H· produced by radiation induced C - H bond cleavage. Another possible reaction involving ethylene production is

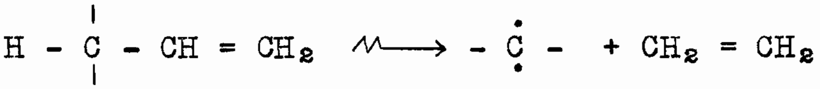

$$H - \overset{|}{\underset{|}{C}} - CH = CH_2 \xrightarrow{\sim\sim} - \overset{\cdot}{\underset{\cdot}{C}} - + CH_2 = CH_2$$

If the composition of the gas from the pure polymer is independent of dose, the number of molecules of ethylene evolved per weight average primary molecule of polymer after a dose of 150 Mrads will be

$$\frac{6.24 \times 10^{17} \ \tilde{M}_{woo} \ 150 \ G_{gp} \ 0.047}{6.02 \times 10^{23}}$$

which reduces to 3.64×10^{-6} $\bar{M}_{woo}$ if the experimental value of $G_{gp} = 0.52$ is employed. It has already been shown that after a dose of 150 Mrads, 8.22×10^{-4} $\bar{M}_{woo}$ vinyl groups have been destroyed per weight average primary molecule and 5.82×10^{-4} $\bar{M}_{woo}$ crosslinks (or 11.64×10^{-4} $\bar{M}_{woo}$ crosslink units) have been formed per weight average primary molecule. Therefore for every crosslink unit formed 0.706 vinyl groups have been destroyed and 0.0031 molecules of ethylene have been evolved. These results imply that vinyl destruction is rarely accompanied by the production of ethylene.

Some of the 8.1% of the gas which is neither ethylene nor hydrogen might be the products of vinyl group destruction. But even if all the uncharacterized gas arises from the destruction of vinyl groups there is still a large discrepancy between the number of vinyl groups destroyed and the amount of this gas produced assuming vinyl group destruction. One might account for this descrepancy by postulating the occurrence of reactions which lead to the destruction of vinyl groups but do not lead to the formation of endlink or crosslink units. Hydrogen scavenging is a reaction of this type.

$$-\overset{|}{\underset{|}{C}} - CH = CH_2 + H\cdot \longrightarrow -\overset{|}{\underset{|}{C}} - \dot{C}H - CH_3$$

The experimentally determined value of the number of crosslinks per molecule of hydrogen is

$$\frac{G_x}{0.871\ G_{gp}} = 3.85$$

The above reaction would account for this high value if crosslinking occurred by a mechanism such as

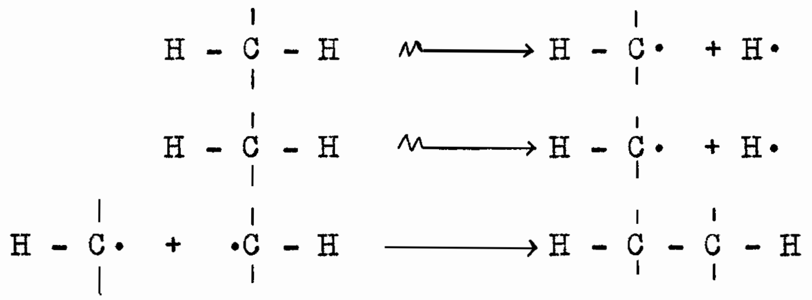

$$\mathrm{H-\overset{|}{\underset{|}{C}}-H} \rightsquigarrow \mathrm{H-\overset{|}{\underset{|}{C}}\cdot + H\cdot}$$

$$\mathrm{H-\overset{|}{\underset{|}{C}}-H} \rightsquigarrow \mathrm{H-\overset{|}{\underset{|}{C}}\cdot + H\cdot}$$

$$\mathrm{H-\overset{|}{\underset{|}{C}}\cdot + \cdot\overset{|}{\underset{|}{C}}-H \longrightarrow H-\overset{|}{\underset{|}{C}}-\overset{|}{\underset{|}{C}}-H}$$

Another possibility which would account for the discrepancy between the amount of vinyl group destruction, the theoretical amount of gas produced by this extent of vinyl group destruction and the actual gas produced, is the occurrence of reactions which would lead to the formation of endlinks or crosslinks and the destruction of vinyl groups. One possible reaction is

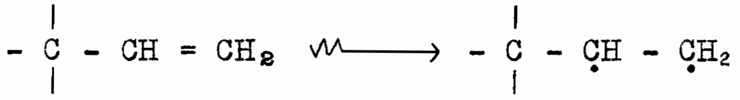

$$\mathrm{-\overset{|}{\underset{|}{C}}-CH=CH_2} \rightsquigarrow \mathrm{-\overset{|}{\underset{|}{C}}-\underset{\bullet}{C}H-\underset{\bullet}{C}H_2}$$

followed by

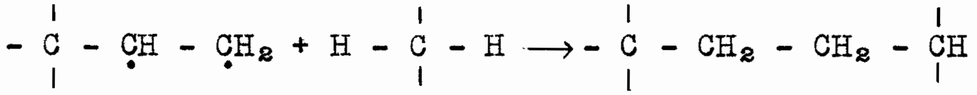

$$\mathrm{-\overset{|}{\underset{|}{C}}-\underset{\bullet}{C}H-\underset{\bullet}{C}H_2 + H-\overset{|}{\underset{|}{C}}-H \longrightarrow -\overset{|}{\underset{|}{C}}-CH_2-CH_2-\overset{|}{\underset{|}{C}H}}$$

where an endlink is formed and no gas is evolved. A second possible reaction is

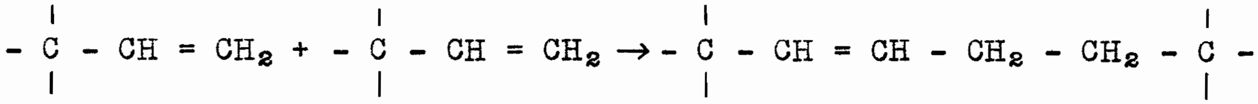

$$\mathrm{-\overset{|}{\underset{|}{C}}-CH=CH_2 + -\overset{|}{\underset{|}{C}}-CH=CH_2 \longrightarrow -\overset{|}{\underset{|}{C}}-CH=CH-CH_2-CH_2-\overset{|}{\underset{|}{C}}-}$$

where a crosslink is formed and no gas is evolved. A reaction scheme in which these two reactions dominate would account for the large number of crosslinks or endlinks formed per molecule of hydrogen evolved.

The results presented in Fig. 29 show that G_x and G_g decrease to a much greater extent over the concentration range 0 - 2% B than is predicted by the "mixture law" (166). But from 2 - 11% B both G_x and G_g are constant. The negative deviation from the "mixture law" over the range 0 - 2% B suggests that the antioxidant, B, is protecting the polymer over this range. The study of the antioxidant destruction shows that this protection must involve some type of excitation energy transfer, charge transfer, or quenching. It is possible that a small amount of radical scavenging occurs in addition to these processes.

If gas evolution and crosslink formation is caused by one mechanism, such as

$$\begin{aligned} RH &\rightsquigarrow R\cdot + H\cdot \\ RH &\rightsquigarrow R\cdot + H\cdot \\ R\cdot + R. &\longrightarrow RR \end{aligned}$$

which is inhibited by B, G_g and G_x would be less than predicted by the "mixture law". Furthermore, if such a mechanism occurs the percentage decrease in G_g and G_x would be the same. However at a 2% B concentration the value of G_x has decreased by approximately twice that of G_g. If only one mechanism occurs both G_g and G_x should increase with increasing dose for a sample containing both polymer and B, because the concentration of B is reduced as the dose increases. In the range 0 - 11% B, G_g and

G_x were independent of dose except for the 0.52% B sample which showed a dose dependence in G_x. Furthermore, when B varied from 2 to 11%, G_g and G_x were constant and independent of B concentration. It is unlikely that these findings could be explained by the occurrence of one reaction mechanism.

If two reaction mechanisms are responsible for gas evolution and crosslink formation and one mechanism is retarded by B and the other is unaffected, the plots of G_g and G_x versus % B would be similar to those given in Fig. 29. However, both G_g and G_x would decrease over the range 2 - 11% B even if one of the reactions is completely suppressed by a 2% concentration in B. G_g and G_x would decrease over this range in a manner predicted by the "mixture law". From 2 - 11% B the value of G_g would decrease by 0.03 units and that of G_x by 0.05 units. It is evident from Fig. 29 that neither G_g nor G_x show such a decrease.

An explanation for the shape of the G_g and G_x versus % B curves might be given on the basis of particle dispersion. If the solubility limit of B in the polymer is attained at a concentration of 2% B, small aggregates of B would be distributed throughout the polymer above this concentration. Above 2% B the protective action would remain constant because the molecules of B in the aggregates would be isolated from the polymer and unable to protect it. In contradiction to this explanation, the results of Angert and Kuz'minskii (180) indicate that the solubility limit is in excess of 10% B. The solubility explanation also fails to account for the constant values of G_g and G_x over the range 2 - 11% B. Both G_g and G_x would decrease over this range to an extent predicted by the "mixture law".

A reaction scheme which does account for the decrease in G_g and Gx over the range 0 - 2% B and also for the constant values of G_g and G_x over the range 2 - 11% B involves two distinct mechanisms. In one of these mechanisms the dependence of G_g and Gx on B concentration exhibits a positive deviation from the "mixture law" and in the other the deviation from the "mixture law" is markedly negative. Fig. 30 shows one possible manner in which two such mechanisms could be affected by B to give a plot similar to that of Fig. 29 for the range 0 - 11% B. Fig. 30 shows that the mechanism which exhibits a negative deviation from the "mixture law" is completely suppressed by a concentration of 2% B. Since the other mechanism involves a positive deviation from the "mixture law", the change in G_g and G_x between 2 and 11% B will be within the experimental error for these quantities (±0.5% for G_g and ±2% for Gx). A concentration of 2% B reduces G_x by 65.6% and G_g by only 28.1%. Therefore the ratio of gas yield to crosslink or endlink yield is smaller for the mechanism which exhibits a negative deviation from the "mixture law" than for the other mechanism. Consequently, for the mechanism exhibiting negative deviation more vinyl groups might be destroyed during irradiation. The destruction of the vinyl groups might be by crosslink or endlink formation or by hydrogen scavenging.

Fig. 30

Theoretical dependence of G_g and G_x on B concentration.

– – – G_g, molecules of gas per 100 e.v. absorbed

——— G_x, crosslinks per 100 e.v. absorbed

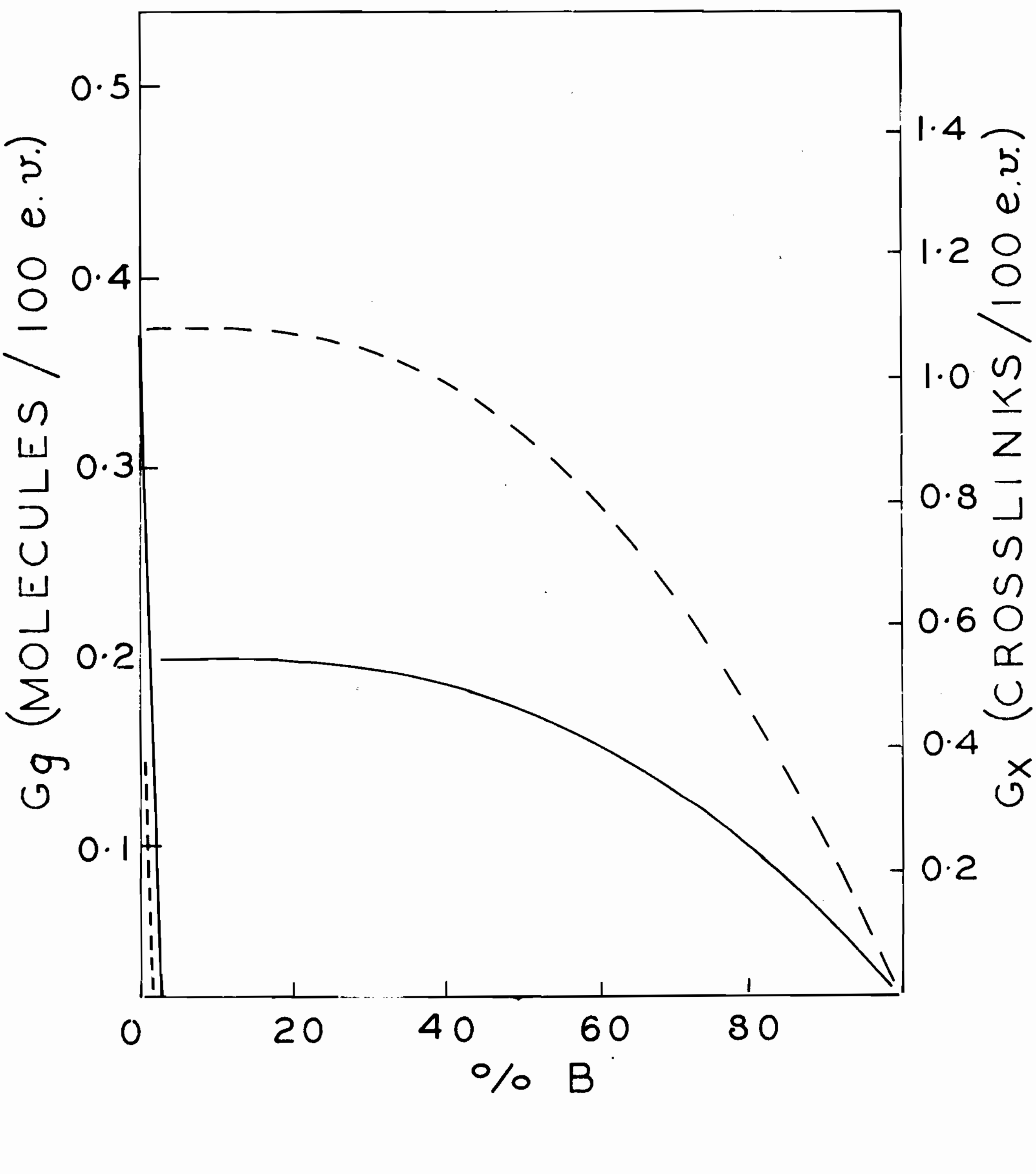
Gg (MOLECULES / 100 e.v.)
0·5
0·4
0·3
0·2
0·1
Gx (CROSSLINKS/100 e.v.)
1·4
1·2
1·0
0·8
0·6
0·4
0·2
0
20
40
60
80
% B

The two mechanisms could involve ions exclusively or excited molecules exclusively. However, because radiation probably produces both ions and excited molecules it is likely that one mechanism involves ions while the other involves excited molecules. B is a secondary amine and a good electron donor. Therefore B would prevent the ionic mechanism by replacing electrons lost by polymer molecules. This implies that the reaction which exhibits a negative deviation from the "mixture law" is ionic. The large number of vinyl groups destroyed per crosslink or endlink for this mechanism also implies that it is ionic because carbonium ions are highly electrophilic and will react very rapidly with olefins (22). The mechanism involving excited molecules would exhibit a positive deviation from the "mixture law" if B transfers excitation energy to the polymer.

This reaction scheme alone does not explain why at low doses G_g for the sample containing 60% B is much greater than G_g for the pure polymer and why G_g for this sample is very dose dependent. One possible explanation for this observation is that a third gas producing mechanism occurs. The gas from this third source probably comes from B, because dose dependency is a characteristic frequently found for low molecular weight organic compounds but not for polymers. If the gas did come from the polymer, G_x for the 60% B sample would probably be greater than for the pure polymer; but the experimental results show that it is less. The third gas producing process must be sensitized by the polymer because the gas yield from this source is greater at 60% B than at either 0% or 100% B. If sensitization occurs G_g will increase in the range 2 - 11% B. The constant value of both G_g and G_X is this range implies that the gas from this third source must be negligible below 11% B. One explanation for the constant values of G_g and G_X is that the process only occurs if B is in the form of aggregates so that the molecules of B are very close to one another. At a concentration of 60% B the solubility limit has been exceeded and aggregates of B are present, but below a concentration of 11%, B is soluble and the molecules of B are isolated.

Conclusions

During irradiation of the polymer the presence of air was found to have a serious effect. Infra-red and ultraviolet analyses revealed that the pure polymer was severely oxidized when irradiated in air, but that polymer containing 2.7% B was only slightly oxidized. The changes in the infra-red spectrum produced by irradiating the polymer in air were similar to those produced when the polymer was oxidized in the absence of radiation. Solubility results for samples irradiated in air indicated that q_o was less than in the absence of air and that p_o/q_o was 0.10 for the pure polymer and 0.25 for the polymer containing 2.7% B. Swelling results were found to overestimate seriously the degree of nonlinearity when the pure polymer was irradiated in air, but were reliable for a sample containing 2.7% B.

From gas yield and gas composition determinations for the pure polymer irradiated in vacuo, it was calculated that after a dose of 150 Mrads 3.64×10^{-6} $\bar{M}_{woo}$ molecules of ethylene are evolved. Infra-red analyses showed that for the same dose 8.22×10^{-4} $\bar{M}_{woo}$ vinyl groups are destroyed per weight average primary molecule. If these values are compared to the corresponding value of the number of crosslinks formed, it can be calculated that for every crosslink unit formed 0.706 vinyl groups have been destroyed and 0.0031 molecules of ethylene have been evolved. Vinyl groups are therefore destroyed mainly by reactions leading to crosslinks or by hydrogen atom scavenging or by both these processes.

For the pure polymer irradiated in vacuo $G_X = 1.59$, whereas $G_X = 0.37$ for a sample containing 2 - 11% B. The corresponding values for G_g are 0.52 and 0.20. Therefore, $G_g/G_X = 0.33$ for the pure polymer and 0.54 for the polymer containing 2 - 11% B. These low values are in agreement with the results of infra-red analyses, for they also indicate that either, (a) vinyl groups react to produce crosslinks or endlinks, or (b) hydrogen arising from crosslink or endlink formation is scavenged by the vinyl groups, or (c) both these processes occur simultaneously.

Ultraviolet analyses show that diene structures are created during the irradiation of the pure polymer in vacuo. It was not possible to estimate the amount of diene formation from the change in the ultraviolet spectrum. Only a small amount of diene formation probably occurs, because at least one molecule of hydrogen is evolved for every crosslink unit formed in a reaction which produces a diene structure.

The large decrease in G_g and G_x caused by a 2% concentration of B indicates that this additive protects the polymer from radiation. The determination of the amount of soluble B in the polymer following irradiation shows that B is an efficient protector. The destruction of one molecule of B corresponds to the prevention of 21.3 crosslink units. This result suggests that protection arises mainly from charge transfer or excitation transfer from the polymer to the antioxidant, or from quenching of the polymer by the antioxidant.

The large decrease in G_g and G_x in the range 0 - 2% B and the constant values of G_g and G_x in the range 2 - 11% B indicate that two distinct mechanisms occur on irradiation of the polymer. One of these mechanisms exhibits a positive, and the other a negative deviation from the "mixture law".

The value of G_g at low doses for the sample containing 60% B was much greater than G_g for the pure polymer. The explanation of this result might be that the polymer sensitizes a reaction which leads to the decomposition of B. This reaction would only occur if the B in the polymer is dispersed as aggregates.

Fig. 31 (A,B,C,D) illustrates some of the many reactions which might occur during the irradiation of pure polymer or a mixture of polymer and B. In this figure RH represents a molecule of polymer and $HN(Ar)_2$ a molecule of antioxidant. The unbracketed numbers beside the arrows are the activation energies (183) in kilocalories per mole for the particular reaction. According to Pearson et al. (184) the activation energy for radiation induced nonlinearity in poly(butadiene-co-styrene) is approximately two. Radicals R· and H· might be either "hot" or thermal. Reactions involving "hot" radicals have activation energies close to zero (183).

The initiating reaction for Fig. 31A is

$$RH \rightsquigarrow RH^{+} + e$$

There are two possible initiating reactions for Fig. 31B.

$$RH^{+} + e \longrightarrow RH^{*}$$
$$RH + e \longrightarrow RH^{*} + e$$

Radical mobility shown in Fig. 31C can occur by two mechanisms. For the first (14) the activation energy (183) is 10 Kcal. per mole.

$$R_1\cdot + R_2H \longrightarrow R_1H + R_2\cdot$$
$$R_2\cdot + R_3H \longrightarrow R_2H + R_3\cdot$$

The activation energy is unknown for the second (185).

$$R_1\cdot + H_2 \longrightarrow R_1H + H\cdot$$

$$H\cdot + R_2H \longrightarrow R_2\cdot + H_2$$

Many of the possible reactions are not represented in this figure. One such reaction is main chain fracture followed by the radicals formed attaching themselves to molecules. Endlinks would be created by this process. Another reaction not included in the figure is sensitization of B by the polymer. Quenching reactions are also not shown.

The relative probability of each reaction in Fig. 31 is given by the nature of the arrows in the figure. A thick line denotes a reaction with a high probability, a dashed line a low probability, and a thin line an unknown probability. The relative probabilities are based on the interpretation of the results given in the body of this thesis.

<u>Fig. 31</u>

Summary of possible reactions.

━━━━ high probability

──── unknown probability

- - - - low probability

Figure 31A

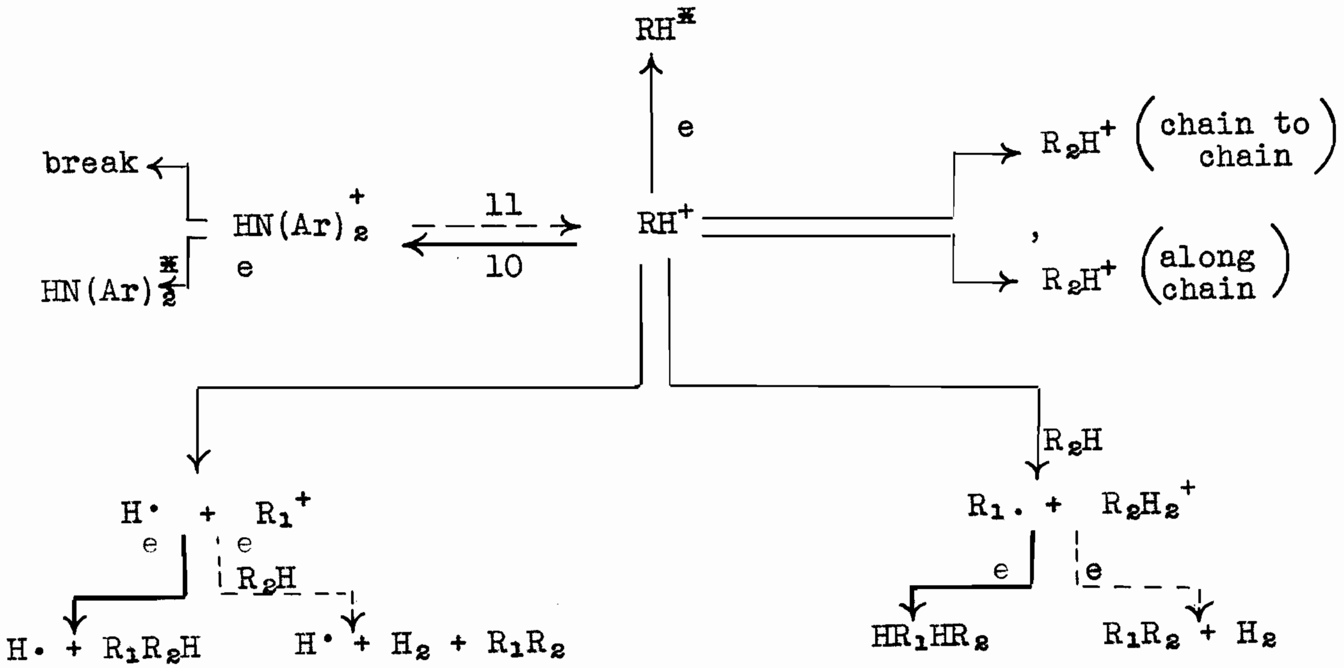
RH^*
e
break
$HN(Ar)_2^+$
$HN(Ar)_2^*$
e
11
10
RH^+
R_2H^+ (chain to chain)
,
R_2H^+ (along chain)
R_2H
$H\cdot + R_1^+$
e
e
R_2H
$H\cdot + R_1R_2H$
$H\cdot + H_2 + R_1R_2$
$R_1\cdot + R_2H_2^+$
e
e
HR_1HR_2
$R_1R_2 + H_2$

Figure 31B

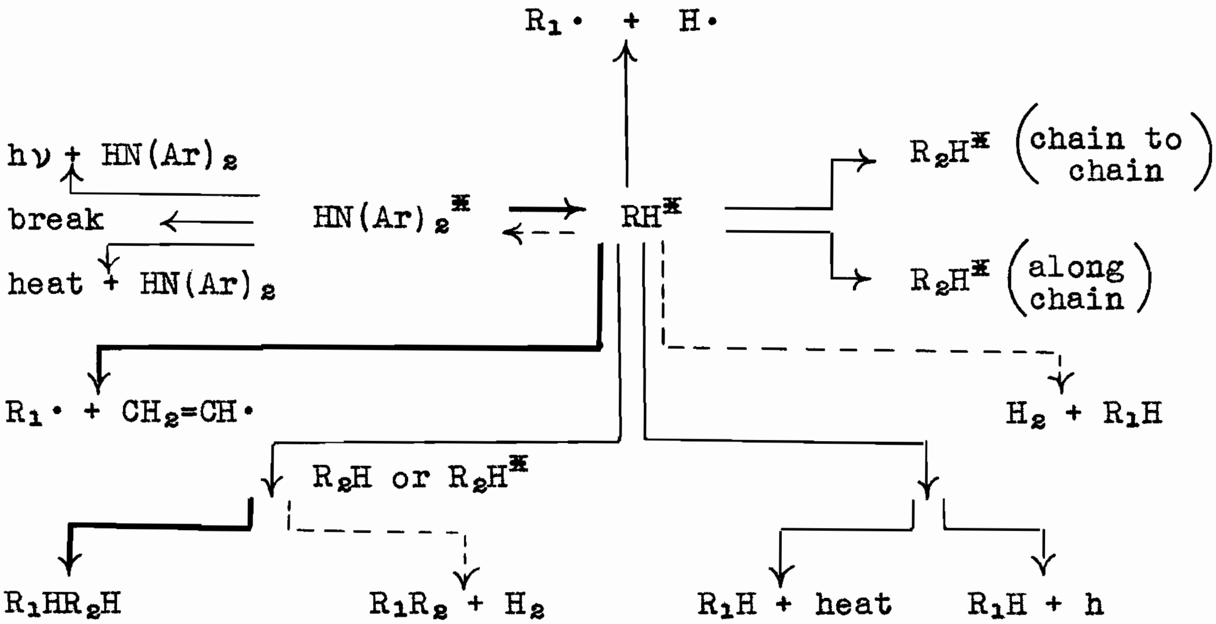

R₁· + H·
hν + HN(Ar)₂
break
heat + HN(Ar)₂
HN(Ar)₂*
RH*
R₂H* (chain to chain)
R₂H* (along chain)
R₁· + CH₂=CH·
H₂ + R₁H
R₂H or R₂H*
R₁HR₂H
R₁R₂ + H₂
R₁H + heat
R₁H + h

Figure 31C

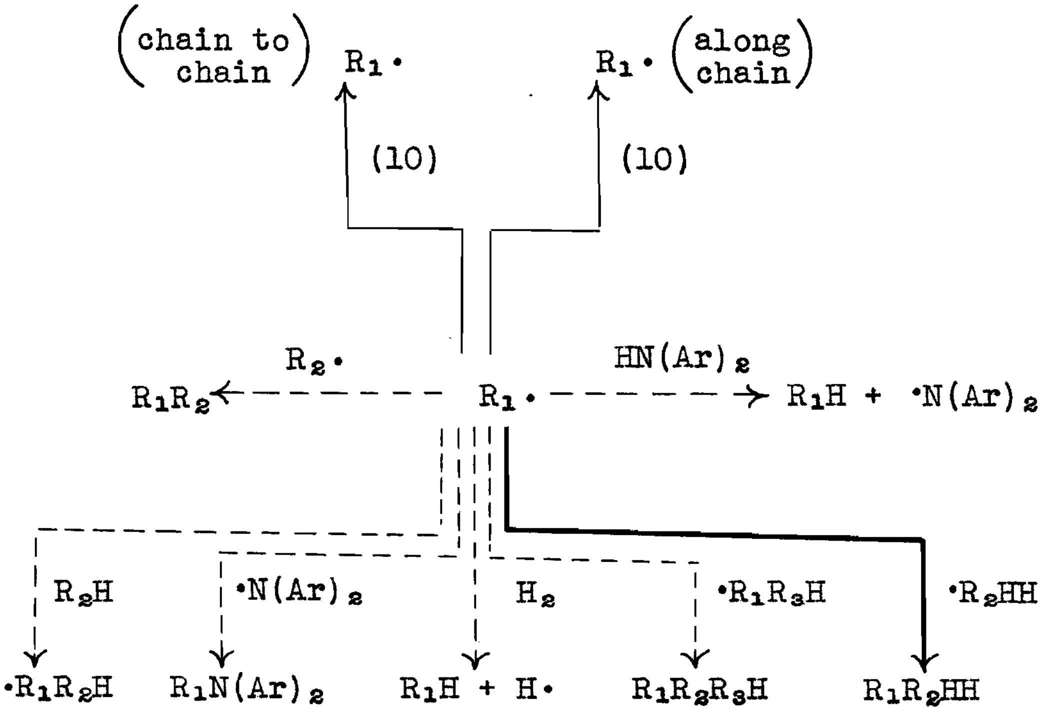
(chain to chain)
R₁•
R₁•
(along chain)
(10)
(10)
R₂•
HN(Ar)₂
R₁R₂
R₁•
R₁H + •N(Ar)₂
R₂H
•N(Ar)₂
H₂
•R₁R₃H
•R₂HH
•R₁R₂H
R₁N(Ar)₂
R₁H + H•
R₁R₂R₃H
R₁R₂HH

Figure 31D

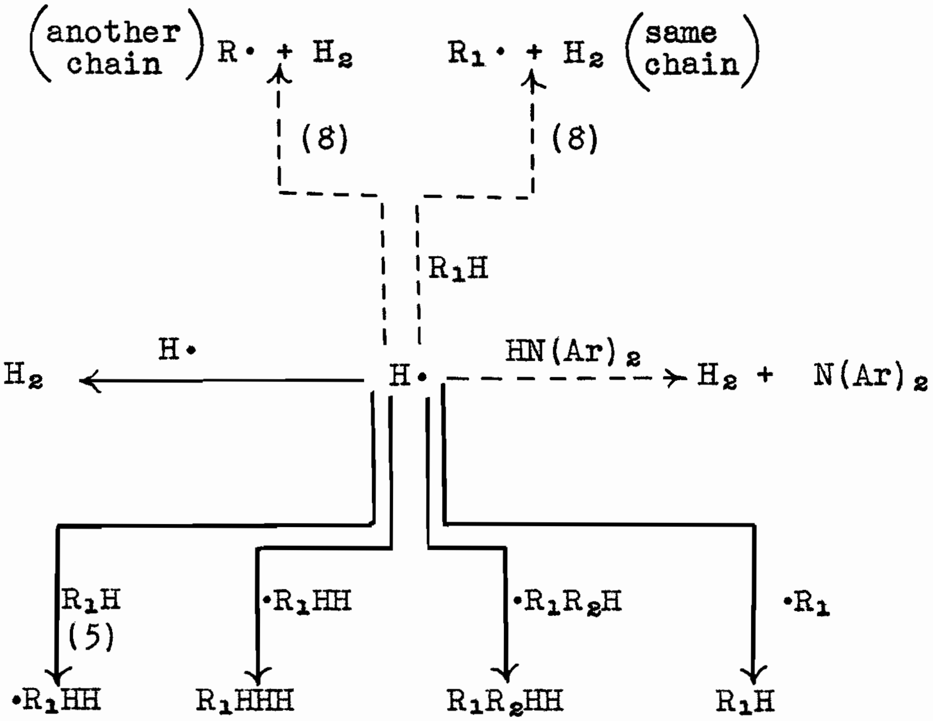
(another chain) R• + H₂
R₁• + H₂ (same chain)
(8)
(8)
R₁H
H•
H₂
H•
HN(Ar)₂
H₂ + N(Ar)₂
R₁H
(5)
•R₁HH
•R₁R₂H
•R₁
•R₁HH
R₁HHH
R₁R₂HH
R₁H

APPENDIX I

Viscosity and Sedimentation Data
for the Polymer Fractions

TABLE IX

Viscosity data for the fractions

Fraction 1

conc. $g.dl.^{-1}$	time sec.	η_r	η_{sp}/c $g.^{-1}dl.$
0.2376	365.8	3.154	9.063
0.1585	256.6	2.222	7.711
0.1188	212.1	1.828	6.968
0.0951	188.5	1.625	6.575
0.0684	161.4	1.391	6.163

$[\eta]$ uncorrected for B 4.87 $g.^{-1}dl.$ $[\eta]$ corrected for B 5.38 $g^{-1}dl.$
slope uncorrected for B 7.50 $g.^{-1}dl.^2$ slope corrected for B 21.5 $g.^{-1}dl.^2$

Fraction 2

conc. $g.dl.^{-1}$	time sec.	η_r	η_{sp}/c $g.^{-1}dl.$
0.3165	512.5	4.418	10.800
0.2111	336.1	2.897	8.986
0.1582	263.0	2.268	8.001
0.1266	227.6	1.962	7.598
0.0845	182.4	1.605	7.160

$[\eta]$ uncorrected for B 4.92 $g.^{-1}dl.$ $[\eta]$ corrected for B 5.13 $g.^{-1}dl.$
slope uncorrected for B 14.27 $g.^{-1}dl.^2$ slope corrected for B 15.60 $g.^{-1}dl.^2$

TABLE IX (Cont'd)

Viscosity data for the fractions

Fraction 3

conc. g.dl.$^{-1}$	time sec.	η_r	η_{sp}/c g.$^{-1}$dl.
0.2641	298.7	2.574	5.961
0.1886	234.3	2.019	5.403
0.1467	202.8	1.748	5.099
0.1200	184.5	1.591	4.925
0.1016	172.2	1.485	4.775

$[\eta]$uncorrected for B 4.04 g.$^{-1}$dl. $[\eta]$ corrected for B 4.30 g.$^{-1}$dl.
slope uncorrected for B 7.20 g.$^{-1}$dl.^{2} slope corrected for B 8.14 g.$^{-1}$dl.^{2}

Fraction 4

conc. g.dl.$^{-1}$	time sec.	η_r	η_{sp}/c g.$^{-1}$dl.
0.2900	269.6	2.325	4.570
0.1934	210.2	1.812	4.200
0.1450	183.2	1.579	3.994
0.1160	167.8	1.446	3.761
0.0965	158.4	1.366	3.792

$[\eta]$uncorrected for B 3.41 g.$^{-1}$dl. $[\eta]$ corrected for B 3.65 g.$^{-1}$dl.
slope uncorrected for B 4.03 g.$^{-1}$dl.^{2} slope corrected for B 4.58 g.$^{-1}$dl.^{2}

TABLE IX (Cont'd)

Viscosity data for the fractions

Fraction 5

conc. g.dl.$^{-1}$	time sec.	η_r	η_{sp}/c g.$^{-1}$dl.
0.3052	251.1	2.165	1.165
0.2035	199.6	1.721	0.721
0.1526	176.2	1.519	0.519
0.1221	163.3	1.409	0.408
0.1016	154.8	1.335	0.335

$[\eta]$uncorrected for B 3.00 g.$^{-1}$dl. $[\eta]$ corrected for B 3.18 g.$^{-1}$dl.
slope uncorrected for B 3.02 g.$^{-1}$dl.^{2} slope corrected for B 3.39 g.$^{-1}$dl.^{2}

Fraction 6

conc. g.dl.$^{-1}$	time sec.	η_r	η_{sp}/c g.$^{-1}$dl.
0.4146	270.6	2.332	3.213
0.2765	210.7	1.816	2.951
0.2073	184.2	1.588	2.836
0.1659	170.0	1.465	2.804
0.1380	160.2	1.381	2.760

$[\eta]$uncorrected for B 2.49 g.$^{-1}$dl. $[\eta]$ corrected for B 2.59 g.$^{-1}$dl.
slope uncorrected for B 1.73 g.$^{-1}$dl.^{2} slope corrected for B 1.86 g.$^{-1}$dl.^{2}

TABLE IX (Cont'd)

Viscosity data for the fractions

Fraction 7

conc. $g.dl.^{-1}$	time sec.	η_r	η_{sp}/c $g.^{-1}dl.$
0.4013	235.9	2.033	2.574
0.2676	190.3	1.641	2.395
0.2006	170.4	1.469	2.293
0.1605	158.6	1.368	2.287
0.1336	151.5	1.306	2.289

$[\eta]$ uncorrected for B 2.11 $g.^{-1}dl.$ $[\eta]$ corrected for B 2.19 $g.^{-1}dl.$
slope uncorrected for B 1.13 $g.^{-1}dl.^2$ slope corrected for B 1.22 $g.^{-1}dl.^2$

Fraction 8

conc. $g.dl.^{-1}$	time sec.	η_r	η_{sp}/c $g.^{-1}dl.$
0.6412	283.5	2.444	2.248
0.4277	218.2	1.881	2.060
0.3206	199.2	1.640	1.996
0.2565	173.6	1.496	1.935
0.2137	162.8	1.401	1.876

$[\eta]$ uncorrected for B 1.74 $g.^{-1}dl.$ $[\eta]$ corrected for B 1.81 $g.^{-1}dl.$
slope uncorrected for B 0.744 $g.^{-1}dl.^2$ slope corrected for B 0.802 $g.^{-1}dl.^2$

TABLE IX (Cont'd)

Viscosity data for the fraction

Fraction 9

conc. g.dl.$^{-1}$	time sec.	η_r	η_{sp}/c g.$^{-1}$dl.
0.6344	245.6	2.117	1.760
0.4232	196.5	1.693	1.638
0.3173	161.6	1.502	1.582
0.2538	162.0	1.396	1.561
0.2114	155.7	1.342	1.617

$[\eta]$uncorrected for B 1.40 g.$^{-1}$dl.$[\eta]$corrected for B 1.48 g.$^{-1}$dl.

slope uncorrected for B 0.567 g.$^{-1}$dl.^{2} slope corrected for B 0.606 g.$^{-1}$dl.^{2}

Fraction 10

conc. g.dl.$^{-1}$	time sec.	η_r	η_{sp}/c g.$^{-1}$dl.
0.8475	253.1	2.182	1.394
0.5653	200.7	1.730	1.291
0.4238	176.2	1.519	1.225
0.3390	162.7	1.403	1.189

$[\eta]$uncorrected for B 1.06 g.$^{-1}$dl. $[\eta]$ corrected for B 1.10 g.$^{-1}$dl.

slope uncorrected for 0.300 g.$^{-1}$dl.^{2} slope corrected for B 0.321 g.$^{-1}$dl.^{2}

TABLE IX (Cont'd)

Viscosity data for the fractions

Fraction 11

conc. g.dl.$^{-1}$	time sec.	η_r	η_{sp}/c g.$^{-1}$dl.
0.4450	126.2	1.358	0.804
0.2968	116.1	1.233	0.785
0.2225	111.8	1.172	0.773
0.1780	109.9	1.139	0.781
0.1188	108.9	1.092	0.774

$[\eta]$uncorrected for B 0.745 g.$^{-1}$dl. $[\eta]$ corrected for B 0.786 g.$^{-1}$dl.

slope uncorrected for B 0.131 g.$^{-1}$dl.^{2} slope corrected for B 0.145 g.$^{-1}$dl.^{2}

Fraction 12

conc. g.dl.$^{-1}$	time sec.	η_r	η_{sp}/c g.$^{-1}$dl.
0.4969	145.0	1.250	0.503
0.3314	135.5	1.168	0.507
0.2485	130.3	1.123	0.496
0.1988	127.8	1.102	0.513
0.1656	125.8	1.082	0.496

$[\eta]$uncorrected for B 0.503 g.$^{-1}$dl. $[\eta]$ corrected for B 0.632 g.$^{-1}$dl.

slope uncorrected for B -- g.$^{-1}$dl.^{2} slope corrected for B -- g.$^{-1}$dl.^{2}

APPENDIX I

TABLE X

Sedimentation data for the fractions.

Fraction 1		Fraction 2		Fraction 3	
c g.dl.$^{-1}$	(1/s)x10^{11} (sec.)$^{-1}$	c g.dl.$^{-1}$	(1/s)x10^{11} (sec.)$^{-1}$	c g.dl.$^{-1}$	(1/s)x10^{11} (sec.)$^{-1}$
0.0614	0.380	0.0727	0.382	0.1128	0.583
0.0925	0.429	0.1038	0.468	0.1410	0.668
0.1098	0.434	0.1555	0.638	0.1695	0.787
0.1255	0.452	0.1915	0.735	0.1880	0.813
0.1423	0.557	0.2080	0.822	0.2255	0.917
0.2145	0.778	0.2590	0.900	0.2540	1.000
0.2710	1.100	0.2870	1.030	0.3065	1.095
0.3610	1.390	1.1750	3.320	0.3850	1.351
0.4520	1.290				
0.4750	1.515				
0.5450	1.460				

Equation

1/s = 0.260c + 2.19

mean % dev'n.

9.54

Equation

1/s = 0.264c + 2.27

mean % dev'n.

3.47

Equation

1/s = 0.2.722c + 2.93

mean % dev'n.

1.93

TABLE X (Cont'd)

Sedimentation data for the fractions.

Fraction 4		Fraction 5		Fraction 6	
c	$(1/s)x10^{11}$	c	$(1/s)x10^{11}$	c	$(1/s)x10^{11}$
$g.dl.^{-1}$	$(sec.)^{-1}$	$g.dl.^{-1}$	$(sec.)^{-1}$	$g.dl.^{-1}$	$(sec.)^{-1}$
0.0749	0.531	0.1020	0.725	0.0771	0.741
0.1134	0.642	0.1322	0.827	0.0964	0.826
0.1498	0.782	0.1690	0.870	0.1350	0.952
0.1875	0.819	0.2080	0.990	0.1870	1.052
0.2155	0.962	0.2880	1.110	0.2400	1.220
0.2710	1.048	0.6900	1.990	0.3190	1.298
0.6420	2.045			0.4000	1.490
				1.4600	3.970
Equation		Equation		Equation	
$1/s = 0.264c + 3.51$		$1/s = 0.212c + 5.24$		$1/s = 0.230c + 6.05$	
mean % dev'n.		mean % dev'n.		mean % dev'n.	
2.72		1.87		2.74	

TABLE X (Cont'd)

Sedimentation data for the fractions.

Fraction 7		Fraction 8		Fraction 9	
c g.dl.$^{-1}$	$(1/s)\times10^{11}$ (sec.)$^{-1}$	c g.dl.$^{-1}$	$(1/s)\times10^{11}$ (sec.)$^{-1}$	c g.dl.$^{-1}$	$(1/s)\times10^{11}$ (sec.)$^{-1}$
0.0768	0.813	0.0866	0.952	0.1160	1.130
0.1047	0.934	0.1252	1.070	0.1355	1.170
0.1250	1.031	0.1733	1.176	0.1548	1.220
0.1538	1.064	0.2115	1.190	0.1742	1.220
0.1922	1.143	0.3650	1.870	0.2130	1.351
0.2305	1.210	0.4470	1.890	0.2515	1.429
0.3840	1.560	0.617	2.240	0.2905	1.471
		1.338	3.965	1.1320	3.560
Equation $1/s = 0.228c + 6.95$ mean % dev'n. 2.28		Equation $1/s = 0.239c + 7.78$ mean % dev'n 2.57		Equation $1/s = 0.241c + 8.27$ mean % dev'n. 1.55	

APPENDIX II

Viscosity, Solubility and Swelling Data
for the Irradiated Polymer

TABLE XI

Viscosity data for sample D4 containing 11.32% B, R = 22.6x10^{+4} rads.

time sec.	conc. g.dl.$^{-1}$	η_r	η_{sp}	η_{sp}/c g.$^{-1}$dl.
225.4	0.33655	1.936	0.936	2.785
183.2	0.22436	1.574	0.576	2.560
164.6	0.16827	1.414	0.414	2.465
153.9	0.13462	1.322	0.322	2.390
147.1	0.11218	1.264	0.264	2.355

time for solvent = 116.1 sec.

$[\eta]$ (uncorrected for B) = 2.16, $[\eta]$ (corrected for B) = 1.86

slope (uncorrected for B) = 2.43, slope (corrected for B) = 2.36

TABLE XII

Viscosity results for unirradiated and irradiated polymer.

$Rx10^{-4}$ rads	$[\eta]$ $g.^{-1}dl.$	slope of η_{sp}/c vs. c $g.^{-1}dl.$	$[\eta]_R/[\eta]_o$	R/R_g
Sample A1, 0.00% B				
0	2.370	2.275	0	0
5.8	2.365	2.440	1.038	0.2875
11.5	2.460	2.580	1.079	0.5750
23.0	2.600	3.380	1.141	1.150
34.5	2.275	1.980	0.998	1.725
Sample B1, 0.52% B				
0	2.330	2.150	1.000	0
5.3	2.300	2.290	0.9890	0.0982
10.5	2.350	2.260	1.009	0.1964
21.0	2.400	2.400	1.030	0.3928
31.5	2.435	2.830	1.045	0.5900
41.9	2.545	3.060	1.092	0.7850
52.4	2.640	3.360	1.133	0.9820
62.9	2.655	3.400	1.139	1.1770
Sample C1, 2.10% B				
0	2.265	2.250	1.000	0
22.9	2.350	2.545	1.038	0.332
45.7	2.515	2.875	1.110	0.661
67.9	2.660	3.230	1.174	0.985
79.2	2.630	4.230	1.161	1.145
Sample D1, 2.10% B				
0	2.340	2.380	1.000	0
11.7	2.410	2.445	1.030	0.1700
23.7	2.450	2.560	1.047	0.3440
35.1	2.480	2.755	1.060	0.5120
52.7	2.620	3.215	1.120	0.7650
58.5	2.650	2.990	1.132	0.8470
70.2	2.660	3.380	1.137	1.030
81.8	2.670	3.150	1.141	1.182

TABLE XII (Cont'd)

Viscosity results for unirradiated and irradiated polymer.

$R \times 10^{-4}$ rads	$[\eta]$ $g^{-1}dl.$	slope of η_{sp}/c vs. c $g^{-1}dl.$	$[\eta]_R/[\eta]_o$	R/R_g
Sample D2, 5.30% B				
0	2.310	2.230	1.000	0
22.6	2.380	2.405	1.030	0.3280
45.2	2.455	2.820	1.063	0.6551
Sample D3, 7.13% B				
0	2.265	2.310	1.000	0
22.6	2.360	2.500	1.042	0.3280
45.2	2.415	2.680	1.066	0.6600
Sample D4, 11.32% B				
0	2.310	2.140	1.000	0
22.6	2.434	2.360	1.054	0.328
45.6	2.500	2.980	1.082	0.660
77.5	2.540	3.260	1.100	1.115
Sample E1, 2.72% B, irradiated in air				
0	2.390	1.940	1.000	0
21.1	2.440	2.025	1.021	0.127
42.2	2.470	1.895	1.034	0.255
87.0	2.530	2.750	1.059	0.527
126.5	2.645	3.255	1.107	0.767
153.8	2.685	3.560	1.124	0.932

TABLE XIII

Solubility and swelling data

$R \times 10^{-4}$ rads	Weight g.	%S	$S + \sqrt{S}$	$1/v_2$	R/R_g	$(I/R) \times 10^8$ (rads)$^{-1}$
Sample E2, 0.00% B						
85.5	0.4167	46.80	1.152	48.2	4.27	117.0
231.0	0.4930	32.10	0.888	24.9	11.55	43.3
280.0	0.4650	25.30	0.756	23.8	14.00	35.7
377.0	0.2611	19.50	0.638	18.4	18.85	26.5
Sample F1, 0.00% B						
567.2	0.5880	12.35	0.475	18.00	28.3	17.60
1155.0	0.5294	5.27	0.282	11.85	57.8	8.65
1698.0	0.4925	2.62	0.188	9.85	84.9	5.87
2350.0	0.5007	1.31	0.128	8.51	117.0	4.26
3120.0	0.5179	0.81	0.098	6.42	156.0	3.20

TABLE XIII (Cont'd.)

Solubility and swelling data

$R\times10^{-4}$ rads	Weight g.	%S	$S + \sqrt{S}$	1/vs	R/R_g	$(I/R)\times10^{8}$ $(\text{rads})^{-1}$
Sample B1, 0.51% B						
428.0	1.8010	44.70	1.115	46.00	8.01	23.36
563.0	1.8159	33.20	0.908	31.40	10.55	17.76
998.0	1.8057	12.34	0.475	13.30	18.65	10.02
1608.0	1.8151	7.42	0.347	9.20	30.15	6.22
Sample B1, 0.51% B						
2350.0	1.8070	5.020	0.274	7.80	44.0	4.26
2930.0	1.8000	3.400	0.218	6.78	54.8	3.41
3520.0	1.8041	2.060	0.164	6.36	65.8	2.84
4700.0	1.8007	1.028	0.112	5.73	88.0	2.13

TABLE XIII (Cont'd.)

Solubility and swelling data

Rx10^{-4} rads	Weight g.	%S	$S + \sqrt{S}$	1/vs	R/R_g	(I/R)x10^8 (rads)$^{-1}$
Sample C1, 2.1% B						
576.4	0.6001	41.80	1.060	41.2	8.35	17.30
1160.0	0.6008	20.70	0.662	18.3	16.80	8.62
1625.0	0.6007	15.60	0.551	14.4	21.30	6.16
1920.0	0.6000	12.50	0.481	12.9	27.80	5.21
3150.0	0.6009	6.10	0.308	8.3	45.70	3.18
4240.0	0.2753	2.91	0.200	7.4	61.60	2.36
5090.0	0.2655	3.36	0.222	6.9	74.00	1.97
Sample D1, 2.1% B						
287.0	0.7003	59.70	1.370	-	4.16	34.80
424.0	0.7001	48.70	1.170	52.50	6.14	23.60
695.0	0.7007	29.80	0.844	30.80	10.05	14.40
948.0	0.6998	22.10	0.691	23.50	13.65	10.80
1320.0	0.7003	19.00	0.627	18.70	19.15	7.58
1870.0	0.7020	8.57	0.387	12.20	27.10	5.51
3470.0	0.6830	5.43	0.283	-	57.40	2.97
5420.0	0.6811	2.57	0.186	7.40	78.70	1.85

TABLE XIII (Cont'd.)

Solubility and swelling data

$Rx10^{-4}$ rads	Weight g.	%S	$S + \sqrt{S}$	1/vs	R/R_g	$(I/R)x10^8$ $(rads)^{-1}$
Sample D4, 11.3% B						
631.0	0.6002	43.4	1.090	34.60	9.15	15.80
1194.0	0.6004	24.9	0.748	21.30	17.32	8.36
1768.0	0.6005	14.8	0.533	15.50	25.65	5.65
2320.0	0.7000	10.8	0.438	13.00	33.70	4.31
3000.0	0.7007	6.5	0.321	9.68	43.50	3.33
3750.0	0.7001	4.9	0.271	8.80	54.30	2.66
Sample C2, 60.3% B						
389.0	0.5997	51.20	1.220	-	3.89	25.70
554.4	0.6050	50.30	1.210	-	5.58	18.00
780.0	0.5993	42.80	1.080	-	7.80	12.80
1735.0	0.6080	23.10	0.712	22.9	17.30	5.76
1777.0	0.7000	20.70	0.662	22.8	17.70	5.63
2730.0	0.5998	11.05	0.443	18.3	27.30	3.66
3160.0	1.0004	3.34	0.219	15.5	31.60	3.17
3750.0	0.5990	6.72	0.326	15.7	37.50	2.67
4270.0	0.5994	5.58	0.292	13.9	42.70	2.34

TABLE XIII (Cont'd.)

Solubility and swelling data

$Rx10^{-4}$ rads	Weight g.	%S	$S + \sqrt{S}$	1/vs	R/R_g	$(I/R)x10^8$ $(rads)^{-1}$
Sample E2, 0.00% B, irradiated in air						
190.5	0.3259	90.00	1.840	-	3.65	52.63
243.5	0.3174	72.40	1.580	-	4.57	41.07
468.0	0.3137	49.80	1.200	14.60	8.78	21.37
883.0	0.3346	18.20	0.609	4.06	16.60	11.32
1460.0	0.3689	8.23	0.369	3.35	27.40	6.85
2280.0	0.3147	6.28	0.313	2.94	42.70	4.39
3880.0	0.3384	3.25	0.213	2.39	73.70	2.58
Sample E1, 2.7% B, irradiated in air						
1038.0	0.3112	45.2	1.120	47.7	6.15	9.64
1630.0	0.3259	39.8	1.029	39.2	9.64	6.13
2650.0	0.3343	22.6	0.701	19.1	15.10	3.77
4480.0	0.3071	10.8	0.486	12.8	26.60	2.23
6100.0	0.3247	10.8	0.486	12.8	36.10	1.64

APPENDIX III

Radiation Induced Gas Yield Data

TABLE XIV

Gas yield data

$Rx10^{-4}$ rads	h_2 cm.	h_1 cm.	$h_2^2 - h_1^2$ $(cm.)^2$	Weight g.	$Y \times 10^6$ moles/g.	G_g molecules/100 e.v.
Sample F1, 0.00% B						
17.0	1.05	0.20	1.06	0.588	0.11	0.610
567.2	5.00	0.20	24.90	0.529	2.64	0.450
1155.0	7.25	0.20	52.50	0.493	6.17	0.517
1698.0	8.50	0.30	72.10	0.501	9.14	0.522
3120.0	11.65	0.30	135.80	0.518	16.40	0.506
Sample E2, 0.00% B						
85.5	2.50	0.30	6.16	0.417	0.93	1.040
231.0	3.50	0.50	12.00	0.493	1.52	0.636
280.0	3.55	0.25	12.00	0.465	1.61	0.555
377.0	3.55	0.30	11.10	0.261	2.49	0.637

TABLE XIV (Cont'd.)

Gas yield data

$Rx10^{-4}$ rads	h_2 cm.	h_1 cm.	$h_2^2 - h_1^2$ $(cm.)^2$	Weight g.	$Y \times 10^6$ moles/g.	G_g molecules/100 e.v.
Sample B1, 0.52% B						
161.4	4.95	0.80	23.8	1.800	0.74	0.460
428.0	7.85	0.25	61.5	1.801	1.98	0.447
563.0	9.10	0.30	82.6	1.816	2.69	0.462
998.0	12.15	0.50	147.4	1.806	5.10	0.492
1608.0	15.60	0.25	243.4	1.815	7.79	0.467
Sample C1, 2.1% B						
42.4	1.2	0.30	1.35	0.350	0.23	0.512
67.7	1.3	0.20	1.65	0.300	0.32	0.457
78.8	1.4	0.30	1.92	0.300	0.37	0.456
576.4	5.0	0.25	24.90	0.600	2.42	0.406
1160.0	7.2	0.35	57.70	0.601	5.03	0.418
1625.0	8.4	0.20	70.40	0.601	6.82	0.406

TABLE XIV (Cont'd.)

Gas yield data

$Rx10^{-4}$ rads	h_2 cm.	h_1 cm.	$h_2^2 - h_1^2$ $(cm.)^2$	Weight g.	$Y \times 10^6$ moles/g.	G_g molecules/100 e.v.
Sample C1, 2.1% B						
1920.0	9.00	0.20	80.9	0.600	7.85	0.395
3150.0	11.40	0.10	29.9	0.601	12.62	0.386
4240.0	9.20	0.40	84.5	0.275	17.88	0.407
5090.0	9.60	0.30	92.1	0.266	20.10	0.382
Sample D2, 5.2% B						
286.0	3.90	0.25	15.1	0.701	1.40	0.423
1132.0	7.65	0.25	58.4	0.701	4.85	0.413
1715.0	9.15	0.50	83.4	0.700	6.92	0.390
2320.0	9.80	0.25	95.9	0.601	11.72	0.512
2850.0	10.80	0.50	116.3	0.600	11.30	0.382
Sample D3, 7.1% B						
64.8	1.35	0.70	1.33	0.299	0.25	0.372
135.4	1.75	0.15	2.94	0.300	0.49	0.393
270.5	2.45	0.30	5.91	0.300	1.10	0.393

TABLE XIV (Cont'd.)

Gas yield data

$Rx10^{-4}$ rads	h_2 cm.	h_1 cm.	$h_2^2 - h_1^2$ $(cm.)^2$	Weight g.	$Y \times 10^6$ moles/g.	G_g molecules/100 e.v.
Sample D3, 7.1% B						
1140.0	4.80	0.25	22.9	0.311	4.22	0.358
1400.0	5.00	0.25	24.9	0.262	5.52	0.381
1405.0	7.55	0.30	56.9	0.311	10.60	0.373
2750.0	3.85	0.20	14.7	0.162	5.29	0.364
3410.0	8.40	0.25	70.4	0.310	13.20	0.373
Sample D4, 11.3% B						
2.3	1.10	0.30	0.72	0.350	0.012	0.504
4.6	0.90	0.20	1.17	0.350	0.020	0.410
6.8	1.40	0.40	1.80	0.320	0.033	0.471
7.9	1.30	0.20	1.65	0.272	0.035	0.432
631.0	5.10	0.20	25.90	0.600	2.530	0.385
1194.0	6.80	0.20	46.20	0.600	4.540	0.363
1768.0	8.20	0.20	67.20	0.601	6.530	0.357
2320.0	10.35	0.30	107.10	0.700	8.920	0.371
3000.0	11.85	0.25	140.40	0.701	11.700	0.376
3750.0	13.10	0.30	171.40	0.700	14.250	0.368

TABLE XIV (Cont'd.)

Gas yield data

$Rx10^{-4}$ rads	h_2 cm.	h_1 cm.	$h_2^2 - h_1^2$ $(cm.)^2$	Weight g.	$Y \times 10^6$ moles/g.	G_g molecules/100 e.v.
Sample C2, 60.3% B						
389.0	6.60	0.70	43.01	0.600	4.48	2.520
554.4	6.00	0.30	35.91	0.605	3.45	1.110
780.0	7.55	0.50	56.75	0.599	6.28	0.732
1735.0	8.35	0.35	69.58	0.608	6.62	0.370
2730.0	9.65	0.45	93.00	0.600	13.80	0.487
3160.0	13.10	0.30	177.50	1.000	10.25	0.313
3750.0	9.90	0.40	97.84	0.599	8.95	0.330
4270.0	10.25	0.20	105.16	0.599	10.92	0.248
Sample G, 100% B						
631.0	1.50	0.30	2.16	1.000	0.256	0.039
2320.0	2.15	0.20	4.59	0.980	0.578	0.024
5420.0	(measured gas yield by mass spectrometer volumes)			26.200	1.180	0.021

SUMMARY AND CONTRIBUTIONS TO KNOWLEDGE

1. A sample of poly(butadiene-co-styrene) was divided into twelve fractions by precipitation from a dilute benzene solution. The intrinsic viscosities $[\eta]$ and weights of all the fractions were measured and the sedimentation rates and coefficients, (s_o), were determined for the nine highest molecular weight fractions. From the sedimentation and viscosity data the number of crosslinks per molecule for each fraction was calculated according to several theories. The results indicated that only four fractions of highest intrinsic viscosity contained nonlinear molecules. The extend of nonlinearity increased with increasing intrinsic viscosity. From these results and the weight of each fraction the number of crosslink units per weight average primary molecule, δ_o, was calculated. The theory of Zimm and Kilb (73) gave $\delta_o = 0.78$, whereas the Stockmayer-Fixman theory (72) and that represented by equation 14 gave much lower values.

2. The value of the Huggins constant, k', was found to be the same for the eight lowest intrinsic viscosity fractions, but progressively increased with increasing intrinsic viscosity for the four fractions of highest intrinsic viscosity.

3. From the number average molecular weight of the unfractionated polymer, $\bar{M}_{no}$, which was determined by osmometry, and the intrinsic viscosity of the unfractioned polymer, δ_o was found to vary from 0.30 to 0.66.

4. The partial specific volume of the polymer in benzene was found by pycnometry to be independent of concentration and equal to 1.02 $g.^{-1}ml$. Using this value and the sedimentation and viscosity data of the nine highest intrinsic viscosity fractions, the molecular weights of these nine fractions were calculated.

5. Two sets of viscosity average molecular weights, $\bar{M}_v$, of the fractions were calculated using two different relations between intrinsic viscosity and molecular weight. These relations were determined by other workers, (134, 135). Values of $\bar{M}_v$ calculated using the relation for low temperature polymerization agreed well with the molecular weights, $M_{\eta s}$, calculated using $[\eta]$ and s_o. However, there was serious disagreement when $\bar{M}_v$ was calculated using the relation for high temperature polymerization.

6. A molecular weight distribution curve has been obtained using the weights of the fractions, and $\bar{M}_{\eta s}$ for the nine highest molecular weight fractions, and $\bar{M}_v$ for the three lowest molecular weight fractions. From this curve it was estimated that the ratio of the weight average to

number average molecular weight of the unfractionated polymer, $\bar{M}_{wo}/\bar{M}_{no}$, was equal to 2.84. This value of $\bar{M}_{wo}/\bar{M}_{no}$ led in turn to a value of 0.36 for δ_o.

7. The degree of nonlinearity of the molecules was increased when the polymer was exposed in vacuo to gamma radiation. Solubility measurements at high doses indicated that the radiation produced very little main chain degradation. These measurements also indicated that nonlinearity was not caused by cyclization or chain reaction crosslinking. It was not possible to determine whether irradiation led to endlinking or crosslinking.

8. From the manner in which the solubility depended on dose, δ_o was estimated to be 0.8. This value approximates that calculated from the fractionation data by the Zimm and Kilb theory (73).

9. The number of crosslink units formed per 100 e.v. absorbed by the sample, G_x, was calculated from $\bar{M}_{wo}$ and from the value of the radiation dose required to produce incipient gelation, R_g. If $\bar{M}_{wo}$ is calculated from $\bar{M}_{no}$ and from the experimentally determined molecular weight distribution, G_x is found to be 9.4. From $\bar{M}_{no}$ and the manner in which solubility decreased with dose, a more reliable value of $G_x = 1.6$ was obtained. The discrepancy in G_x values

suggests that $\bar{M}_{wo}$ calculated from the experimentally determined M.W.D. is less than the true value. Therefore the experimentally determined molecular weight distribution was narrower than the true M.W.D. If G_x is equal to 1.6 when calculated from R_g and $\bar{M}_{wo}$, the ratio $\bar{M}_{wo}/\bar{M}_{no}$ must be approximately 8. This value for $\bar{M}_{wo}/\bar{M}_{no}$ corresponds to $\delta_o = 0.8$, therefore δ_o must be approximately 0.8. This implies that all the viscosity theories considered, except that of Zimm and Kilb, underestimate the effect of nonlinearity on viscosity.

10. The degree to which the polymer swelled in benzene decreased as the radiation dose increased. From an analysis of the dependence of swelling on dose it was concluded that $G_x = 1.6$. Therefore swelling data provided further evidence that $\delta_o = 0.8$.

11. The increase in intrinsic viscosity caused by irradiating the polymer was considerably less than that predicted by several theories (90, 81, 92, 75). This result is consistent with the fact that these same theories gave a value of δ_o which was much less than 0.8. Apparently these theories underestimate the effect of nonlinearity.

12. Mass spectrometric analyses revealed that the gas evolved on irradiating the pure polymer contained 87.1% hydrogen, 4.8% ethylene and 8.1% higher mass number constituents.

The number of molecules of gas evolved per 100 e.v. absorbed, G_g, has been determined by gas yield measurements. For the pure polymer $G_g = 0.52$. From this value of G_g, from $G_x = 1.59$ and from the gas composition, it was calculated that for every crosslink unit formed 0.0031 molecules of ethylene were evolved.

13. The composition of the gas evolved from pure antioxidant, B, after a high dose was 53.1% hydrogen and 46.9% higher mass number constituents. G_g for pure B was slightly dependent on dose and had an average value of 0.2 over the range examined.

14. G_g was found to be independent of dose over the range 0 - 11% B, but G_g was very dose dependent for a sample containing 60% B.

15. After irradiating the pure polymer in vacuo to a dose of 150 Mrads infrared analyses showed many vinyl groups were destroyed. Ultraviolet analyses indicated that irradiation in vacuo caused the formation of diene and triene groups. By a calculation using $G_x = 1.6$ it was found that for every crosslink unit formed 0.71 vinyl groups were destroyed.

16. When B was added to the polymer both G_x and G_g were reduced by a much greater extend than predicted by the "mixture law".

This deviation indicates that B protects the polymer from radiation. The percentage decrease in G_x was greater than in G_g. The extent of the protection increased with increasing B content up to a concentration of 2% B. A constant degree of protection was observed from 2 - 11% B.

17. For a sample containing 0.52% B the degree of protection decreased with increasing dose. The degree of protection was independent of dose for samples containing more than 2% B.

18. Solvent extraction of irradiated protected polymer showed that 21.3 potential crosslink units were prevented for every molecule of B destroyed or attached to the polymer. Therefore, protection must involve either charge transfer, excitation energy transfer, or quenching.

19. Infra-red and ultraviolet analyses revealed that the extent of oxidation which occurred when the pure polymer was irradiated in air was much greater than in the absence of radiation. Only a small amount of oxidation occurred when polymer containing B was irradiated in air. Solubility results indicated that when either pure polymer or polymer containing antioxidant was irradiated in air fewer crosslinks were formed than when irradiation was in vacuo, but main chain degradation occurred in air.

20. A reaction mechanism is proposed to account for the radiation induced effects in pure polymer and polymer containing B. Radiation induced nonlinearity and gas evolution are considered to be caused by two distinct processes each of which leads to crosslink or endlink formation and gas evolution. One of the processes involves ions and exhibits a negative deviation from the "mixture law," because of charge transfer to B. The other process involves excited molecules and exhibits a positive deviation from the "mixture law" because of excitation energy transfer from B. To account for the high value of G_g for the sample containing 60% B it is proposed that in addition to the two processes mentioned above a third gas producing process occurs. The gas associated with this process results from the decomposition of B. This third process is sensitized by the polymer, but it can only occur if B is dispersed in aggregates.

SUGGESTIONS FOR FURTHER WORK

1. The fractions studied in the present work were probably somewhat polydisperse. If a refractionation technique were employed or if a large number of fractions were obtained, the polydispersity of the fractions would be low. With such fractions the validity of the theories relating molecular nonlinearity to intrinsic viscosity could be tested more accurately.

2. A solvent should be found which would give clearer and more pronounced ultracentrifuge schlieren patterns than those obtained with benzene. With such a solvent the sedimentation coefficient for the low molecular weight fractions might be determined. Furthermore, a more suitable solvent might make it possible to estimate the molecular weight distribution of each fraction.

3. The number average molecular weight of each fraction should be determined. From this the degree of polydispersity could be determined by comparing the number average molecular weight to the molecular weight calculated from the intrinsic viscosity and the sedimentation coefficient.

4. When a linear polymer is irradiated the change in the intrinsic viscosity might be investigated. Such an investigation would indicate whether the deviation from theory obtained in the present work is related to non-random crosslinking and degradation produced by nonlinear units, or to inherent inadequacies of the theories

5. G_g in the present work was greater at low doses than at high doses. This dose dependency can arise from nonlinear units formed during polymerization causing degradation or from errors in sample preparation. The determination of gas composition and G_g for linear polymer irradiated to low doses would reveal the relative importance of the two possibilities above.

6. The possibility of a third gas producing process could be examined by measuring G_g and gas composition over the entire range of antioxidant concentration.

7. Infra-red analyses following the irradiation of a polymer containing B would indicate the extent to which B protected the vinyl groups. This information could then be related to the decrease in G_x and G_g caused by B and to the gas composition of a sample containing B.

BIBLIOGRAPHY

1) H.R. Anderson, Jr. J. Appl. Polymer Sci. 3, 316 (1960).

2) A. Charlesby. Atomic Radiation and Polymers. Pergamon Press Ltd., London. 1959. p.37.

3) M. Burton, J.L. Magee and A.H. Samuel. J. Chem. Phys. 20, 760 (1950).

4) R.L. Platzman. Radiation Research, 2, 1 (1955).

5) E.U. Condon. Phys. Rev. 28, 1182 (1926);
32, 858 (1928);
35, 658 (1930).

6) A. Charlesby. Atomic Radiation and Polymers. Pergamon Press Ltd., London. 1959. p.443.

7) L.H. Gray. Physical Aspects of Radiobiology in Chemical and Biological Actions of Radiations. Edited by M. Haissinsky. Masson, Paris. 1955. p.1.

8) A. Chapiro. Radiation Chemistry of Polymeric Systems. John Wiley and Sons Inc. London. 1962. p.58.

9) National Bureau of Standards (U.S.) Handbook. 62 (1957).

10) A. Charlesby. Proc. Roy. Soc. (London), A, 230, 120 (1952)

11) E.J.A. Lawton, A.M. Bueche and J.S. Balwit. Nature, 172 76 (1953)

12) A.A. Miller, E.J. Lawton and J.S. Balwit. J. Polymer Sci. 14, 503 (1954).

13) L.A. Wall. J. Polymer Sci. 17, 141 (1955).

14) M. Dole, D.C. Milner and T.F. Williams. J. Am. Chem. Soc. 79, 4809 (1957).

15) W.H.T. Davison. Chem. and Ind. 662 (1957).

16) A. Charlesby. Proc. Roy. Soc. (London), A, 215, 187 (1952)

17) M. Dole, C.D. Keeling and D.G. Rose. J. Am. Chem. Soc. 76, 4304 (1954)

18) B.J. Lyons. Nature, 195, 690 (1962)

19) K. Schumacher. Kolloid Z. 157, 16 (1958)

20) A. Charlesby. Atomic Radiation and Polymers. Pergamon Press Ltd., London. 1959. p.190.

21) J. Weiss. J. Polymer Sci., 29, 425 (1958).

22) W.F. Libby. J. Chem. Phys., 35, 1714 (1961).

23) R.W. Pearson. J. Polymer Sci., 25, 189 (1957); Chem. and Ind. (London), 209 (1957).

24) A. Charlesby. Radiation Research, 2, 96 (1955).

25) M.A. Golub. J. Am. Chem. Soc., 82, 5093 (1960).

26) P. Alexander and A. Charlesby. J. Polymer Sci., 23, 355 (1957)

27) E. Witt. J. Polymer Sci., 41, 507 (1959).

28) M. Burton and S. Lipsky. J. Phys. Chem., 61, 1461 (1957).

29) M. Dole, D.C. Milner and T.F. Williams. J. Am. Chem. Soc., 80, 1580 (1958).

30) P. Alexander and D. Toms. J. Polymer Sci., 22, 343 (1956).

31) W.C. Sears and W.W. Parkinson. J. Polymer Sci., 21, 325 (1956).

32) P.J. Flory. Principles of Polymer Chemistry. Cornell Univ. Press, Ithaca, N.Y. 1953. p.560.

33) G.V. Schulz. Z. physik. Chem. B,47, 155 (1940).

34) P.J. Flory. Principles of Polymer Chemistry. Cornell Univ. Press, Ithaca, N.Y. 1953. p.408.

35) P.J. Flory. Principles of Polymer Chemistry. Cornell Univ. Press, Ithaca, N.Y. 1953. p.425.

36) M. Kurata and H. Yamakawa. J. Chem. Phys., 29, 311 (1958).

37) T. Svedberg and K.O. Pedersen. The Ultracentrifuge. Oxford Univ. Press, London. 1940. p.10.

38) H.C. Brinkman. Applied Sci. Res., A,1, 27 (1947).

39) P. Debye and A.M. Bueche. J. Chem. Phys., 16, 563 (1948); 16, 573 (1948).

40) J.G. Kirkwood and J. Riseman. J. Chem. Phys., 16, 565 (1948).

41) A. Peterlin. J. Colloid Sci., 10, 587 (1955).

42) L. Mandelkern and P.J. Flory. J. Chem. Phys., 20, 212 (1952).

43) P.J. Flory. Principles of Polymer Chemistry. Cornell Univ. Press, Ithaca, N.Y. 1953, Chap. XIV.

44) L. Mandelkern, W.R. Krigbaum, H.A.Scheraga and P.J. Flory. J. Chem. Phys., 20, 1392 (1952)

45) J. Oth and V. Desreux. Bull. soc. chim. Belg., 66, 303 (1957).

46) H.A. Scheraga and L. Mandelkern. J. Am. Chem. Soc., 75, 179 (1953).

47) W.R. Krigbaum and D.K. Carpenter. J. Phys. Chem., 59, 1166 (1955).

48) W.H. Stockmayer, M. Kurata and A. Roig. J. Chem. Phys., 33, 151 (1960).

49) P.F. Onyon. Viscometry. in Techniques of Polymer Characterization. Edited by P.W. Allen. Butterworth, London. 1959. p.194.

50) M.L. Huggins. J. Am. Chem. Soc., 64, 2716 (1942).

51) R.B. MacFarlane and L.A. McLeod. Proc. Third Rubber Tech. Conference. 214 (1954).

52) L.H. Cragg and C.C. Bigelow. J. Polymer Sci., 16, 177 (1955).

53) R. Simha. J. Colloid Sci., 5, 386 (1950).

54) D.A.I. Goring and A. Rezanowich. J. Colloid Sci., 15, 472 (1960).

55) M.H. Jones. Can. J. Chem., 34, 1027 (1956).

56) H.K. Schachman. Ultracentrifugation in Biochemistry. Academic Press. New York. 1959. p.92.

57) J.M. Burgers. Proc. Acad. Sci., Amsterdam, 45, 9 (1942).

58) M. Wales and K.E. Van Holde. J. Polymer Sci., 14, 81 (1954).

59) J. Bisschops. J. Polymer Sci., 17, 81 (1955).

60) P.Y. Cheng and H.K. Schachman. J. Polymer Sci., 16, 19 (1955).

61) S. Newman, L. Loeb and C.M. Conrad. J. Polymer Sci., 10, 463 (1953).

62) H. Mark. Der feste Korper. Hirzel, Leipzig. 1938. p.103.

63) R. Houwink. J. prakt. Chem., 157, 15 (1940).

64) P. J. Flory. Principles of Polymer Chemistry. Cornell Univ. Press, Ethaca, N.Y. 1953. p.312.

65) H. Tompa. Polymer Solutions. Academic Press, New York. 1956.

66) Q.A. Trementozzi. J. Phys. Chem., 54, 1227 (1950).

67) D. Cleverdon, D. Laker, and P.G. Smith. Trans. Faraday Soc., 47, 908 (1951).

68) J.A. Manson and L.H. Cragg. Can. J. Chem., 30, 482 (1952).

69) O.J. Walker, Jr. and C.A. Winkler. Can. J. Research, B 28, 298 (1950).

70) B.H. Zimm and W.H. Stockmayer. J. Chem. Phys., 17, 1301 (1949).

71) C.D. Thurmond and B.H. Zimm. J. Polymer Sci., 8, 477 (1952).

72) W.H. Stockmayer and M. Fixman. Ann. New York Acad. Sci., 57, 334 (1953).

73) B.H. Zimm and R.W. Kilb. J. Polymer Sci., 37, 19 (1959).

74) F. Bueche. J. Polymer Sci., 41, 549 (1959).

75) A.M. Kotliar and S. Podgor. J. Polymer Sci., 55, 423 (1961).

76) A.M. Kotliar. J. Polymer Sci., 55, 71 (1961).

77) F.R. Senti, N.N. Hellman, N.H. Ludwig, G.E. Babcock, R. Tobin, C.A. Glass and B.L. Lamberts. J. Polymer Sci., 17, 527 (1955).

78) L.H. Cragg and D.F. Switzer. Can. J. Chem., 31, 868 (1953).

79) L.H. Cragg and G.R.H. Fern. J. Polymer Sci., 10, 185 (1953).

80) L.M. Hobbs, S.C. Kothari, V.C. Long and G.C. Sutaria. J. Polymer Sci., 22, 123 (1956).

81) R.W. Kilb. J. Phys. Chem., 63, 1838 (1959).

82) W. Cooper, G. Vaughan, D.E. Eaves and R.W. Madden. J. Polymer Sci., 50, 159 (1961).

83) W. Cooper, D. E. Eaves and G. Vaughan. J. Polymer Sci., 59, 241 (1962).

84) J.A. Manson and L.H. Cragg. Can. J. Chem., 36, 858 (1958).

85) D.J. Pollock, L.J. Elyash and T.W. DeWitt. J. Polymer Sci., 15, 335 (1955).

86) L.D. Moore, Jr., G.R. Greear and J.O. Sharp. J. Polymer Sci., 59, 339 (1962).

87) B.H. Zimm. J. Chem. Phys., 16, 1099 (1948).

88) W.H. Stockmayer. J. Chem. Phys., 11, 45 (1943); 12, 125 (1944).

89) O. Saito. J. Phys. Soc. Jap., 13, 198 (1958); 13, 1451 (1958).

90) A.R. Schultz, P.I. Roth and G.B. Rathmann. J. Polymer Sci., 22, 495 (1956).

91) R.W. Kilb. J. Polymer Sci., 38, 403 (1959).

92) K. Katsuura. J. Phys. Soc. Jap., 15, 2310 (1960).

93) S. Kataoka. Busseironkenkya, 66, 102 (1953).

94) M. Dole. J. Phys. Chem., 65, 700 (1961).

95) A. Charlesby. Proc. Roy. Soc. (London), A, 222, 542 (1954).

96) A. Charlesby. J. Polymer Sci., 11, 513 (1953); 11, 521 (1953).

97) A. Charlesby. Proc. Roy. Soc. (London), A, 231, 521 (1955).

98) A. Charlesby. Proc. Roy. Soc. (London), A, 241, 495 (1957).

99) A. Charlesby, V. Wycherley and T.T. Greenwood. Proc. Roy. Soc. (London), A, 244, 54 (1958).

100) P.J. Flory. J. Chem. Phys. 18, 108 (1950).

101) J.A.E. Bardwell. Ph.D. Thesis. McGill University, Montreal, Que. 1948.

102) J. Scanlan. J. Polymer Sci., 43, 501 (1960).

103) L. Mullins and A.G. Thomas. J. Polymer Sci., 43, 13 (1960)

104) H.M. James and E. Guth. J. Polymer Sci., 4, 153 (1949); J. Chem. Phys. 31, 1039 (1953).

105) F.T. Wall and P.J. Flory. J. Chem. Phys., 19, 1435 (1951).

106) J.J. Hermans. J. Polymer Sci., 59, 191 (1962).

107) J.C.H. Hwa. J. Polymer Sci., 58, 715 (1962).

108) J.J. Hermans. Trans. Faraday Soc., 43, 591 (1947).

109) W. Kuhn, R. Pasternak and H. Kuhn. Helv. Chim. Acta. 30, 1705 (1947).

110) L. Mullins. J. Polymer Sci., 19, 225 (1956).

111) A.F. Blanchard and P.M. Wooton. J. Polymer Sci., 34, 627 (1957).

112) P.J. Flory. Principles of Polymer Chemistry. Cornell Univ. Press, Ithaca, N.Y. 1953. p.461.

113) P.J. Flory. J. Am. Chem. Soc., 69, 30 (1947).

114) L.E. St. Pierre, H.A. Dewhurst and A.M. Bueche. J. Polymer Sci., 36, 105 (1959).

115) G.M. Bristow. J. Polymer Sci., 36, 526 (1959).

116) A.M. Bueche. J. Polymer Sci., 15, 97 (1955).

117) T.A. Orofino and P.J. Flory. J. Chem. Phys., 26, 1067 (1957).

118) P.J. Flory and H. Daoust. J. Polymer Sci., 25, 429 (1957).

119) J.L. Binder. Ind. Eng. Chem., 46, 1727 (1954); Anal. Chem., 26, 1877 (1954).

120) A.W. Craig and D.A. Henderson. J. Polymer Sci., 19, 215 (1956).

121) J. Schurz and E.H. Immergut. J. Polymer Sci., 9, 279 (1952).

122) G. Kegeles. J. Am. Chem. Soc., 74, 5532 (1952).

123) I.M. Kolthoff, C.W. Carr, and B.J. Carr. J. Polymer Sci., 2, 637 (1947).

124) H.K. Schachman. Ultracentrifugation in Biochemistry. Academic Press. New York. 1959. p.75.

125) J. Oth and V. Desreux. Bull. soc. chim. Belg., 63, 133 (1954).

126) R.L. Baldwin and K.E. Van Holde. Fortschr. Hochpolym-Forsch. 1, 451 (1958).

127) N. Gralen. Dissertation. University of Uppsala. 1944.

128) T. Svedberg. J. Phys. and Colloid Chem., 51, 1 (1947).

129) P.O. Kinell and B.G. Rånby. Advances in Colloid Sci., 3, 161 (1950).

130) A.F.V. Eriksson. Acta. Chem. Scand., 7, 623 (1953).

131) I. Jullander. J. Polymer Sci., 2, 329 (1947).

132) International Critical Tables. McGraw-Hill Book Co., Inc., New York. 5, 27 (1933); 3, 33 (1933).

133) T. Svedberg and K.O. Pedersen. The Ultracentrifuge. Oxford Univ. Press, London. 1940. p.62.

134) D.M. French and R.H. Ewart. Ind. Eng. Chem., Anal. Ed., 19, 165 (1947).

135) A.S. Novikov, M.B. Khaikina, T.V. Dorokhina and M.J. Arkhangelskaya. Colloid J., 15, 51 (1953).

136) D. Cleverdon and D. Laker. J. Appl. Chem. (London), 1, 6 (1951).

137) P.J. Flory. J. Am. Chem. Soc., 69, 2893 (1947).

138) M. Morton. Ann. New York Acad. Sci., 57, 432 (1953).

139) Q.A. Trementozzi. J. Polymer Sci., 23, 887 (1957).

140) J.K. Breasley. J. Am. Chem. Soc., 75, 6123 (1953).

141) C. Booth and L.R. Beason. J. Polymer Sci., 42, 81 (1960).

142) H.W. McCormick. J. Polymer Sci., 36, 341 (1959).

143) M. Morton, T.E. Helminiak, S.D. Gadkary and F. Bueche. J. Polymer Sci., 57, 471 (1962).

144) G. Friedlander and J.W. Kennedy. Nuclear and Radiochemistry. John Wiley and Sons, Inc. New York. 1955. p.374.

145) A. Chapiro. Radiation Chemistry of Polymeric Systems. John Wiley and Sons, Inc. New York. 1962. p.21.

146) W.O. Baker. Ind. Eng. Chem., 41, 511 (1949).

147) R. Freeman. Proc. Third Rubber Tech. Conference 3 (1954).

148) A.C. Baskett. Intern Symp. Macromol. Chem. Milan-Torino 1954. Ricercu Sci., Suppl. A, 379 (1955).

149) P.J. Flory, N. Rabjohn and M.C. Shaffer. J. Polymer Sci., 4, 225 (1949).

150) L.A. Wood, Physical Chemistry ofSynthetic Rubbers. in Synthetic Rubber. Edited by G.S. Whitby. Wiley and Sons, Inc. New York. 1954. p.350.

151) G.M. Bristow and W.F. Watson. Trans. Faraday Soc., 54, 1731 (1958).

152) G. Vaughan, D.E. Eaves and W. Cooper. Polymer, 2, 235 (1961).

153) L.A. Wall and D.W. Brown. J. Phys. Chem., 61, 129 (1957).

154) P.J. Flory. Principles of Polymer Chemistry. Cornell Univ. Press, Ithaca, N.Y. 1953. p.187.

155) F. Harlen, W. Simpson, F.B. Waddington, J.D. Waldron and A.C. Baskett. J. Polymer Sci., 18, 589 (1955).

156) A. Charlesby and S.H. Pinner. Proc. Roy. Soc. (London), A,249, 367 (1959).

157) A. Charlesby. Atomic Radiation and Polymers. Pergamon Press Ltd., London. 1959. p.156.

158) D.T. Turner. Polymer, 1, 27 (1960).

159) A.S.T.M. Standards, Part 11, Am. Soc. Testing Materials, Philadelphia. 1961. p.619.

160) R.H. Hampton. Anal. Chem. 21, 923 (1949).

161) M.B. Evans, G.M.C. Higgins and D.T. Turner. J. Appl. Polymer Sci., 2, 340 (1959).

162) A.D. Cross. Introduction to Practical Infra-red Spectroscopy. Butterworths Scientific Publications. London. 1960. p.21.

163) E.J. Meehan. J. Polymer Sci., 1, 175 (1946).

164) L.G. Angert and A.S. Kuz'minskii. J. Polymer Sci., 32, 1 (1958)

165) J. Rehner, Jr., F.W. Banes and S.B. Robison. J. Am. Chem. Soc., 67, 605 (1945).

166) P.J. Dyne and J. Denhartog. Can J. Chem., 40, 1616 (1962).

167) F.W. Banes and L.T. Eby. Ind. Eng. Chem. 18, 535 (1946).

168) F.C. Foster and J.L. Binder. J. Am. Chem. Soc., 75, 2910 (1953).

169) A.S. Kuzminsky, T.S. Nikitina, E.V. Zhuravskaya, L.A. Oxentievich, L.L. Sunitsa and N.I. Vitushin. Geneva Conference. 29, 258 (1958).

170) M. Dole and T.F. Williams. Disc. Faraday Soc., 27, 74 (1959).

171) R.C. Giberson. J. Phys. Chem., 66, 463 (1962).

172) G.H. Miller, V.R. Larson and G.O. Pritchard. J. Polymer Sci., 61, 475 (1962).

173) R.G. Bauman and J.W. Born. J. Appl. Polymer Sci., 1, 351 (1959).

174) B.A. Dogadkin. Kolloid Z. 30, 260 (1958).

175) J.E. Field, D.E. Woodford and S.D. Gehman. J. Polymer Sci., 15, 51 (1955).

176) E.J. Lawton, P.D. Zemany and J.S. Balwit. J. Am. Chem. Soc., 76, 3437 (1954).

177) P.J. Dyne and J. A. Stone. Can. J. Chem., 39, 2381 (1961).

178) I. Ya Petrov and V.L. Karpov. Trudy I Vsesyuz. Soveshchaniga po Radiatsionnoi Khim. Academy of Sciences of the U.S.S.R. Moscow. 279 (1958).

179) M.E. Jayko and W.M. Garrison. J. Chem. Phys., 25, 1084 (1956).

180) L.G. Angert and A.S. Kuz'minskii. J. Polymer Sci., 55, 489 (1961).

181) J. Lamborn and A.J. Swallow. J. Phys. Chem., 65, 920 (1961).

182) M.S. Matheson. Ann. Rev. Phys. Chem., 13, 77 (1962).

183) A. Chapiro. Radiation Chemistry of Polymeric Systems. John Wiley and Sons Inc. London 1962. pp.434-436.

184) R.W. Pearson, J. Benett and I. Miller. Chem. and Ind. 1572 (1961).

185) M. Dole and F. Cracco. J. Am. Chem. Soc., 83, 2584 (1961).